Norwegian University of Life Sciences

Master's Thesis 2021 60 ECTS
Faculty of Bioscience

Transfection optimization and gene editing method establishment for fish cells

Subash Sapkota
M.Sc. Aquaculture

Transfection optimization and gene editing method establishment for fish cells

Norwegian Veterinary Institute, Department of fish health research

and

The Norwegian University of Life Sciences, Faculty of Bioscience, Department of Animal and Aquacultural Sciences (IHA)

Acknowledgments

This work for the master's thesis was developed under an ongoing project (Bio-Direct) at the Norwegian Veterinary Institute (NVI). The laboratory work was carried out between August 2020 and May 2021.

I would first and foremost like to thank my main scientific supervisor Aderito Loius Monjane (Researcher) and co-scientific supervisor Maria K Dahle (senior researcher and Professor II v/UiT) from the Norwegian veterinary institute (NVI) for the trust, guidance, and support. Thanks for being always available and guiding me throughout the year. I would like to thank my internal supervisor Simen Rød Sandve (associate professor, NMBU) for all the supervision and support.

I would like to thank many people from NVI who helped me carry out this project. I am thankful to Trude Vrålstad for facilitating my work at NVI. A special thanks to Anita Solhaug for helping with cell lines, growth media, and flow cytometry. Thanks to Mona Gjessing for providing ASG-10 cells and Hilde Sindre for LG-1 cells. Thanks to Kathrine Andersen for initiating ASG-10 transfection work before I started. I must thank other helping peoples without whom it would have been difficult to work like Unni Grimholt, Randi Faller, Cathrine Arnason Bøe, Ingebjørg Modahl, and Lone T Engerdahl.

Being separated from family during this pandemic was a very hard time but I am thankful to my family, dad, mom, and sister who always motivated, the daughter who send the reason for the smile and support of my wife in every step. My friends and relatives, I am always grateful for your help in this journey.

Subash Sapkota

Summary

Aquaculture is one of the fastest-growing industries around the world, and salmonoid aquaculture is a very big industry for Norway. Ensuring fish health and welfare is essential for aquaculture, also to avoid economic loss. To solve these challenges, researchers need to build new knowledge and understanding through research. To avoid the overuse of fish for in-vivo experiments, researchers need good *in vitro* cell models. Such cell models can be used to study the effects of infectious diseases, environmental impact, and functions of associated genes with the help of gene editing. Effective and optimized methods are essential for successful gene editing using the CRISPR Cas9 method. Electroporation is a very effective method for the transfection of cell lines. This project was aimed to optimize transfection protocols for fish gill cell lines using two electroporation methods and attempting to perform genome sediting based on the CRISPR/CAS9 system in the Atlantic salmon gill (ASG)-10 cell line.

Fish cell lines (ASG-10 and LG-1) developed within the Veterinary Institute of Norway were transfected using pmaxGFP™ plasmid and eSpCas9-GFP protein, on the Neon™ transfection system and Nucleofector™ 2b electroporation devices. Transfected cells were analyzed using a fluorescence microscope and flow cytometry. The best program identified was used for CRISPR-Cas9 transfection in the ASG-10 cell line. CYP1a was used as a target gene as it is important for detoxification, functional assays were available, and the gene is expressed in ASG-10. Two different Cas9 enzymes were used (GFP tagged and untagged) to make ribonucleoprotein (RNP) complexes. The analysis of gene editing from CRISPR-Cas9 transfection was performed using Cleavage assay and Sanger sequencing. From the analysis, edits were not detected, most likely due to low editing efficiency.

The master project was successful in optimizing transfection protocols for plasmid and protein transfection in gill cell lines, as well as in establishing a CRISPR-Cas9 gene editing workflow.

Abbreviations

ASG-10	Atlantic salmon gill cells
BME	Beta mercaptoethanol
BP	Base pair
Ca^{2+}	Calcuim
CHSE 214	Chinook salmon embryo cells
CRISPR/Cas9	Clustered regularly interspaced short palindromic repeats, associated protein9
crRNA	CRISPR-derived RNA
CYP1a	Cytochrome P450 1A
DNA	Deoxyribonucleic acid
DSB	Double-strand break
FACS	Fluorescence-activated cell sorting
FBS	Fetal bovine serum
FCS	Fetal calf serum
GFP	Green fluorescent protein (GFP)
HDR	Homology directed repair
IPTG	Isopropyl β-D-1-thiogalactopyranoside
gRNA	Guide ribonucleic acid
LG-1	Lumpsucker gill cells
Mg^{2+}	Magnesium
NHEJ	Non-homologous end joining
NMBU	Norges miljø- og biovitenskapelige universitet
NVI	Norwegian Veterinary Institute
PAM	Protospacer adjacent motif
PBS	Phosphate-buffered saline
PCR	Polymerase chain reaction
qPCR	Quantitative polymerase chain reaction
RNA	Ribonucleic acid
ssa11	*Salmo salar* chromosome 11
ssa 26	*Salmo salar* chromosome 26
TBE	Tris borate EDTA
tracrRNA	Trans-activating CRISPR RNA

Table of Contents

1 Introduction 1

1.1 Aquaculture 1

1.2 Salmonidae 2

1.2.1 Atlantic Salmon (*Salmo salar*) 3

1.2.2 Chinook Salmon (*Oncorhynchus tshawytscha)* 4

1.3 Lumpsucker (Cyclopterus lumpus) 5

1.4 Gill 6

1.5 Fish cell lines 7

1.6 Cyp1A gene 8

1.7 Transfection 9

1.8 Clustered Regularly Interspaced Short Palindromic Repeats (CRISPR)-Cas9 System 11

1.8.1 Background introduction 11

1.8.2 CRISPR Cas9 11

1.8.3 CRISPR-based immunity in bacterial systems 12

1.8.4 Structure and mechanism of CRISPR/Cas9 type II 13

1.9 Genome editing in fish cells using CRISPR- Cas9 method 16

2 Aims of thesis 17

3 Material 18

3.1 Equipment 18

3.2 Kits 18

3.3 Reagents and chemicals 19

3.4 Cell lines 19

4 Methods 20

4.1 Preparations of cells 20

4.2 Transfection by electroporation of cells with GFP-Plasmid and GFP-Cas9 (protein) 22

4.2.1 Plasmid (pMaxGFP™) transfection using Neon™ transfection system 23

4.2.2 Protein (eSpCas9-GFP) transfection using the Nucleofector™ 2b Device 25

4.2.3 Analysis of transfection efficiency of cells using Flow cytometry 25

4.3 Gene editing attempt in ASG-10 cells 27

4.3.1 Identification of target gene for gene editing 28

4.3.2 Target sequence selection for gRNA design 28

4.3.3 Primer Design for PCR and sequencing 28

4.3.4 gRNA synthesis using *In Vitro* Transcription (IVT) kit 28

4.3.5 Selection of positive control Slc45a2 gene 29

4.3.6 Protocol for ribonucleoprotein (RNP) complex transfection 29

4.4 Analysis of gene edits after CRISPR/Cas9 transfection 31

4.4.1 Cleavage detection assay 31

4.4.2 Gel electrophoresis 32

4.4.3 PCR Clonning 33

4.4.4 Sanger Sequencing 33

5 Results 34

5.1 Transfection of ASG-10 cells with pmaxGFP™ plasmid using the Neon™ transfection system 34
5.1.1 Transfection of fully confluent ASG-10 cells 34
5.1.2 Transfection of ASG-10 cells at 70% -80% confluency 37
5.1.3 Transfection of cells at 70% -80% confluency with $5*10^5$ cells 39
5.1.4 Replicate experiment of transfection of cells at 70% -80% confluency with $5*10^5$ cells 42

5.2 Transfection of CHSE 214 cells 42
5.2.1 Transfection of 70-80% confluent CHSE 214 cells using Neon™ transfection system 42
5.2.2 pmaxGFP™ Plasmid transfection using of CHSE 214 cells using Nucleofeter™ system. 45

5.3 Transfection of LG-1 cells 47

5.4 eSpCas9-GFP protein transfection of cells by NucleofectorTM 2b Device 51
5.4.1 Transfection of ASG10 cells 51
5.4.2 Transfection of CHSE 214 53

5.5 Gene editing attempt in ASG-10 cells 55
5.5.1 Identification of CYP1a gene in Atlantic salmon 55
5.5.2 Identification of target sequences using ChopChop browser 55
5.5.3 Design of DNA oligos for IVT synthesis of gRNA 57
5.5.4 PCR assembly of DNA oligos 57
5.5.5 Primers designed for PCR 59
5.5.6 PCR of target gene CYP1a 59
5.5.7 Genomic cleavage detectation assay 62
5.5.8 Results from PCR clonning 63
5.5.9 Sanger sequencings 65

6 Discussion 71

6.1 Identification of factors affecting transfection efficiency in GFP tagged plasmid DNA transfection . 71

6.2 Identification of Nucleofector™ 2b device programs giving higher transfection efficiency in protein transfection 72

6.3 Attempt to gene edit in ASG-10 cells 73
6.3.1 Analysis of target gene (CYP1a) and identification of target sequences 73
6.3.2 Analysis of gene editing after RNP transfection 74

6.4 Future perspective 75

7 Conclusion 76

8 References 77

9 Appendix 84

1 Introduction

1.1 Aquaculture

Aquaculture is the farming of aquatic animals like fishes, mollusks, crustaceans, and seaweeds. It is the fastest-growing food production sector in the world (Little et al., 2016). Aquaculture has a long history dating to ancient civilizations in China, Egypt, and the Roman empire (Costa-Pierce, 2010; Smith, 2014). It is believed that aquaculture started 4000 years ago during the period 2000–1000 BCE in China (Rabanal, 1988). Now, traditional aquaculture has changed into modern aquaculture with the incorporation of new knowledge and technologies such as breeding and selection, feeding and nutrition, disease diagnostic,s and vaccination This rapid change in the modernization of aquaculture and the drive to making it one of the most productive fields of agriculture is known as the "Blue Revolution"; a revolution that's risen to the challenge of fulfilling the requirements of a nutritious diet, food security, and adding economical values to societies (Ahmed & Thompson, 2019).

Between 1961 and 2017 the global fish consumption increased by 3.1% compared to the population growth rate of 1.6% (Food and Agriculture Organization of the United Nations, 2020). Between 1990 and 2016, global aquaculture production increased six-fold, and there was an average annual growth rate of 5.8% during the period 2000–2016 (Food and Agriculture Organization of the United Nations, 2018). In 2018, the contribution of world aquaculture to global fish production reached 46%, which corresponds to 82.1 million tonnes of fish along with 32.4 million tonnes of aquatic algae and 26000 tonnes of ornamental seashells and pearls, bringing the total to an all-time high of 114.5 million tonnes (Food and Agriculture Organization of the United Nations, 2020). According to the Food and Agriculture Organization (FAO) report of Scottish White Fish Producers' Association (SWFA) 2020, China has been the top producer and main exporter since 2002, and the third major importing country in terms of value since 2011. Norway has been the second major exporter since 2004, followed by Viet Nam since 2014, India since 2017, and Chile and Thailand as the top five countries in terms of export (Food and Agriculture Organization of the United Nations, 2020).

The beginning of modern aquaculture in Norway date back to the 1850s when the first hatcheries for rainbow trout and Atlantic salmon for restocking purposes were established (Paisley et al., 2010). In the early days, most of the supply was from traditional sea catches which caused overfishing and overexploitation of wild stocks. This raised concern, which paved the way for modernizing aquaculture with the enforcement of fisheries laws and integration of new technologies in the 1960s (Gezelius, 2008; Mikalsen & Jentoft, 2003). In Norway specifically,

modern aquaculture started in the early 1970s (Stickney & Treece, 2000), with the first fish cages being installed at sea for farming, and the first set of production figures being recorded (Paisley et al., 2010). Now, aquaculture is an important sector that contributes to the national economy. In Norway, for the last five years, the annual production of salmon and trout have been approximately 1.4 million tons of round fish (Atlantic salmon and Rainbow trout), and within the same period, the value of this fish has increased from NOK 30 billion to NOK 67 billion (Table 1) (BarentsWatch, 2020).

Table 1. Aquaculture production in Norway by fish types in the year 2018-2019 (SSB Norway, 2020)

Aquaculture.					
	Fish for food (tonnes)	Share	Change in percent 2018 - 2019	First-hand value (NOK million)	Change in percent 2018 - 2019
2019					
Total	1,452,928	100	7.2	71,735	5.7
Salmon	1,364,044	93.9	6.4	67,990	5.4
Rainbow trout	83,489	5.7	22.2	3,477	13.8
Char	519	0	80.2	31	52
Halibut	1,525	0.1	-17.2	155	-14.9
Shellfish	2,164	0.1	25.7	29	-24

Aquaculture production is increasing. However, for it to fulfill the needs of a growing human population various challenges must be overcome including sustainable feeds, control of environmental pollution, disease management, fish welfare, and vulnerabilities associated with the effects of global climate change and increases in sea temperature (Elisabeth Ytteborg & Lynne Falconer, 2020; Martos-Sitcha et al., 2020; Sandersen et al., 2020). The economic value of marine aquaculture is increasing but the vulnerabilities associated with infectious diseases and parasites are challenging its economic growth (Lafferty et al., 2015; Rodger, 2016).

1.2 *Salmonidae*

The family *Salmonidae* belongs to the order *Salmoniformes* which includes 176 species in 11 genera and is grouped into three subfamilies (ITIS, 2020). The three genera *Oncorhynchus*,

Salmo, and *Salvelinus* which comprises of the commercially valuable farmed salmonids as well as other species that are valuable for recreational fishing (Pennell & Prouzet, 2009). This group includes fish that have high economic value, nutrient content, and taste (Colombo & Mazal, 2020; Criddle & Shimizu, 2014; Hamilton et al., 2005).

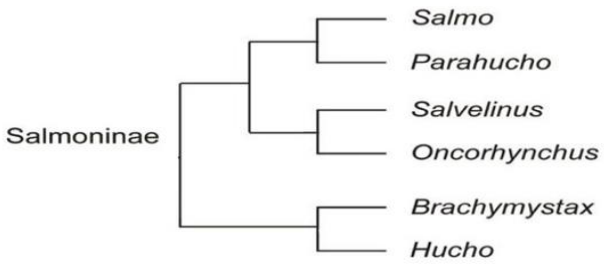

Figure 1. Cladogram showing sub-family Salmoninae along with nearest genera (Gauld, 2016)

1.2.1 Atlantic Salmon (*Salmo salar*)

The Atlantic Salmon is an anadromous species that is native to the North Atlantic region. This is a species that typically lives in freshwater for two to three years, then migrates to the sea, and comes to freshwater rivers for reproduction. *Salmo salar* is found in the Atlantic Ocean in the temperate regions and arctic zones in the northern hemisphere like the North Atlantic Ocean, Iceland, and Greenland, as well as the Ungava region of northern Quebec in Canada (CABI, 2020). Landlocked species are found in Norway, North America, Russia, Finland, and Sweden (Kazakov, 1992).

Genetically improved Atlantic salmon are now farmed in various parts of the world including Norway, Canada, USA, Chile, Australia, New Zealand, Ireland, Scotland, Spain, France, Russia, Iceland, and the Faeroe Islands (CABI, 2020; MacCrimmon & Gots, 1979). Atlantic salmon harvested from farms contribute to more than 72% of total salmon production, and the top four producers of Atlantic salmon based on export are Norway, Chile, Scotland, and Canada (Bloodworth et al., 2019). In Norway, the supply of farmed Atlantic salmon has increased by 443% since 1995, with an average annual growth of 8% (MOWI, 2019). The total supply of all farmed salmon exceeded 1.3 million tonnes in 2018 (Table.1) (Iversen et al., 2020).

Due to the increase in demand lead to extensive production, the aquaculture industry face challenges like lack of reduced fish health and welfare associated with sea lice and infectious diseases (Bailey & Eggereide, 2020; Bergheim, 2012; MOWI, 2019). Disease management is

one of the major challenges faced by the aquaculture industry due to intensive farming (Collet et al., 2015). Research is important to understand fish health and biology, including the mechanism of disease development, and to find potential solutions. To avoid extensive use of live fish for experimental trials, research is shifting towards alternative approaches and methods, like *in vitro* models (Drennan et al., 2007; Noguera et al., 2017). Additionally, when working with live fish, research labs must obtain permission according to rules and regulations defined by the EU Directive 2010/63 and Norway animal welfare act (European Union, 2010; The Norwegian National Research Ethics Committees, 2015).

Figure 2. Atlantic Salmon (Salmo salar) (Sekkingstad AS, 2021)

1.2.2 Chinook Salmon (*Oncorhynchus tshawytscha)*

Pacific salmon belongs to the genus *Oncorhynchus* known as *Oncorhynchus tshawytscha*. Like Atlantic salmon, chinook salmon are also anadromous. This salmon is also known as king salmon due to its large size among Pacific salmons. They can be as long as 149 cm and weigh up to 58.5 kg, but typically mature fish are about 92 cm long and weigh about 13.6 kg (NOAA Fisheries, 2021).

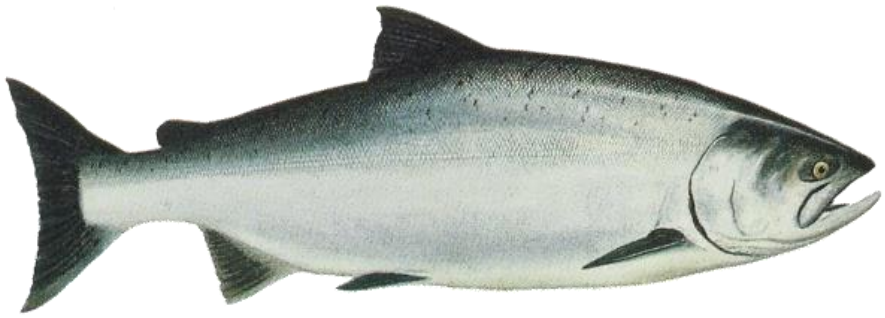

Figure 3. Chinook salmon (Rice, 2013)

The natural habitat of Chinook salmon are the colder upper reaches of the Pacific Ocean and they breed in the freshwater rivers and streams of the Pacific Northwest region (National Wildlife Federation, 2020). This includes most parts of the USA (Alaska, California, Oregon, Idaho) and in Canada, Japan, and Russia (CAB International, 2021). Commercially they are grown in New Zealand and Chile (FAO, 2021; Waples et al., 2004). But the worldwide production is less than 1% of the total farmed salmon. Despite low production, Chinook salmon is considered to have the highest nutritional contents, flavor, and texture (National Institute of Water and Atmospheric Research, 2016).

1.3 Lumpsucker (*Cyclopterus lumpus*)

The Atlantic lumpfish (*Cyclopterus lumpus*), also known as lumpsucker, is a marine teleost that belongs to the order *Scorpaeniformes* and family *Cyclopteridae* (Erkinharju et al., 2021; Nelson et al., 2016). The lumpfish is typically found in colder regions of the northern hemisphere. It is a relatively new aquaculture species and broodstocks are wild-caught mature fish (Torrissen et al., 2013). The sea lice problem is very big in Atlantic salmon aquaculture farms, and the use of cleaner fish like lumpfish to remove sea lice from salmon is a biological method that is more environmentally friendly than chemical methods (Powell et al., 2018), and less harmful for the salmon than mechanical methods. Studies have shown lower sea lice infestation levels on affected salmon after the use of lumpfish (Imsland et al., 2018). However, due to their intensive use, these fish are highly exploited, and they are vulnerable due to poor husbandry management and disease outbreaks (Froese & Pauly, 2014; Gutierrez Rabadan et al., 2021). The welfare concern of this fish is increasing, and there is a great need for more knowledge (Brooker et al., 2018).

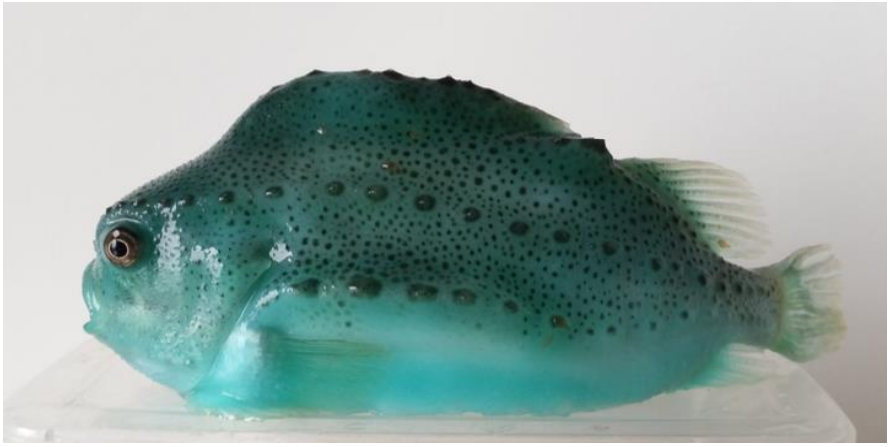

Figure 4. Lumpsucker (Institute of Marine Research, 2020)

1.4 Gill

The fish gill is a multifunctional organ that has many essential functions including O_2-CO_2 exchange, ion regulation, osmoregulation, acid-base balance, ammonia excretion, hormone production, modification of circulating metabolites, and immune defense (Rombough, 2007). The gill is composed of different cells with different functions (Fig. 5). The gill epithelium is composed of several types of cells but primarily consists of pavement cells (PVCs) and mitochondrion-rich cells (MRCs), which comprise more than 90% and less than 10% of the epithelial surface area, respectively (Fig. 6) (Evans et al., 2005).

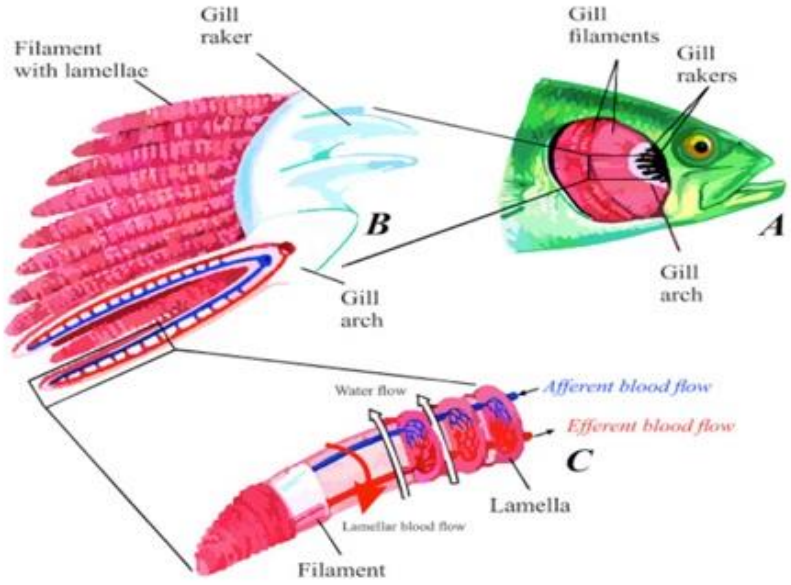

Figure 5. Diagram showing the gill structure of a bony fish. (A) Gills in the gill chamber without the operculum. (B) The segment of the gill showing gill rakers and filaments. (C) Part of an enlarged single filament. It also shows the water exchange and blood flow in single filament (McMillan & Harris, 2018).

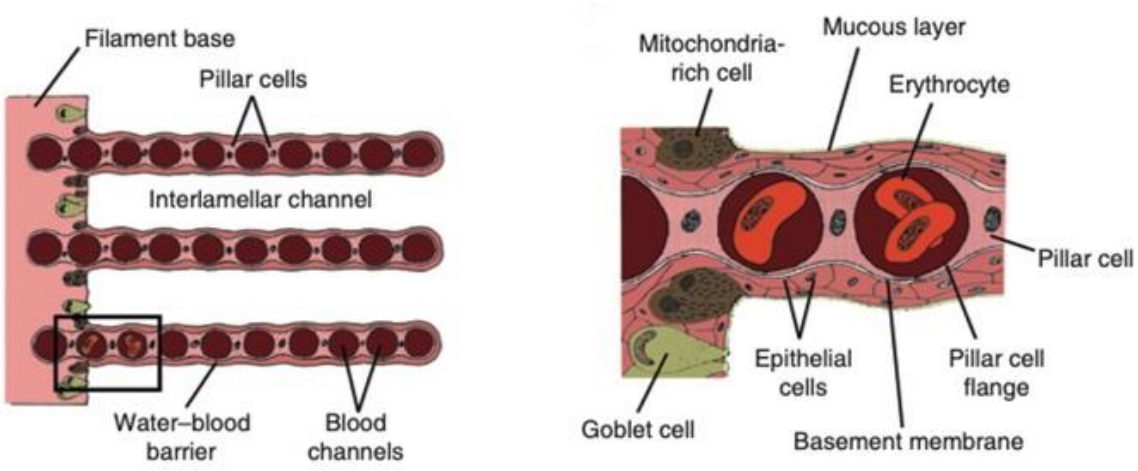

Figure 6. Diagram showing cross-section of lamella from single filament base and detailed diagram of a single lamella segment (Wegner, 2011)

The fish gills faces challenges as they form a semi-permeable barrier for exchange between blood flowing inside gills and the water environment through the countercurrent exchange process (Koppang et al., 2015). As fish gills are directly exposed to the water environment, they are vulnerable to any insults like physical trauma, infectious agents, and toxic compounds. Gill diseases can be defined as any disease with an effect on gill health and function, either due to invasion of infectious agents or of non-infectious origin (Foyle et al., 2020; Gjessing et al., 2019).

Cell lines from gills are important for the study of fish gill functions, gill diseases and for toxicological studies, treatment testing, and effects of water quality, which are easier to perform on cell lines than on whole organisms (Lee et al., 2009). In teleost fish various cell lines from gills, have been developed and work has been carried out to explore the toxicological effects and disease responses against pathogens. These models can reduce the use of live fish or *in vivo* research for study of disease response (Lee et al., 2009; Trump et al., 2000; Wood et al., 2002).

1.5 Fish cell lines

Fish cell lines are very important tools to study toxicology, cellular physiology, and gene regulation and function associated with interaction with pathogens and toxic compounds (Goswami Mukunda, 2018; Segner, 1998). Several cell lines have been developed so far from various tissues or organs from Atlantic salmon, including cell lines from kidney, endothelial tissue, blood cells (Lakra et al., 2011).

Different kinds of cell lines that are available are ASH (Atlantic salmon heart) which are monolayer fibroblast cells from the heart (Nicholson & Byrne, 1973), Salmon head kidney 1 (SHK-1) from the head kidney (Dannevig et al., 1997), TO from head kidney leukocytes (Wergeland & Jakobsen, 2001), RGE from gill (Butler & Nowak, 2004), ASK from kidney, SSP-9 from kidney tissue (Rodriguez Saint-Jean et al., 2014), ASHE from endothelial cells of Atlantic salmon (Pham et al., 2017) and, Atlantic salmon gills cells ASG-10 and ASG-13 (Gjessing et al., 2018). The ASG-10 cell line was developed from juvenile Atlantic salmon and was tested for successful passage and viral infection and confirmed to be an epithelial gill cell line that is capable of continuous growth (Gjessing et al., 2018).

There are some fish cell lines available from Chinook salmon isolated from different organs. Cell lines that are commercially available and popular for research and diagnostic tests are CHSE 114 and CHSE 214 (Lannan et al., 1984).

Cell lines from Lumpsucker are becoming relevant for in vitro experimental research, but there are few reports on cell lines available from lumpsucker. The commercially available cell line from this species is Cyclopterus Lumpus Fin (CLF) derived from fin (Fryer & Lannan, 1994).

Fish health and welfare is a growing concern in today's aquaculture industry as it has greater significance on the ability of fish to withstand stress, different pathogens like viruses, bacteria, ectoparasites (sea lice) (Cflow, 2021). So, the development of cell lines and cell models helps to safeguards the fish's health and welfare, etc. by reducing experimental trials (Iaria et al., 2019). This concept is based on the idea of using animal alternatives or the replacement of living species with *in-vitro* cultured models (Russell & Burch, 1959). The cell model helps to solve various ethical, social, and political issues associated with fish welfare like pain, stress, anesthetic treatment, and proper handling (Sloman et al., 2019).

1.6 Cyp1A gene

Cytochrome P450 molecules (CYPs) are a group of heme-thiolate monooxygenase enzymes that catalyze the oxidation of organic compounds (Nelson et al., 1993; Rahman & Thomas, 2012). Among the CYP superfamily, the CYP1a family of enzymes are extensively studied as they play a major role in the biotransformation of various endogenous substances such as lipids, steroids, vitamins, or toxic compounds like halogenated aromatic hydrocarbons (HAHs), polycyclic aromatic hydrocarbons (PAHs), and polychlorinated biphenyls (PCBs) (Goldstone et al., 2007; Leaver & George, 2000; Lewis et al., 1998). CYP1 genes are among the most intensively studied P450 genes (Rees, Christopher B. et al., 2005; Uno et al., 2012). Research on the P450

detoxification system is important to understand how the organism handles exposure to organic toxic compounds. The P450 CYPA1 enzyme system has been studied using different methods like next-generation sequencing, RT-qPCR, EROD assay, immunohistochemistry, and Western blot techniques in Atlantic salmon (Krøvel et al., 2008; Rees et al., 2003; Rees, Christopher B et al., 2005). The regulation and expression of CYPA1 in Atlantic salmon have been studied in response to different conditions such as hypoxic stress levels, temperature, salinity, and xenobiotics (Arukwe et al., 1997; Olsvik et al., 2013; Rahman & Thomas, 2012; Sanden & Olsvik, 2009).

The aryl hydrocarbon receptor (AHR) pathway is responsible for the expression of CYP1A subfamily members (Hahn et al., 1998). This pathway is activated when AHR binds to ligands dioxin-like like chemicals (DLCs) and polycyclic aromatic hydrocarbons (PAHs), which results in dimerization with AHR nuclear transporters (ARNT) forming a transcriptionally active complex that binds to xenobiotic response elements (XRE) and upregulates the transcription of CPYP1a (Di Giulio & Clark, 2015).

1.7 Transfection

Transfection is a method that introduces foreign nucleic acids or proteins into cells to genetically modify or alter cellular functions (Ruedel & Bosserhoff, 2012). It is a powerful tool to enable an analysis of the function of genes and gene products within the cells (Kim & Eberwine, 2010). The introduced nucleic acids can express protein within cells either stably or transiently based on the nature of the genetic material introduced (Glover et al., 2005; Recillas Targa, 2006). The transfection methods are broadly classified into three groups: biological, chemical, and physical (Table 2). Physical transfection is the method that uses mechanical or electrical forces to deliver foreign agents inside the target cells, for example, microinjection, electroporation, biolistic particle delivery (Kim & Eberwine, 2010). The chemical method is based on using positively charged chemical compounds (cationic polymers) that can form complexes with negatively charged nucleic acid components and delivery them inside the cell by the process of endocytosis or phagocytosis (Csiszár et al., 2010; Felgner et al., 1987). Biological methods use a virus (adenovirus, lentivirus) to deliver foreign genes into cells (Mali, 2013; Pfeifer & Verma, 2001).

Electroporation the commonly used physical method for transfection is suitable for many cells due to its simplicity, ease of use, and high efficacy (Fajrial Apresio K et al., 2020; Neumann et al., 1982). This method uses high voltage electric shock to create a pore in the cell and nuclear membrane to introduce genetic material into the cell (Potter H, 2001). Both stable and transient transfection is possible with this method (Potter, 2003). The result of this method is cell viability

and transfection efficiency which depends on various factors like voltage applied, electric pulse and time, vector concentration, cell type and density, and properties of the electroporation buffer (Potter, 2003; Sherba et al., 2020). These variables can affect cell viability due to excessive heat, pH changes, and ionic imbalance that occur after transfection (Lesueur et al., 2016). Different cell types require different electroporation conditions and parameters to obtain good transfection efficiency and results, so each new cell type needs optimization to find suitable parameters (Andreason & Evans, 1989; Gresch & Altrogge, 2012; Guo et al., 2012). Electroporation has been a successful method for the delivery of the CRISPR/Cas9 system into different types of cells from different species with varying degrees of gene editing results (Fajrial Apresio K et al., 2020; Gratacap et al., 2020b; Liang et al., 2015). The method of CRISPR-Cas9 transfection with electroporation and using ribonucleoprotein has an advantage in enhancing the on-target effect lowering off-target effect compared to other methods a ribonucleoprotein starts editing process faster than plasmid transfection where expression starter slower and takes a long time for expression (Farboud et al., 2018; Kim et al., 2014). Electroporation techniques for ribonucleoprotein transfection are quite novel in the transfection of fish cell lines (Gratacap et al., 2020b).

Table 2.Table showing conventional methods of transfections with advantages, disadvantages, and examples (Kim & Eberwine, 2010)

Class	Methods	Advantages	Disadvantages	Examples
Biological	• Virus-mediated	- High-efficiency - Easy to use - Effective on dissociated cells, slices, and in vivo	- Potential hazard to laboratory personnel - Insertional mutagenesis - Immunogenicity - DNA package size limit	Herpes simplex virus, Adeno virus, Adeno-associated virus, Vaccinia virus, Sindbis virus
Chemical	• Cationic polymer • Calcium phosphate	- No viral vector - High-efficiency	- Chemical toxicity to some cell types - Variable transfection efficiency by cell type or condition	DEAE-dextran, polyethyleneimine, dendrimer, polybrene, calcium phosphate, lipofectin, DOTAP, lipofectamine, CTAB/DOPE, DOTMA
	• Cationic lipid	- Easy to use - Effective on dissociated cells and slices - Plenty of commercially available products - No package size limit	- Hard to target specific cells	
Physical	• Direct injection	- Simple principle and straightforward	- Needs special instruments	Micro-needle, AFM tip, Gene Gun, Amaxa Nucleofector, phototransfection, Magnetofection
	• Biolistic particle delivery	- Physical relocation of nucleic acids into cell	- Vulnerable nucleic acids	
	• Electroporation	- No need for vector	- Demands experimenter skill, laborious procedure	
	• Laser-irradiation	- Less dependent on cell type and condition		
	• Sonoporation	- Single-cell transfection		
	• Magnetic nanoparticle			

1.8 Clustered Regularly Interspaced Short Palindromic Repeats (CRISPR)-Cas9 System

1.8.1 Background introduction

Modern genome editing is based on the use of engineered nucleases that are capable of binding a specific DNA site, and which is a fused composition of sequence-specific DNA-binding domains with a non-specific DNA cleavage module (Carroll, 2011; Urnov et al., 2010). The high efficiency of genome editing relies on the ability to make a targeted DNA double-strand break (DSB) in the targeted sequence of interest (Carroll, 2017). There are three powerful classes of nucleases that are capable to make programmed DSBs at essentially any desired target; the zinc-finger nucleases (ZFNs), transcription activator-like effector nucleases (TALENs), and CRISPR-Cas (Carroll, 2014).

ZFNs and TALENs are both based on creating the targeted DSBs by DNA cleavage activity of *Fok*I, a Type IIS restriction enzyme(Gupta & Musunuru, 2014; Miller et al., 2007). ZFNs are hybrids between a DNA cleavage domain from a bacterial protein and sets of zinc finger DNA binding domains (Ede et al., 2017; Hillary et al., 2020). TALENs employ the same bacterial cleavage domain but link it to DNA recognition modules from transcription factors produced by plant pathogenic bacteria (Joung & Sander, 2013). The TALEN technology is considered easier to design than ZFN and is reported to be more specific and less toxic to cells compared to ZFN (Joung & Sander, 2013; Sun & Zhao, 2013). In the last decade, the development of the CRISPR-Cas9 method of gene editing has overshadowed other methods like TALEN and ZFN.

1.8.2 CRISPR Cas9

CRISPR is known as clustered regularly interspaced short palindromic repeats and is associated with a nuclease known as Cas9. CRISPR/Cas was first discovered in bacteria and archaea as an acquired immune system against viruses and phages (Horvath & Barrangou, 2010; Ishino et al., 1987). CRISPR/Cas9-mediated genome editing depends on the generation of DSB at a precise location guided by single-stranded guide RNA (sgRNA) and Cas9, and a subsequent repair mechanism (Jinek et al., 2012; Nishimasu et al., 2014). This method has received extensive attention due to ease of manipulation, high editing efficiency, and that it applies to genome editing in different animals, plants, and organisms for a wide range of purposes (Lee et al., 2020; Song et al., 2016).

The history of the discovery of CRISPR repeats started in 1987 when Ishino et al accidentally discovered CRISPR repeats in *Escherichia coli* (Ishino et al., 1987). The CRISPR/Cas 9

mechanism was first demonstrated in 2008 and opened the door for a better understanding of this mechanism (Brouns et al., 2008; Koonin & Makarova, 2009). In 2012, Jennifer Doudna, Emmanuelle Charpentier, and their teams elucidated a clear picture of the biochemical mechanism of CRISPR technology (Charpentier et al., 2012). The use of the CRISPR Cas system as the gene-editing tool began in 2013, with the observation that Type II CRISPR systems from *Streptococcus thermophilus* (StCas) and *Streptococcus pyogenes* (SpCas9) could be engineered to edit mammalian genomes (Mali et al., 2013, Cong et al., 2013).

1.8.3 CRISPR-based immunity in bacterial systems

The original function of the CRISPR Cas9 system is to control virus/phage and conjugative plasmid infections within bacteria and archaea (Terns & Terns, 2011). CRISPR-based immunity works by integrating short virus sequences in the cell's CRISPR locus which allows the cell to remember, recognize and clear infections by distinguishing between genomic and invading foreign DNA (Fig. 7) (Marraffini & Sontheimer, 2010; Rath et al., 2015).

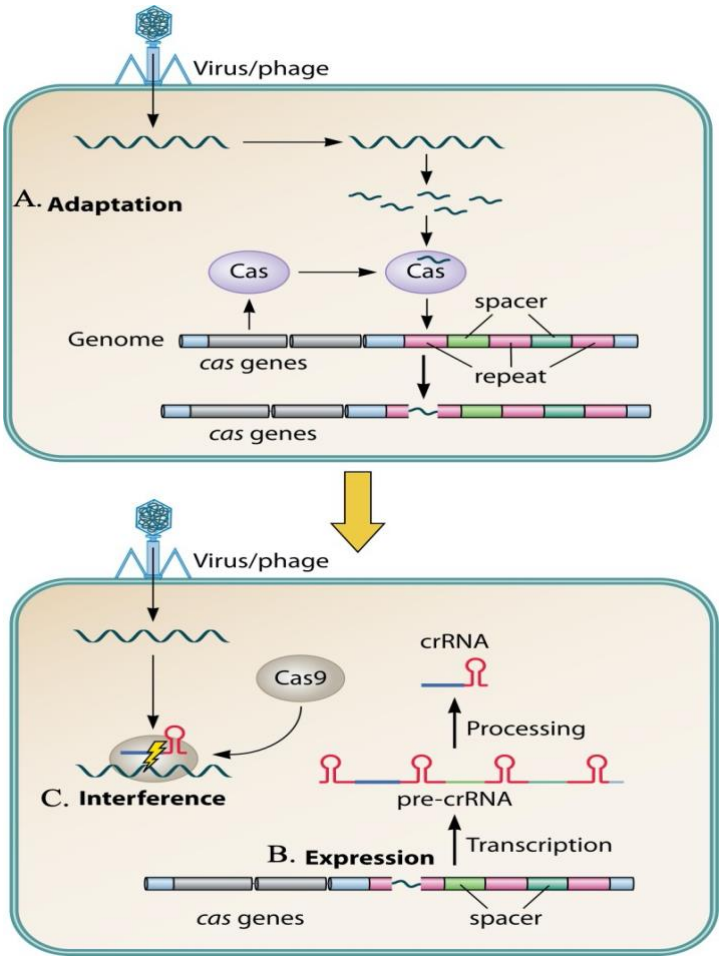

Figure 7. Diagram showing the process of acquiring Crispr-Cas mediated immune system in bacteria where the top diagram shows adaption mechanism and bottom diagrams shows expression mechanism (Ishino et al., 2018). Description: The CRISPR-Cas mediated defense pathway functions in three stages. The first stage A. is adaptation where invaders lead to the insertion of new spacers in the CRISPR locus. The second stage B. is an expression where the system prepares for pre-crRNA biogenesis by expressing the cas genes. Subsequently, the pre-crRNA is processed into mature crRNA by Cas proteins and accessory factors. The last or third stage C. is interference also known as silencing where foreign nucleic acid (invader particle) is recognized and destroyed by the combined action of crRNA and Cas protein.

1.8.4 Structure and mechanism of CRISPR/Cas9 type II

There is an enormous number of CRISPR/Cas systems identified so far like Cas1, Cas2, Cas3, etc. Based on structure, function, and effector molecules of Cas protein the CRISPR/Cas system is divided into two classes which are further divided into six types where class I includes type I, III, and IV, and class II includes type II, V, and VI (Koonin & Makarova, 2019; Makarova et al., 2015).

Table 3.Table: General characteristics of Crispr classes, subtypes, and associated Crispr protein with functions (Clark et al., 2019).

Class	Type	Subtypes	General Characteristics
1	I	I-A through I-F, and I-U	Uses Cas3 Targets double-stranded DNA Requires a PAM sequence
	III	III-A through III-D	Uses Cas10 Introduces single-stranded breaks in both DNA and RNA targets Does not require a PAM sequence
	IV	None characterized	Lacks many conserved *cas* genes and often a CRISPR array
2	II	II-A, II-B, II-C	Uses Cas9 and requires both crRNA and tracrRNA Produces blunt-ended, double-stranded breaks in target DNA Requires a PAM sequence
	V	V-A, V-B, V-C	Cpf1, C2c1, or C2c3 single protein effectors (sometimes called Cas12), depending on subtype Produces staggered, double-stranded breaks in target DNA Requires a PAM sequence Type V-B effector (C2c1) requires both crRNA and tracrRNA
	VI	VI-A, VI-B, VI-C	Uses C2c2 (sometimes called Cas13) single protein effector Produces single-stranded breaks in target RNAs Requires a PFS

The type II CRISPR Cas9 system is first identified and obtained from *S. pyogenes* which comprises of three components: CRISPR RNAs (crRNAs), trans-activating crRNA (tracrRNA), and a Cas 9 protein (Manghwar et al., 2019). In type II systems, the small RNAs, also known as crRNAs, are associated with Cas9 inside bacterial cells to recognize and cleave subsequent invading nucleic acids with sequences identical to that of the spacer (Garneau et al., 2010). crRNAs function with tracrRNA and CRISPR-associated (Cas) proteins to introduce double-stranded breaks in target DNA where target cleavage by Cas9 requires base pairing between the crRNA and tracrRNA as well as crRNA and the target DNA (Doudna & Charpentier, 2014). Protospacer-adjacent motif (PAM) typically represented by the tri-nucleotide sequence 'NGG' facilitates target recognition by crRNA (Sternberg et al., 2014). The PAM sequence is different in differing CRISPR/Cas systems. The PAM sequence is different in different CRISPR/Cas systems. Type II CRISPR-Cas systems are further classified into three subtypes (II-A, II-B, and II-C), two of which were introduced in the updated classification (Makarova et al., 2011). CRISPR Cas9 from type II is a widely used system in genome editing due to its effectiveness and higher efficiency.

Mechanism

Genome editing using the CRISPR system requires a Cas9 protein and an engineered single guide RNA which targets the DNA at a specific locus (Fig. 8) (Jinek et al., 2014). The tracrRNA and the crRNA can be combined to make a single guide RNA (gRNA) or it is now possible to have a completely chemically synthesized gRNA (Moon et al., 2019). The gRNA construct has a 5' region with 20 nucleotides and a 3' region composed of the crRNA fused to the 5' extremity of tracrRNA producing a hairpin structure recognizable by the Cas9 nuclease. The length of gRNA for Cas9 is approximately 100 nucleotides (Sekine, 2018). A PAM sequence is required to direct the gRNA to the target DNA, (Sternberg et al., 2014). When the target is recognized, Cas9 induces site-specific cleavage creating double-stranded breaks (DSBs), which can be repaired by non-homologous end-joining (NHEJ) or homology-directed repair (HDR) (Cong et al., 2013; Hsu et al., 2014; Liang et al., 1998; Pastwa & Błasiak, 2003; Ran et al., 2013). NHEJ is used to knock out genes as the process is error-prone and likely to creates small insertions or deletions that disrupt gene function`. In the HDR mechanism, a DNA repair template can be provided to knock in desired sequences into the break site via homologous recombination (Pattanayak et al., 2014).

.

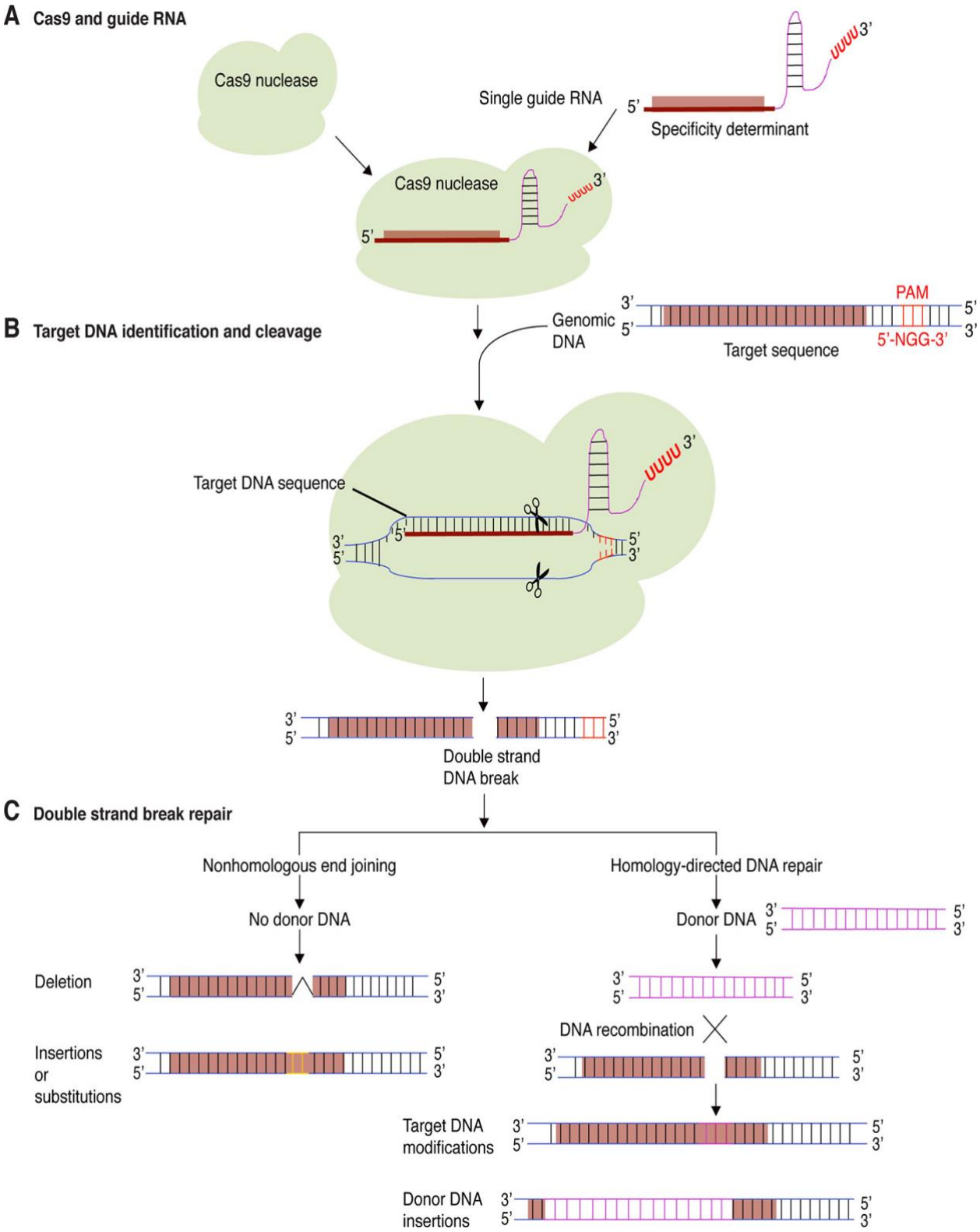

Figure 8. Schematic description of genome editing using CRISPR Cas9 system. A) Cas9 protein with target-specific gRNA .B) Formation of the complex between Cas9 and gRNA which cleaves and creates DSB C) Initiation of repair mechanism, Non-homologous End Joining (NHEJ) leading to insertion or deletion and Homology Directed Repair (El Mounadi et al., 2020).

1.9 Genome editing in fish cells using CRISPR- Cas9 method

Genome editing in fish is getting very popular for finding solutions to infectious diseases, parasites, target trait improvement, production of sterile fish, and studying gene function and regulation in vitro and in vivo (Gratacap, R. et al., 2019; Wargelius, 2019; Yue et al., 2018). CRISPR/Cas9 mediated genome editing of different targeted genes has successfully been applied in vivo or cell lines of several major aquaculture species like *Salmo salar*, *Oncorhynchus mykiss* (rainbow trout), *Oreochromis niloticus*, and many others (Edvardsen et al., 2014; Gratacap, R. et al., 2019; Li et al., 2014; Wargelius, 2019). Methods like microinjection of vector inserts for CRISPR/Cas9 mediated genome editing in fertilized fish eggs are popular to study gene functions (Datsomor et al., 2019; Straume et al., 2020). Lentiviral delivery systems are also used for the delivery of CRISPR-Cas9 components (Gratacap, R. L. et al., 2019). All the used methods are equally not suitable for all cell lines, eggs, or embryos as they are hard to transfect, achieve higher editing efficiency, and develop a clonal line of cells (Collet et al., 2018). The use of the electroporation method to deliver the gRNA Cas9 (ribonucleoprotein) complex has shown higher transfection efficiency and gene editing in fish cells (Gratacap et al., 2020a; Liu et al., 2018). There is an increasing demand for genome-edited fish cell lines for research in studying functional genomics associated with disease development (Collet et al., 2018). But still, there are various obstacles to efficient genome editing, development of stable genome-edited cell lines, so the research is continuously going all around the world to solve this challenge (Collet et al., 2018; Dehler et al., 2016; Escobar Aguirre et al., 2019).

2 Aims of thesis

1. To optimize transfection efficiency, using the Neon™ transfection system with GFP tagged plasmid in ASG-10 and LG-1 and Nucleofector™ 2b device with GFP tagged protein in ASG-10 and CHSE 214 fish cell lines preparing the foundation that leads to CRISPR/Cas9 transfection.

2. To establish a CRISPR/cas9 transfection system and attempt to perform genome editing based on the CRISPR/Cas9 system in the ASG-10 cell line.

3 Material

3.1 Equipment

Table 4. List of equipments and manufacturer.

Equipment	Manufacturer
Nucleofector™ 2b Device	LONZA
Neon™ Transfection System	Invitrogen™
TC20™ automated cell counter	BIO-RAD
BD Accuri™ C6 flow cytometer	BD Inc.
Inverted Laboratory Microscope Leica DM IL LED	Leica
Agilent 2100 Bioanalyzer system	Agilent
Qubit™ 4 Fluorometer, with WiFi	Invitrogen™
T100™ thermal cycler	BIO-RAD
Incubator 20-22 degree Celsius	Labnet International Inc.
NanoDrop™ 2000/2000c Spectrophotometers	Thermo Scientific™
ChemiDoc XRS+ System	BIO-RAD

3.2 Kits

Table 5. List of kits and manufacturer.

Kits	Manufacturing Company
Neon™ Transfection System 10 µL Kit	Invitrogenn
GeneArt™ Genomic Cleavage Detection Kit	Invitrogen™
GeneArt™ Precision gRNA Synthesis Kit	Invitrogen™
PureLink™ Genomic DNA Mini Kit	Invitrogen™
TrueCut™ Cas9 Protein v2	Invitrogen™
Cell Line Nucleofector™ Kit V	LONZA
eSpCas9-GFP Protein	Sigma-Aldrich
Bioanalyzer DNA Kits & Reagents	Agilent

3.3 Reagents and chemicals

Table 6. List of Reagents and manufacturers

Product	Manufacturing company
Fetal Calf Serum	Gibco™
Penicillin-Streptomycin	Gibco™
PBS 1X	In house media production
Gibco™ 2-Mercaptoethanol (BME)	Gibco™
Opti-MEM™ I Reduced Serum Medium	Gibco™
Leibovitz's L-15 Medium, GlutaMAX™ Supplement	Gibco™

3.4 Cell lines

Table 7. List of cell lines and source

Name	Source	Developer
ASG-10	Atlantic Salmon gill cell	Norwegian veterinary institute (NVI)
CHSE 214	Chinook salmon embryonic cell	Public Health England
LG-1	Lumpsucker gill cell	Norwegian veterinary institute (NVI)

4 Methods

4.1 Preparations of cells

ASG-10, CHSE 214, and LG-1 were collected from the cell culture collection of cell lab at the Norwegian Veterinary Institute. ASG-10 is a gill epithelial cell from Atlantic salmon (Gjessing et al., 2018), LG-1 from the gill of lumpsucker fish (not published yet), and CHSE 214 from Chinook salmon embryo (Public Health England, 2021).

L-15 media with different compositions were used for cell growth (Table 8). The cells were maintained at a temperature of 15- 20 °C. Different cells grow differently so, they were split on different days, and they were handled separately to avoid cross-contamination. CHSE 214 and LG-1 were maintained by the cell lab itself, so they were ordered per needed for transfection work.

Table 8. List of cell line and media compositions for respective cell lines.

Cell line	Media composition
ASG-10	1. Leibovitz's L-15 Medium GlutaMAX™ Supplement (Gibco 31415-029) was added with 10% Fetal Calf Serum (FCS) and 1% PenStrep antibiotics for preparing complete growth media. The total 100 ml media contained 10 ml of FCS, 1 ml of Penicillin Streptomycin solution (100 I.U./ml penicillin and 100 µg/ml streptomycin). 2. BME; 30µM (Beta-mercaptoethanol) BME in complete media to control ROS activity and improve cell viability.
CHSE 214	1. Leibovitz's L-15 Medium,) was added with 2mM L-glutamine (Gibco™ L-Glutamine (200 mM), 1% nonessential amino acids (NEAA), 5% Fetal Bovine Serum (FBS) and 1% PenStrep (100 I.U./ml penicillin and 100 µg/ml streptomycin). antibiotics for preparing complete growh media.
LG-1	**1.** Leibovitz's L-15 Medium GlutaMAX™ Supplement (Gibco 31415-029) was added with 10% Fetal Bovine Serum (FBS) and 1% PenStrep antibiotics for preparing complete growth media. The total 100 ml media prepared contained 10 ml of FBS, 1 ml of Penicillin Streptomycin solution (100 I.U./ml penicillin and 60 µg/ml streptomycin).

Protocol for cell splitting and growth of ASG-10 in T75 flask

1. Old-growth media was aspirated by pipetting gently.
2. Cells were washed with 10 ml PBS (Ca^{2+} / Mg^{2+} free) to remove serum.
3. 2 ml trypLE (Thermo Fisher) was added for trypsinization of cells
4. The growth flask was incubated at room temperature, approx. two to four minutes. The bottle was tapped gently and observed for cells detaching from the plastic bottom surface. These cells come off with no need to tap the bottle hard.
5. 5-10 ml of complete medium was added to inhibit trypsinization.
6. Then cells were split in 1: 2 ratios.
7. The seeding cell density was 132,000 / cm^2.
8. These cells need to grow for 10-14 days at 20°C to reach confluency.

4.2 Transfection by electroporation of cells with GFP-Plasmid and GFP-Cas9 (protein)

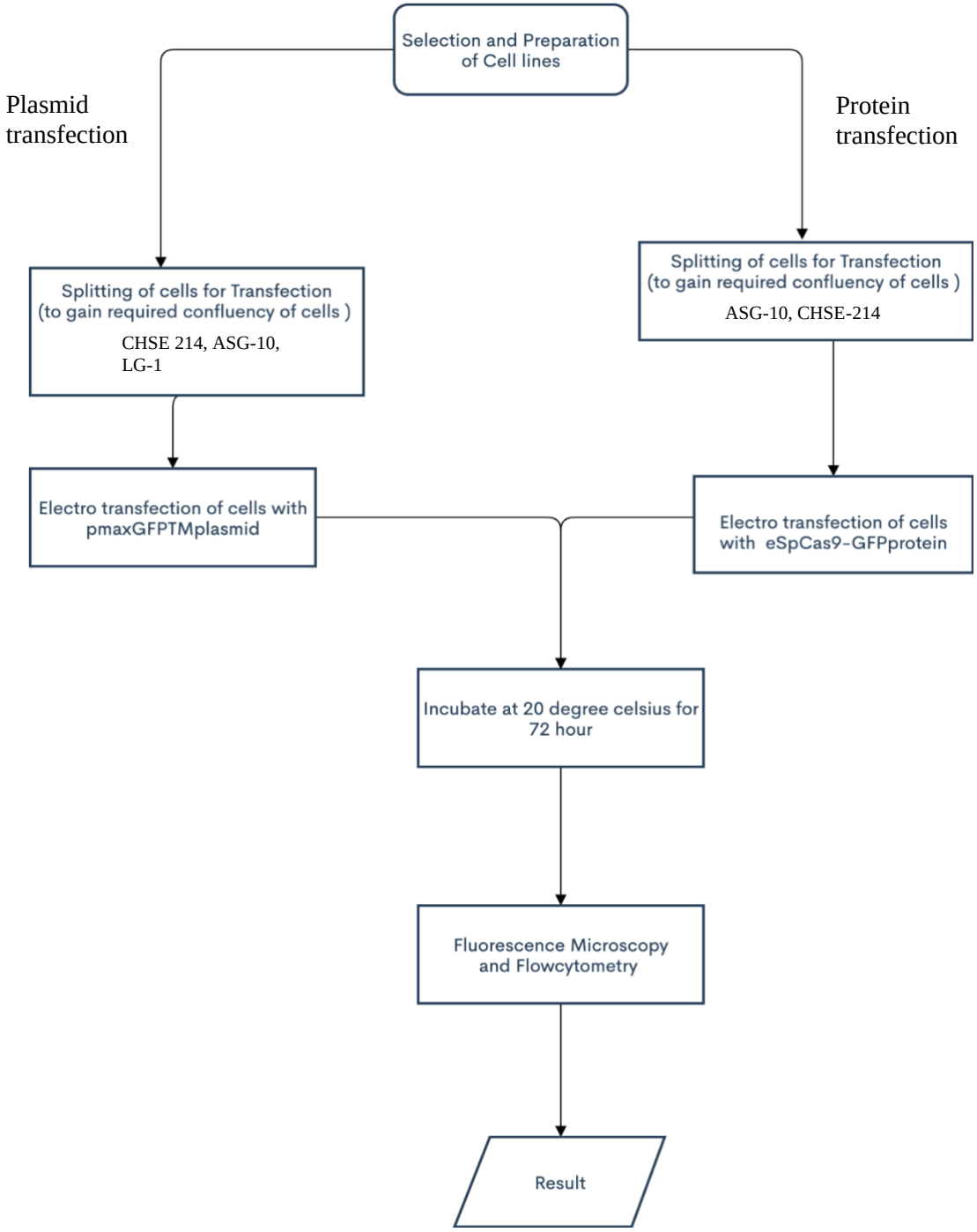

Figure 9. Flow diagram showing steps in plasmid transfection and protein transfection uisng different cell lines.

4.2.1 Plasmid (pMaxGFP™) transfection using Neon™ transfection system

All three cell lines (ASG-10, CHSE 214, LG-1) were transfected with pmaxGFP™ plasmid from Cell Line Nucleofector™ Kit V, using the Neon™ device and Neon™ Transfection 10µl Kit.

Preparation for Transfections

1. The required number of cells were grown in T75 cell culture flask for all three cell lines.
2. The cells were split and grown for 3-10 days before electroporation such that different degree of cells confluency was obtained on the day of the experiment.
   - For 70-80% confluency, cells were grown for three days after splitting at 20
   - For full confluency, ASG-10 and CHSE 214 cells were grown for 10 day and 14 days for LG-1 at 20 °C.
3. On the day of transfection, the working area was cleaned, and the aseptic protocol was followed strictly to avoid contaminations. The cell hood was sterilized with UV light for 15 mins before working, working surface and materials that were used within the hood were cleaned with 70% ethanol.
4. The media was aspirated, and the cells were rinsed using PBS (without Ca^{2+} and Mg^{2+}). 10 ml PBS was added and rinsed once for ASG- 10 in a 75 cm^2 flask. Other adherent cells like CHSE 214 and LG-1 required 2-times PBS wash.
5. The cells were trypsinized using 3 ml TrypLE Express in a 75 cm^2 flask for ASG 10 where CHSE 214 cells require first wash with TrypLE and then again incubation with TrypLE to increase the speed of trypsinization.
6. The cells were harvested in a seven ml growth medium with 10% fetal calf serum (FCS).
7. Aliquots of trypsinized cells were taken from suspension and counted to determine the cell density.
8. The required number of cells was transferred to one 1.5 mL microcentrifuge tube per transfection. ASG-10 and CHSE 214 cells were centrifuged at 400 × g for 5 minutes at room temperature. LG-1 cell suspension was centrifuged at 400 × g for 6 minutes as the cells were not pelleted well like in the other two cell lines uses the same parameters. The supernatant was removed, and cells were washed with PBS (without Ca^{2+} and $Mg^{2+)}$ by centrifugation at 400 × g for 5 minutes at room temperature. For LG-1, 400 × g for 6 minutes.
9. The PBS was aspirated, and the cell pellets were resuspended in either:
   - Neon™ transfection system: 10 µl pti-MEM® I Reduced-Serum Medium
   - Nucleofector™ 2b Device: 100 µl RT Nucleofector® Solution V with supplement solution (in 4.5:1 ratio)
10. The cells were pipetted gently to obtain a single-cell suspension.

11. Prepared 12 well plates for culturing after transfection by filling every second well with 2 mL and 24 plates with 1ml of culture medium containing serum and supplements, but without antibiotics. Pre-incubate in the cell incubator. 24 well plates were used for Neon™ transfection system with 10 µl kits, whereas for Nucleofector™ transfections 12 well plates were used.
12. The cells were transfected with pmaxGFP™ plasmid using Neon™ transfection system or Nucleofector™ 2b Device.

Neon™ transfection system

i. Neon® Tube with 3 mL Electrolytic Buffer (use Buffer E for 10 µL Neon® Tip) was set up into the Neon® Pipette Station.
ii. Then the program was set up on the device based on the cell type
iii. 1 µg of plasmid DNA (1-2 µg used for 10 µL Neon® Tip) was transferred into a sterile, 1.5 ml microcentrifuge tube. The concentration of plasmid was 0.5 µg and the volume taken was 2 µl.
iv. The cells were added to the tube containing plasmid DNA and gently mix.
v. Opti-MEM™ I Reduced Serum Medium was used as a buffer instead of Buffer R or T from the kit.
vi. The sample was pipetted, and the pipette was fixed to run the program, after the complete message was shown cell suspension was immediately transferred to the pre-warmed media.
vii. After 24 hrs complete media with antibiotics 500 µl was added.
viii. Cells were grown for 72 hours before analysis.

Nucleofector™ 2b Device

i. 1 µg plasmid DNA (pMaxGFP from the kit, 0.5 µg/µl) was added per tube prepared with cell solution. The cell solution was composed of the required number of cells and 100 µl RT Nucleofector® Solution V with supplement solution (in 4.5:1 ratio).
ii. The cell solution was transferred into certified cuvettes according to the experimental protocol. Care should be taken so that the sample covers the bottom of the cuvette without air bubbles.
iii. The cuvette was covered with the cap.
iv. The appropriate Nucleofector® Program was set up according to the experiment and cell type.
v. The cuvette with cell/DNA suspension was inserted into the Nucleofector® Cuvette holder and the selected program was entered.
vi. The cuvette was taken out of the holder as soon as possible once the program was finished

vii. Immediately, 500 µl pre-equilibrated culture medium was added to cuvet and the sample was gently transferred into the prepared well in the 12-well plate for adherent cells.

viii. After 24 hrs, 500 µl complete media with antibiotics was added.

ix. Cells were grown for 72 hours before analysis.

4.2.2 Protein (eSpCas9-GFP) transfection using the Nucleofector™ 2b Device

1. 10 µg eSpCas9-GFP (5 µg/µl *2 µl) per 1.5 µl tube was mixed with the prepared cell solution. The cell solution was composed of the required number of cells and 100 µl RT Nucleofector® Solution V and supplement solution (in 4.5:1 ratio). (The mixture shouldn't be stored for a long time at room temperature as GFP gets degraded and the GFP activity will disappear with long time light exposure.)
2. The cell solution was transferred into certified cuvettes and care was taken so that sample covered the bottom of the cuvette without air bubbles.
3. The cuvette was covered with the cap.
4. The appropriate Nucleofector® Programs were set up according to the experiment and cell type.
5. The cuvette with cell/DNA suspension was inserted into the Nucleofector® Cuvette holder and entered the selected program.
6. The cuvette was taken out of the holder as soon as possible once the program is finished
7. Immediately 500 µl pre-equilibrated culture medium was added to the cuvette and the sample was gently transferred into the prepared well in the 12-well plate for adherent cells.
8. After 24 hrs, 500 µl complete media with antibiotics was added.
9. Cells were grown for 72 hours before analysis.

4.2.3 Analysis of transfection efficiency of cells using Flow cytometry

A flow cytometer is an advanced instrument that can measure multiple physical characteristics of a single cell, like size and granularity, simultaneously as the cell flows in suspension through a measuring device (Adan et al., 2017). The main working principle of this system is the emission of light from an emission source (laser beam), and when striking the cell, light scattering and fluorescence emission can be measured by detectors.

Light scattering is directly proportional to the physical properties of the cell while fluorescence emission derived from a fluorescence probe is proportional to the amount of fluorescent probe in the cell or bound to the cell (Adan et al., 2017). We have used a BD Accuri™ C6

flow cytometer (BD Bioscience, 2013). It has four different detectors that can work in different laser wavelengths and filters. We have used the FL1 filter for GFP fluorescence and FL3 for Propidium iodide. Both excite in a 488nm laser wavelength and FL1 uses a 533/30 filter and FL3 for Propidium iodide uses 670 LP. FL1 was used for measuring transfection efficiency and FL3 to measure viability. First cells were measured on forward scatter and side scatter emission, then the sample was gated for live cells which were further analyzed for transfection efficiency and viability.

Protocol for preparing cells for flow cytometry

1. All the media was aspirated from the well
2. The cells were washed with 500 µl 1xPBS /12 well and 1ml 1xPBS/ 24 well plate
3. PBS was removed
4. 50 µl of TrypLE was added per well
5. Cells were checked to make sure they had detached.
6. After enough cells had detached, they were re-suspended with 700 µl media.
7. The suspension was transferred to a 1.5 µl tube and centrifuged at 400*g for 5 min
8. Media was removed and 200 µl of cold PBS was added to resuspend the cells
9. PI (10 µg/ml) was added to cells in the ratio of 1:100 for staining the cells
10. ACCURI BD6 flow cytometer was used for flow cytometry and ACCURI BD6 flow cytometer software for data analysis. The software manual was used to calibrate the system and for data analysis.

4.3 Gene editing attempt in ASG-10 cells

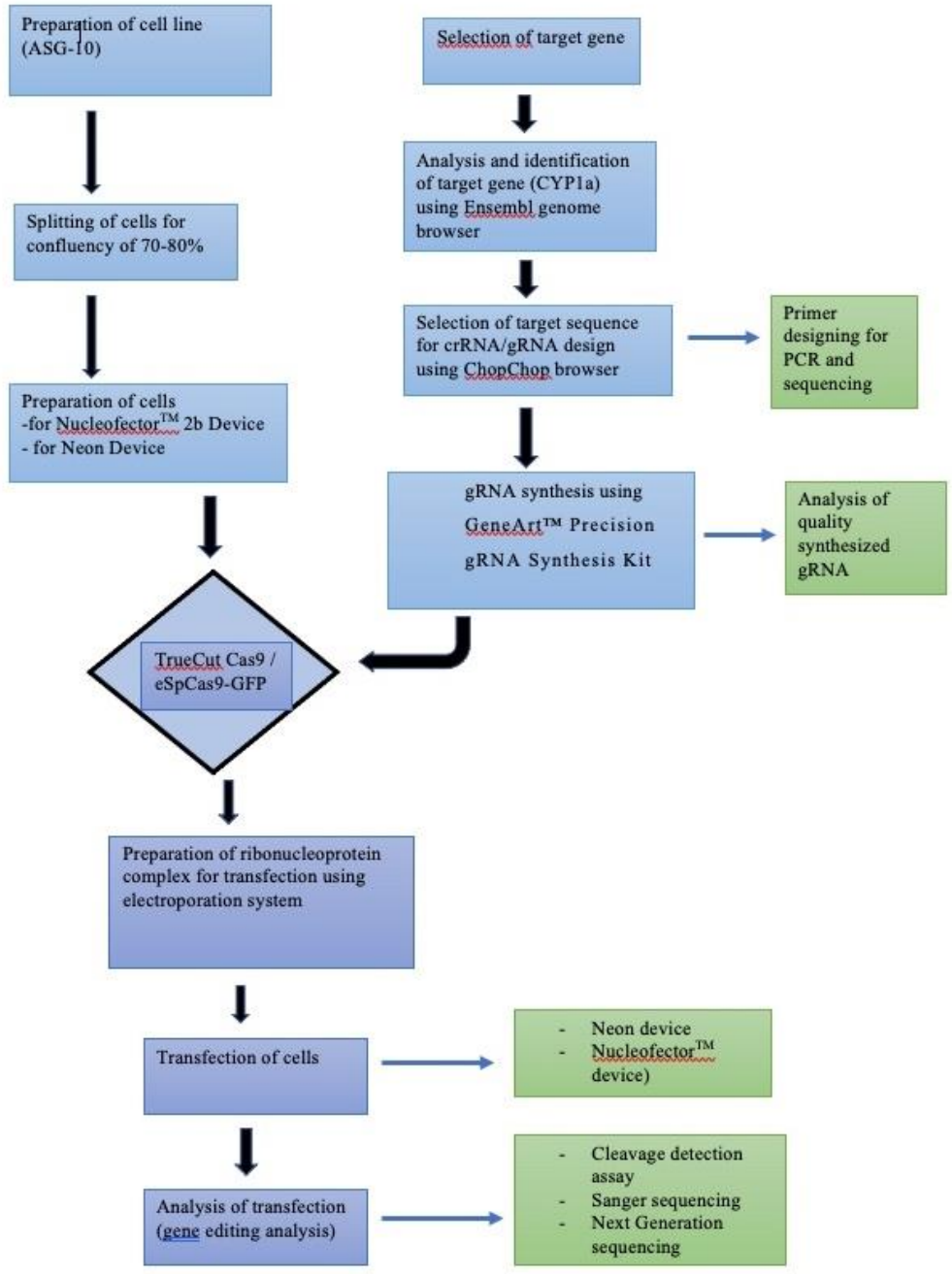

Figure 10. Flow diagram showing steps in CRISPR/Cas9 transfection.

4.3.1 Identification of target gene for gene editing

For this experiment, the Atlantic salmon Cyp1a gene was chosen as a target. The genome location and number of homologous of this gene were identified using the Ensembl genome browser (https://www.ensembl.org/index.html) (Howe et al., 2021). The Cyp1a gene was searched against the Atlantic Salmon genome. Results from this search were used to identify the gene sequences and exons. Gene sequences from different chromosomes were downloaded in Fasta format. These sequences were aligned using Mega7 Software (Kumar et al., 2016) using algorithm muscle for sequence alignment.

4.3.2 Target sequence selection for gRNA design

The ChopChop online browser (https://chopchop.cbu.uib.no/) (Labun et al., 2019) was used for gRNA identification on the target gene, as this software gives the best gRNAs that fulfill the requirements (consider minimizing off-target effects), and selected gRNA sequences were downloaded. The downloaded gRNA sequences were given as input in Mega7 to find their location in all homologous gene sequences by sequence alignment. This was crucial to find out where the gRNA can induce the editing. This was also important for us to be able to design a primer to detect the editing result using cleavage assay and sequencing.

4.3.3 Primer Design for PCR and sequencing

For primer design, the Geneious software 8.0 (Geneious, 2014) was used, and this software uses the Primer3 program for the Tm calculation of primers. Gene sequences in Fasta format were imported into the software, primer designing parameters were set and the program identified forward, and reverse primers based on the criteria provided.

4.3.4 gRNA synthesis using *In Vitro* Transcription (IVT) kit

The GeneArt™ Precision gRNA Synthesis Kit was used following product mannual (invitrogen, 2016) for the whole process of oligos design, gRNA synthesis, and purification of gRNA.

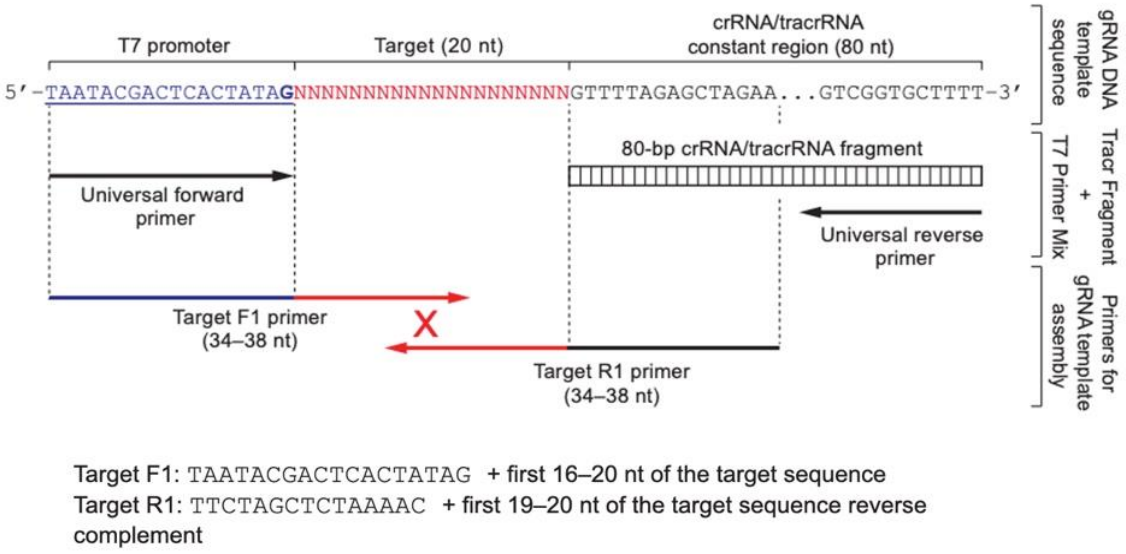

Figure 11. Figure showing the principle and different components of in-vitro transcription kit for the synthesis of DNA oligos (invitrogen, 2016).

The target sequences were selected as above in section 4.3.2, and the same sequences were used to design forward and reverse sequences with the T7 promoter region in the forward sequence and tracrRNA homology in the reverse sequence to synthesize DNA oligos (Fig.12). The synthesized DNA oligos was used for *in vitro* transcription that gave gRNA. A Qubit device was used for RNA quantitation, according to Qubit™ RNA BR Assay Kit.

4.3.5 Selection of positive control Slc45a2 gene

The Slc45a2 gene was selected as a positive control for the gene-editing experiment, taken from the published work from the paper "Efficient genome editing in multiple salmonid cell lines using ribonucleoprotein complexes" (Gratacap et al., 2020). The target sequence for gRNA synthesis and primers for PCR and sequencing were based on the same paper. Then the above-mentioned method in section 3.2.6.4 was used for IVT synthesis of gRNA for Slc45a2. The Slc45a2 gene is present on chromosome 1 (ssa1).

4.3.6 Protocol for ribonucleoprotein (RNP) complex transfection

1. 12 well plate for and 24 well cell culture plate was prepared, with fresh growth media for prewarm up.
2. Cell culture flasks with 70-80% confluent cells were used.
3. Old-growth media was removed by pipetting gently.
4. Cells were washed with 10 ml PBS (Ca^{2+} / Mg^{2+} free) to remove serum.

5. 3 ml trypLE (Thermo Fisher) was added for trypsinization of cells
6. The growth flask was incubated at room temperature, approx. two to minutes.
7. The cells were harvested in a seven ml growth medium with 10% FCS serum.
8. Cells were counted using a TC20™ automated cell counter. Then $2*10^6$ cells were pelleted in 1.5ml tube for Nucleofector™ 2b Device transfections, and 5*10ˆ5 cells were pelleted in 1.5ml tubes for the Neon™ transfection system.
9. The pelleted cells were resuspended using 93µl RT Nucleofector® Solution V and supplement solution (in 4.5:1 ratio) for Nucleofector™ 2b Device and Neon™ transfection system cells were resuspended using 10 µl Opti-MEM™ I Reduced Serum Medium.
10. Preparation of gRNA Cas9 Complex for Nucleofector™ 2b Device
    i. TrueCut™ Cas9 and eSpCas9-GFP were prepared with a concentration of 5 µm from the stock.
    ii. gRNAs produced by IVT synthesis were prepared at concentrations of 15 µm
    iii. The ratio of the concentration of Cas9 to sgRNA was 10:30 µm so, the ratio was 1:3.
    iv. The total volume of the complex was adjusted to 4 µl. The complex mix was incubated at room temperature for 5 mins.
    v. The complex was transferred to a tube with cells and mixed gently.
    vi. The total 100 µl of the solution was transferred to a cuvette for electroporation.
    vii. The best program for the GFP-Cas9 from an earlier experiment was used to transfect the cells.
    viii. The cells after transfection were added with 500 µl fresh media and then transferred to the culture plate with prewarmed growth media.

11. **Preparation of gRNA Cas9 Complex for Neon™ transfection system**
    i. The TrueCut™ Cas9 was prepared with 6.1 µm concentration from the stock.
    ii. gRNAs from IVT synthesis were prepared to the concentration of 18.3 µm.
    iii. The ratio of the concentration of Cas9 to sgRNA was 6.1: 18.3 µm so, the ratio was 1:3.
    iv. The total volume of the gRNA complex was adjusted to 2 µl. The complex mix was incubated at room temperature for five minutes.
    v. The complex was transferred to the tube with cells and mixed gently.
    vi. The 10 µl pipet tips were used to pipet out the cells and the gRNA Cas9 complex for transfection, using specific programs in the Neon device.
    vii. After transfection, the cells were transferred to the prewarmed media in 24 well cell culture plates
    viii. After 24-hours, old media was aspirated and new media with antibiotics was added
    ix. Media was changed after four days, and cells were grown until they reached confluence

12. At confluence, the cells were split and scaled up to 6 well plates. When the cells reached high enough numbers, some were used for genomic DNA extraction, and some were allowed to grow continuously.
13. The PureLink™ Genomic DNA Mini Kit was used for genomic DNA extraction of $1*10^6$ cells following the user manual from the kit and concentration of DNA was measured using NanoDrop™ 2000/2000c.
14. For the dirty extraction of genomic DNA reagents from GeneArt™ a Genomic Cleavage Detection Kit was used.

4.4 Analysis of gene edits after CRISPR/Cas9 transfection

4.4.1 Cleavage detection assay

The principle behind this assay is that when the PCR amplified DNA is denatured and allowed to be reannealed, any mismatches in a heteroduplex will create a bulge of nucleotides, and this will be typical at the point of edit where endonuclease enzymes acts (Sentmanat et al., 2018). Then incubating with an endonuclease that is particularly directed against mismatches, the DNA sequence will be cut at the point where the bulge is created. GeneArt™ Genomic Cleavage Detection Kit from Invitrogen™ (Life Technologies Corporation, 2014) and Alt-R® Genome Editing Detection Kit from Integrated DNA Technologies (Integrated DNA Technologies, 2021), Inc were used for such detections, by following the user manual

Protocol:

1. Two different kits were used: GeneArt™ Genomic Cleavage Detection (GCD) Kit from Invitrogen™ and Alt-R® Genome Editing Detection Kit from Integrated DNA Technologies, Inc. These kits were used sepratley for seprate samples.
2. For GCD cleavage assay, the genomic DNA was first extracted using the PureLink™ Genomic DNA Mini Kit which gave high-quality purified DNA. This product was used in cleavage assay using GeneArt™ Genomic Cleavage Detection Kit. For the cleavage assay using the Alt-R® Genome Editing DetectKit kit, the genomic DNA was extracted using a dirty extraction method where Extraction reagents from GeneArt™ Genomic Cleavage Detection Kit were used.
3. The PCR protocol and ampliTaq Gold 360 PCR Master Mix from the GeneArt™ Genomic Cleavage Detection Kit was used for PCR amplification of the sample DNA.
4. The 8 µl PCR product was added with 1µl buffer and ran with the manufacturer protocol (program for thermocycler). The programs were different for different kits and manufacturers (Integrated DNA Technologies, 2021; Life Technologies Corporation, 2014) .

5. Then the 1 µl cleavage enzyme was added and incubated for 1 hour. This step was the same for both kits.
6. After incubation, the samples were analyzed using the 2100 Bioanalyzer system.

4.4.2 Gel electrophoresis

Gel electrophoresis is a standard separation method in the laboratory that is used to separate DNA, RNA, or proteins based on their molecular size or base-pair length (bp). This method is based on the principle of charged base separation, so negatively charged DNA molecules move towards the positive pole through an agarose gel in an electric field. To observe molecules on the gel, a gel dye like (gel red or ethidium bromide is used, which acts as intercalating agents with DNA.

Gel electrophoresis of DNA

1. One percent agarose gel was prepared on 1x Tris Borate EDTA (TBE) solution.
2. The GelRed® 10,000X stock reagent was added into the molten agarose gel solution at the ratio of 1:10,000 and mix thoroughly.
3. 12 µl of the sample was used to mix with 2 µl gel loading buffer (1the /6 of the gel)
4. The gel was run using Voltage ranging from 90 V to 105 V based on the size of gel.
5. Then gel was analyzed using the ChemiDoc XRS+ System and Image Lab™ software from Bio-Rad.

Gel electrophoresis of gRNA

1. One percent agarose gel was prepared on 1x TBE solution.
2. The GelRed® 10,000X stock reagent was added into the molten agarose gel solution at the ratio of 1:10,000 and mixed thoroughly.
3. 7.5 µl of the sample was used to mix with 7.5ul RNA loading buffer
4. Before loading the mixture, it was heated at 70 degrees for 10 mins.
5. The gel was run using Voltage ranging from 100 V based on the size of gel.
6. Then gel was analyzed using the ChemiDoc XRS+ System and Image Lab™ software from Bio-Rad.

For analysis of samples with low concentrations, the 2100 Bioanalyzer system with software 2100 Expert was used. 2100 Bioanalyzer software was run using Bioanalyzer DNA Kits & Reagents following the system manual (Agilent Technologies, 2016). Samples from cleavage assay of CYP1a PCR product were analyzed using the Agilent4200 TapeStation system with D1000 screen tapes, D1000 reagents, and D1000 ladder.

4.4.3 PCR Clonning

i. PCR amplified products were ligated with pGEM®-T Vector System. The transformations were done using the ligated vector and E. coli competent cells. The protocols form Promega manual was followed for ligation and transformation (Promega corporation, 2018). 150 µl of SOC media with transformed cells were spreaded on selective media plate (LB agar + ampicillin 100 µg/ml, 0.5mM IPTG and X-Gal 80µg/ml) and the plates were incubated overnight at 37 ºC.

ii. After 24 hours the blue-white selection was done, and 10 white colonies were grown on three ml LB agar broth with ampicillin 100 µg/ml, for 24 hours in 37ºC in shaking incubator (200 rpm).

iii. The plasmid recovered from the growth media was purified using GeneJET Plasmid Miniprep Kit from Thermo Scientific™.

iv. To verify that the correct sized band was cloned into pGEM®-T Vector System or not, restriction enzyme digestion of purified products was done using restriction enzyme Xmnl from New England Bio Lab (NEB) using NEB cutsmart buffer. The protocol for restriction digestion was obtained from Product manual and additional it was checked using NEBcloner for restriction digestion (http://nebcloner.neb.com/#!/redigest).

v. The restirction digested product was ran on regular agarose gel.

Protocol

i. 1% agarose gel was prepared on 1x Tris Borate EDTA (TBE) solution.

ii. The GelRed® 10,000X stock reagent was added into the molten agarose gel solution at the ratio of 1:10,000 and mix thoroughly.

iii. 12 µl of the sample was used to mix with 2 µl gel loading buffer (1the /6 of the gel)

iv. The gel was run using Voltage ranging from 90V to 105 V based on the size of gel.

v. Then gel was analyzed using the ChemiDoc XRS+ System and Image Lab™ software from Bio-Rad.

4.4.4 Sanger sequencing

1. PCR amplicons were prepared for us direct Sanger sequencing. The PCR samples were diluted to make the concentration of 10 ng and sent for sequencing.
2. After confirming the success of ligation, purified plasmid with sample concentration of 20 ng was sent for Sanger sequencing.
3. The result from sanger sequencing was anlayzed using Geneious 8.0 software.

5 Results

5.1 Transfection of ASG-10 cells with pmaxGFP™ plasmid using the Neon™ transfection system

The ASG -10 cells were transfected using three different programs (AP1:1400-20-2, AP2:1200-40-1 and, AP3:1200-30-2) which had different parameters like voltage, width, and pulses. Different programs have different transfection efficiency and viability. The test programs were designed randomly following the recommendation for transfection on epithelial cells of different species (Gratacap et al., 2020; Scientific, 2021). Cells were transfected with pmaxGFP™ Plasmid. The cells after transfection were observed and images were captured with an Inverted laboratory fluorescence microscope Leica DM IL LED and digital camera associated with the microscope.

5.1.1 Transfection of fully confluent ASG-10 cells

The experiment was performed based on assumptions, as the ASG-10 cell line is fragile and sensitive so, to get healthy cells, they must be grown for 10 to 14 days. Total $1*10^5$ cells were transfected with GFP tagged plasmid. The transfected cells were observed in the fluorescence microscope after 72 hours of transfection, and green fluorescence were seen (Fig.12) The density of green fluorescence cells was different for a different program. Compare to the two programs (AP1 and AP3), AP2 program had fewer green fluorescence cells.

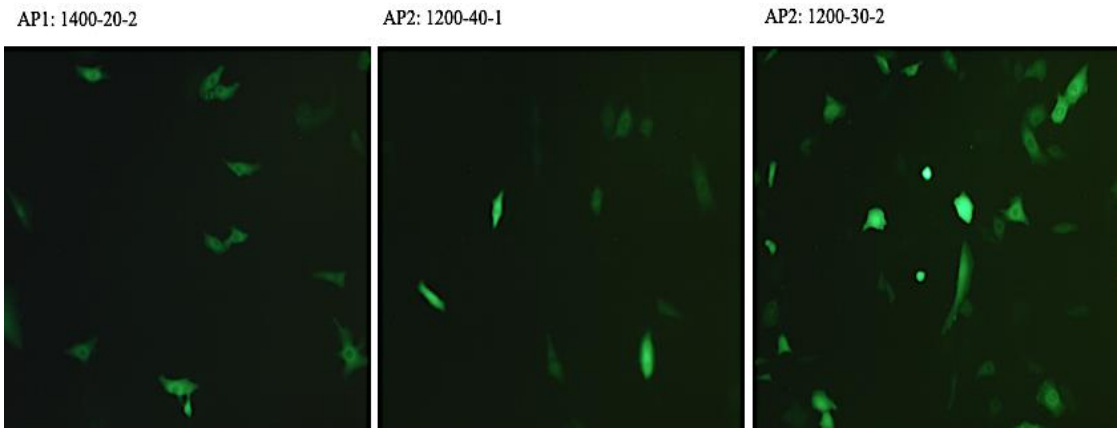

Figure 12. Fluorescence microscopy image of ASG-10 cells after 72 hours of transfection. This figure shows green fluorescence image for $1*10^5$ cells transfected with pmaxGFP™ plasmid by program AP1:1400-20-2, AP2:1200-40-1, and AP3:1200-30-2 in Neon device.

The cells were analyzed by flow cytometry to find the transfection efficiency and viability of each program after observing on a fluorescence microscope (Table. 9). From the flow cytometric analysis, images were captured (Fig.14). The viability of cells was found around 98% for all three programs but transfection efficiency was lower.

Table 9. Flow cytometry analysis results for fully confluent cells.

Program	Transfection efficiency %	Viability %
Control	0	100-0.7 = 99.3
AP1:1400-20-2	45.9	100 – (2.7-0.7) = 98
AP2:1200-40-1	31.4	100- (2.5-0.7) =98.2
AP3:1200-30-2	41.9	100- (3.1-0.7) =97.6

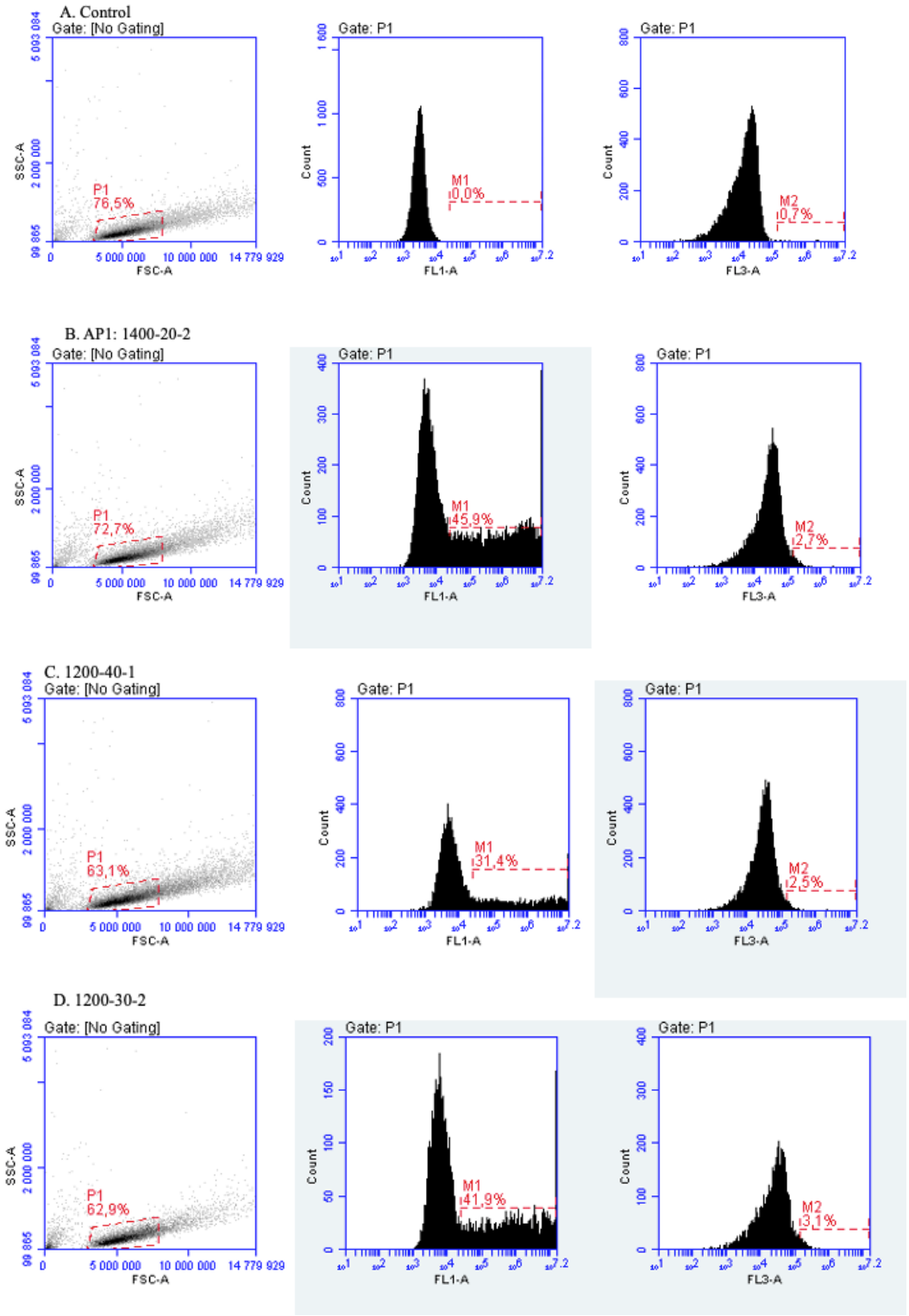

Figure 13. Pictures from flowcytometry analysis of transfection of fully confluent ASG-10 cells. Pictures from flowcytometry analysis of Transfection of fully confluent $1*10^5$ ASG-10 cells. There are three images for each sample first image is sample gating, second is FL1 image for transfection efficiency and third is FL3 image for viability. These images in rows are for A. control cells (not transfected), B. cells transfected with program AP1:1400-20-2, C. cells transfected with program AP2:1200-40-1 and D. cells transfected with program AP3:1200-30-2 Neon™ device.

5.1.2 Transfection of ASG-10 cells at 70% -80% confluency

After observing lower transfection efficiency from the first experiment, the next approach was to attempt to increase the transfection efficiency with less confluent cells. Confluency is considered one of the important characteristics for better transfection efficiency based on the transfection protocols provided by transfection systems and kits (Promega Corporation, 2021; ThermoFisher Scientific, 2021). The second experiment used 70%-80% confluent $1*10^5$ cells extracted after splitting two days. Programs (AP1, AP2, and AP3) designed in the first experiment were used. The fluorescence microscopy results showed higher green fluorescence cells in program AP1 and AP3 compared to program AP2 (Fig.14).

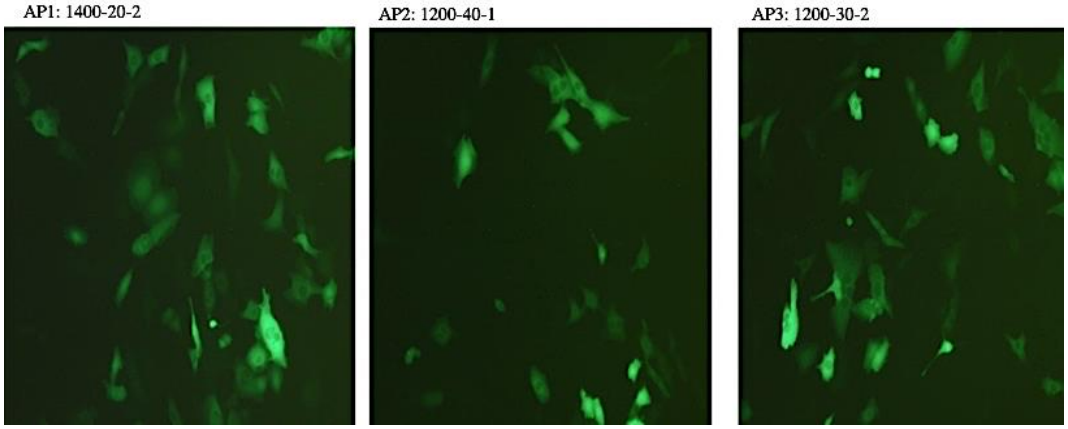

14. Fluorescence microscopy image of 70-80 % confluent $1*10^5$ ASG-10 cells after 72 hours of transfection. This figure shows green fluorescence image for ASG-10 cells transfected with pmaxGFP™ plasmid by program AP1:1400-20-2, AP2:1200-40-1, and AP3:1200-30-2 in the Neon™ device.

This experiment showed increased transfection efficiency but decreased in viability compared to the first experiment from flow cytometry analysis (Table 10). The images for specific programs were also captured (Fig.16). The highest transfection efficiency 68.2% was obtained from program AP1.

Table 10.Flow cytometry results for 70% -80% confluent transfected cells.

Program	Transfection efficiency %	Viability
Control	0	100-1= 99%
AP1:1400-20-2	68.2	100-(5.7-1) = 93.3
AP2:1200-40-1	50.2	100- (4.6-1) = 96.4
AP3:1200-30-2	67.2	100- (8-1) = 93

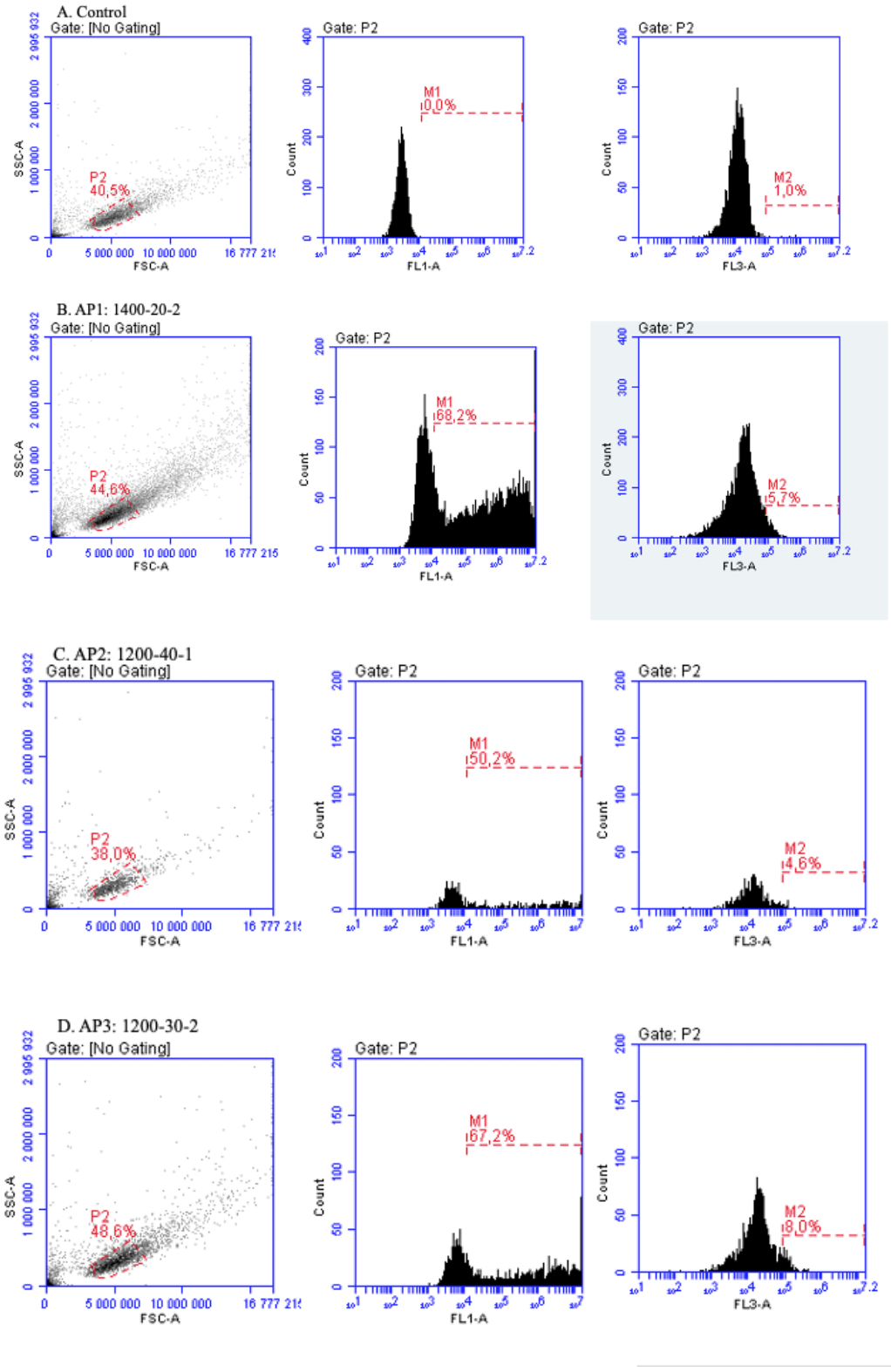

Figure 15. Pictures from flow cytometry analysis of transfection of 70-80% confluent ASG-10 cells. There are three images in the row for each sample first image is sample gating, second is image (FL1 detector) for transfection efficiency and third image (FL3 detector) for viability. These images in rows are A. control, B. cells transfected with program AP1:1400-20-2, C. cells transfected with program AP2:1200-40-1and, D. cells transfected with program AP3:1200-30-2 in the Neon™ device.

5.1.3 Transfection of cells at 70% -80% confluency with $5*10^5$ cells

From the second experiment, it came to know using 70-80% confluent cells increases transfection efficiency with good viability. Then again to improve transfection efficiency higher cell amounts were used. The cell amount was increased five times ($5*10^5$ cells) compared to previous experiments. The cells after transfection were observed using fluorescence microscopy which showed higher GFP positive cells in AP1 and AP3 compared to AP2 (Fig. 16).

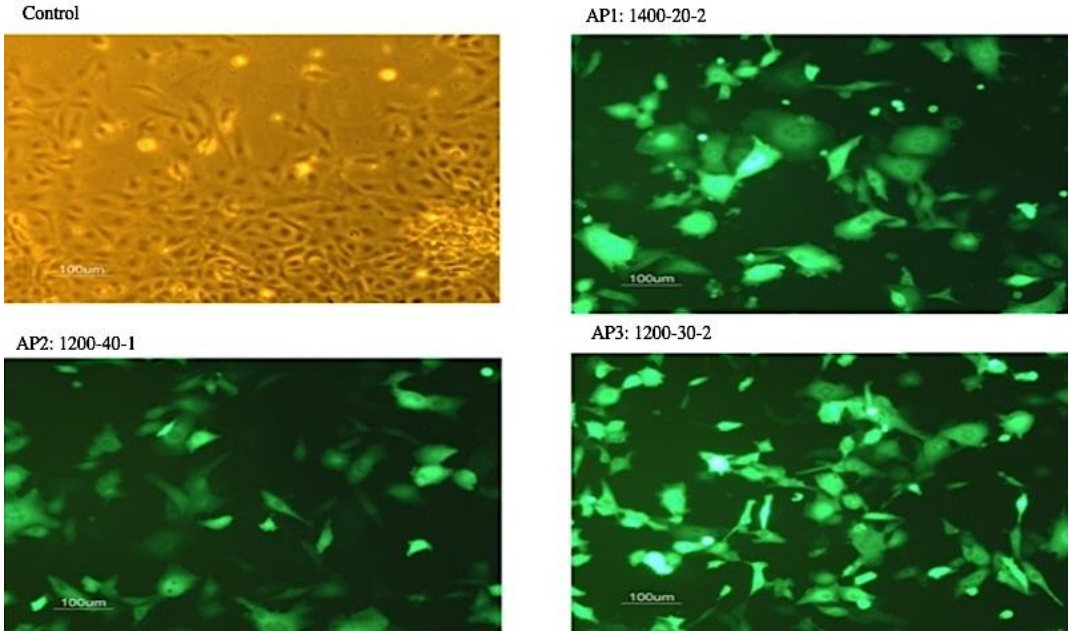

Figure 16. Fluorescence microscopy images of 70-80% confluent $5*10^5$ cells. The figure shows ASG-10 cells transfected with pmaxGFP™ plasmid by programs AP1:1400-20-2, AP2:1200-40-1, and AP3:1200-30-2 in the Neon device. The fist image is for control, which is GFP negative, so image was captured in light microscope.

The total count of cells was done just after transfecting the cells to see the number of live cells. This helps to know what percent of cells are lost during transfection. The result showed program three (AP3) was more efficient with the high number of cell survival after transfection using TC20™ automated cell counter from Bio-Rad (Table 11).

Table 11. Result of transfection anlaysis using TC20™ BioRad automated cell counter.

Program	Total cells	Live cells	Viability %	Total live cells compared to control %
AP1:1400-20-3	9.59×10^4	7.57×10^4	79	12.74
AP2:1200-40-1	1.46×10^5	1.16×10^5	79	19.5
AP3: 1200-30-2	2.62×10^5	2.02×10^5	77	34
Control	6×10^5	5.94×10^5	99	99

Flow cytometry analysis was done after 72 hours of transfection to observe the transfection efficiency and viability of the cells. In this experiment, the transfection efficiency was increased highly (Table 12). Program one (AP1) and program three (AP3) achieved around 91 % transfection. Program three (AP3) has higher viability around 89%. So, the AP3 was an effective program for transfection of ASG-10 using the Neon™ transfection system. The images for specific program from flowcytometry was also captured for analsysis (Fig. 17).

Table 12. Result from flowcytometric analysis of transfected 70% -80% confluent cells with five times more cell count number cells after 72 hours

Program	Percentage gated %	Transfection efficiency %	Viability %
Control	39.8	0	100-0.2= 99.8
AP1:1400-20-3	31.2	91.8	100-(15-0.2) = 85.2
AP2:1200-40-1	44.4	84.3	100-(10.6-0.2) = 89.6
AP3: 1200-30-2	34.4	91.5	100-(10.8-0.2) = 89.4

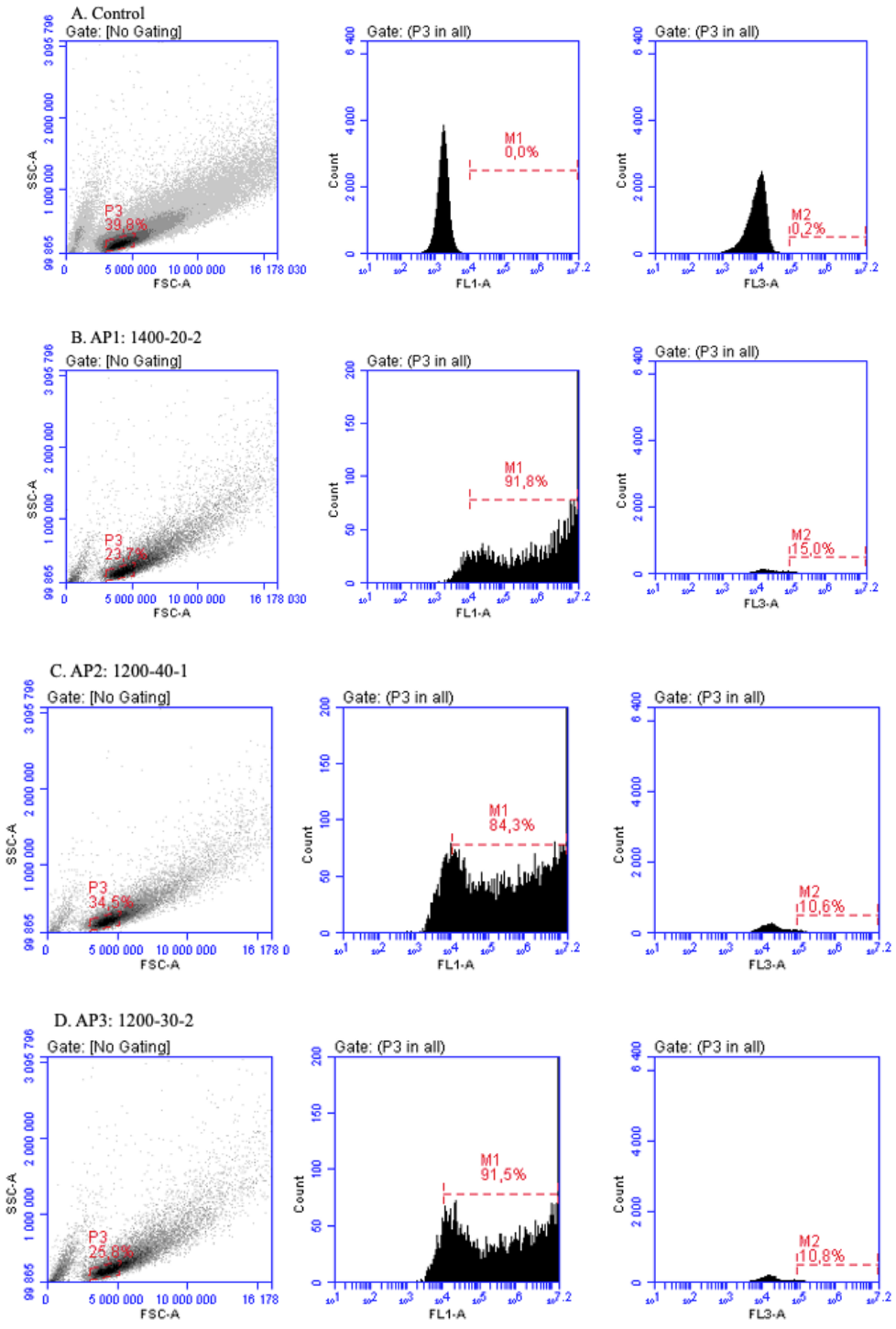

Figure 17. Pictures from flow cytometry analysis of transfection of 70-80% confluent $5*10^5$. ASG-10 cells. There are three images in the row for each sample first image is sample gating, second image is (FL1 detector) for transfection efficiency and third image is (FL3 detector) for viability. These images in rows are a. control, b. AP1:1400-20-2, c. AP2:1200-40-1and d.AP3:1200-30-2 in the Neon™ device.

5.1.4 Replicate experiment of transfection of cells at 70% -80% confluency with $5*10^5$ cells

This was the replicate experiment for the transfection like in section 5.1.3. The flow cytometry result from this experiment was comparable with the previous experiment (Table 12) with the same condition but in this experiment, there was an error during the preparation of cells for transfection with program three (AP3: 1200-30-2). In AP3 transfection cells were diluted more due to remaining PBS and the volume was more than 10 µl so there was a decrease in transfection efficiency (Table 13).

Table 13. Result from flowcytometric analysis of transfected 70% -80% confluent cells with $5*10^5$ cells after 72 hours for replicate experiment.

Program	Percentage gated %	Transfection efficiency %	Cell viability %	Remarks
Control	39.8	0	100-0.2= 99.8	
AP1= 1400-20-3	35.17	93.4	84.2	
AP2= 1200-40-1	40.37	80.4	92.5	
AP3= 1200-30-2	26.46	71.9	92.6	remaining of PBS giving dilution effect

5.2 Transfection of CHSE 214 cells

5.2.1 Transfection of 70-80% confluent CHSE 214 cells using Neon™ transfection system

Three different programs (CNP1= 1400-30-1, CNP2= 1600-10-3, and CNP3= 1700-20-1) Program CNP2= 1600-10-3 was chosen from the reference paper (Gratacap et al., 2020). Other programs CNP1= 1400-30-1, and CNP3= 1700-20-1 were designed randomly to test new programs too. 70-80% confluent $1*10^5$ cells were transfected. This setup was designed to check the effectiveness of the transfection protocol. The cells after transfection were observed and images were captured with an Inverted laboratory flurosence microscope Leica DM IL LED and digital camera associated with the microscope.

Observation of cells after transfection with plasmid under fluorescence microscope showed green fluorescence cells (Fig.18). Programs two (CNP2) and three (CNP3) were observed with more GFP cells compared to program one (CNP1).

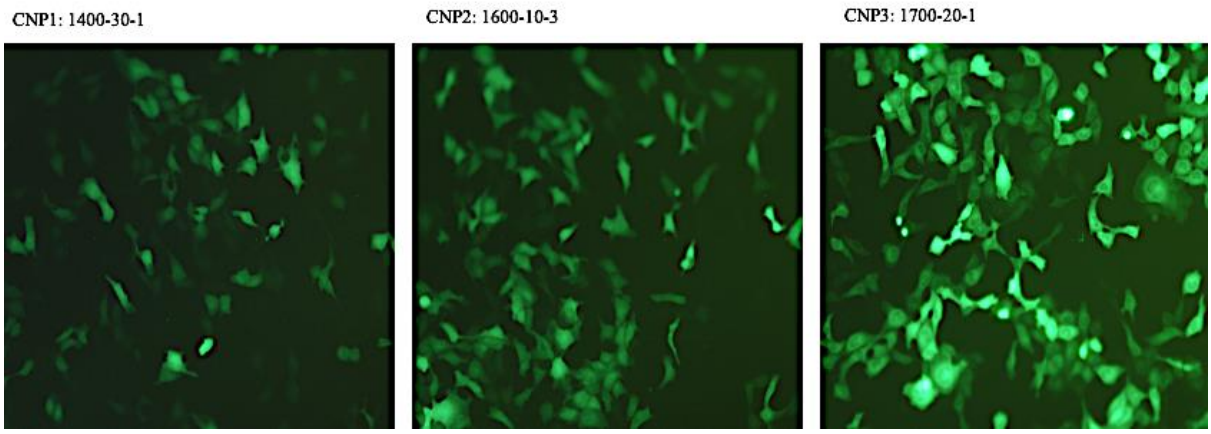

Figure 18. Flurosence microscopy image of transfection of 70-80% confluent CHSE 214 cells using Neon system. The green flourosence images are from cells transfected with programs CNP1: 1400-30-1, CNP2: 1600-10-3 and CNP3: 1700-20-1.

Flowcytometry analysis was done after 72 hours of transfection to observe the transfection efficiency. Programs CNP2 and CNP3 gave higher transfection efficiency around 97% compared to program CNP1 with 82.4 % (Table 14). The images from flowcytometry for specific programs were also captured (Fig.20).

Table 14. Results from flow cytometric analsyis of transfected CHSE 214 cells after 72 hours.

Programs	Transfection efficiency %
CNP1= 1400-30-1	82.4
CNP2= 1600-10-3	97.6
CNP3= 1700-20-1	97.3
Control	0

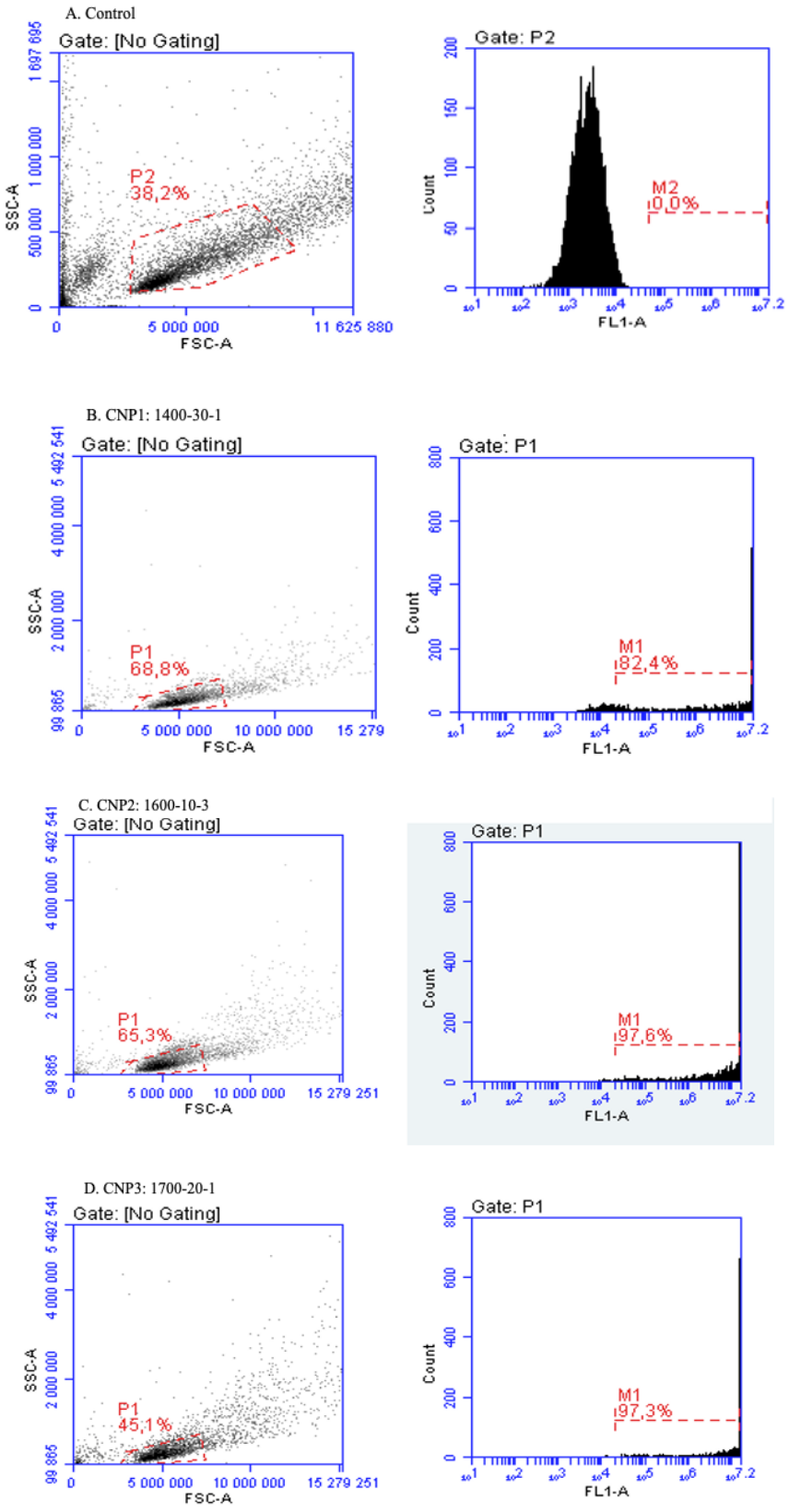

Figure 19. Pictures from flowcytometry analysis of transfection of 70-80% confluent CHSE 214 cells with 1*10^5 cell count. There are two images in the row for each sample first image is sample gating, second is image (FL1 detector) for transfection efficiency. These images in rows are a. Control b. CNP1: 1400-30-1, c. CNP2: 1600-10-3 and d. CNP3: 1700-20-1.

5.2.2 pmaxGFP™ Plasmid transfection using of CHSE 214 cells using Nucleofeter™ system.

One million 70-80 % confluent CHSE 214 cells were transfected with two programs Y-001 and T-20. These programs were selected from papers which had used these programs in transfection of fish cells (Markussen et al., 2013). After 72 hours of transfection, the cells were analyzed using a fluorescence microscope where green fluorescence positive cells were observed (Fig.20). In both programs, cells were comparatively equally green fluorescence positive.

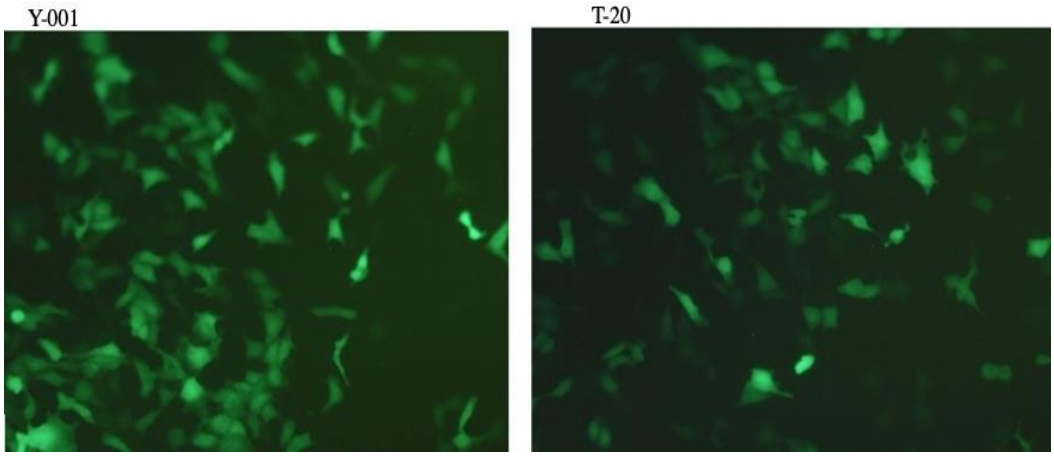

Figure 20. Flurosence microscopy image of transfection of 70-80% confluent 1*10^6 CHSE 214 cells using Nucleofector™ 2b Device. First image is for cells tranfected with the program Y-001 and second image is for the program T-20.

The transfected cells from two programs were analysed using flowcytometer (Fig.22). Transfection program Y-001 gave higher transfection efficiency 51% compared to T-20 with 47.8% (Table 15).

Table 15. Results from flowcytometry analsysis of Nucleofector™ 2b Device transfected cells after 72 hours.

Program	Transfection efficiency
Control	0
Y-001	51
T-20	47.8

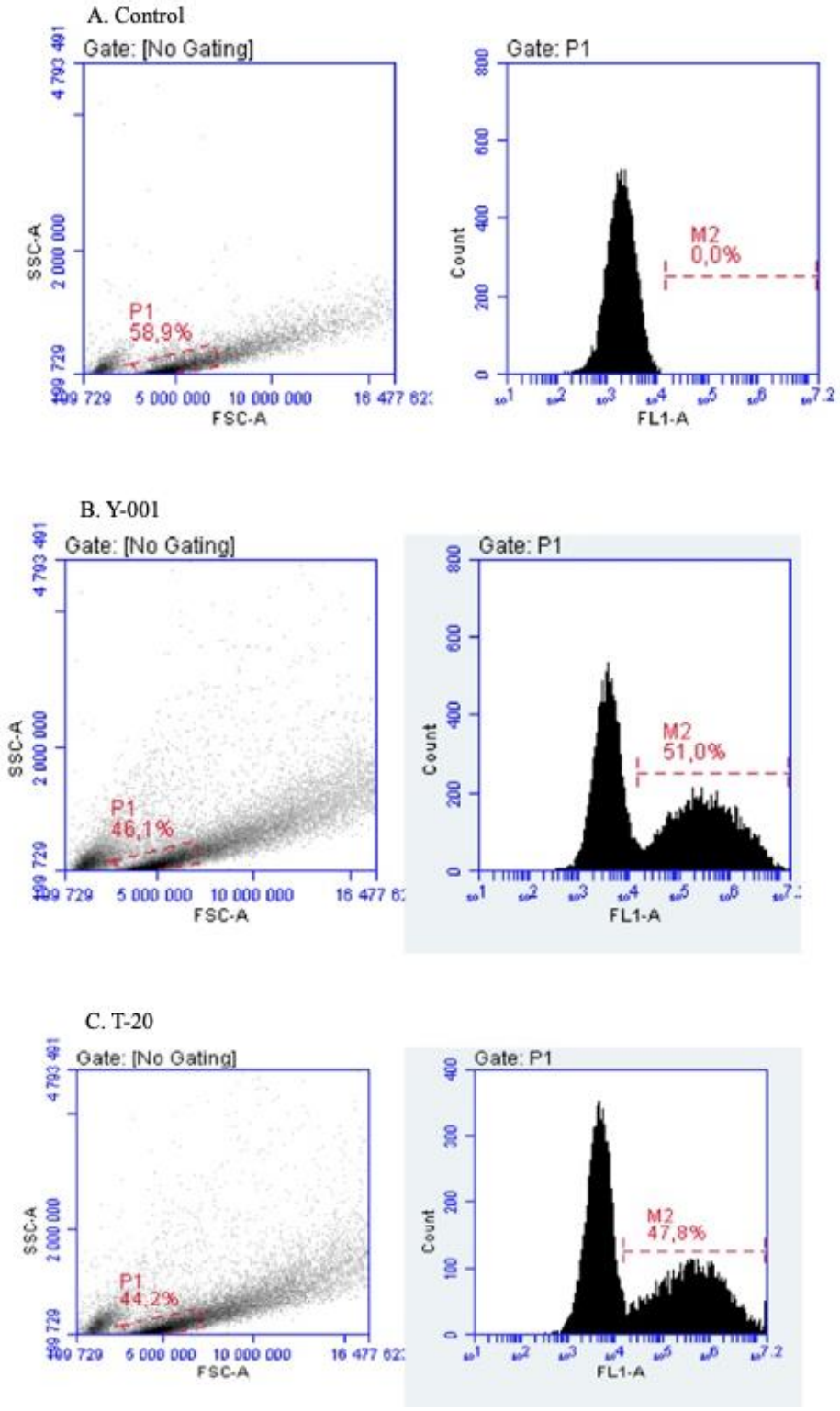

Figure 21. Pictures from flowcytometry analysis of transfection of 70-80% confluent CHSE 214 cells with one million cells transfected by NucleofectorTM 2b Device. There are 3 images in the row for each sample first image is sample gating, second is image (FL1 detector) for transfection efficiency and third image (FL3 detector) for viability. These images in rows are A. control, B. program Y-001 and, C. program T-20.

5.3 Transfection of LG-1 cells

LG-1 is the new in-house cell line from lumpsucker which has huge potential for future research work. Various randoms programs were designed by guessing the characteristics of the cell as the characterization of the cell line was still in the process. Seven Programs LP1: 1000-40-1, LP2: 1200-40-1, LP3: 1300-30-1, LP4: 1400-20-2, LP5: 1500-20-1, LP6:1600-10-3, and LP7: 1700-20-1 were designed and entered in the Neon^{TM} transfection system for transfection of $1*10^5$ cells. The fully confluent cells were used in this experiment.

After 72 hours of transfection, the cells were observed, and images were captured with an Inverted laboratory flurosence microscope Leica DM IL LED and digital camera associated with the microscope. Cells transfected with all seven programs were observed and images were captured (Fig.22). It was difficult to see the cells in a light microscope because the cells were transparent in monolayer. All the programs were able to show green fluorescence cells but program three (LP3) showed a relatively higher number of GFP cells.

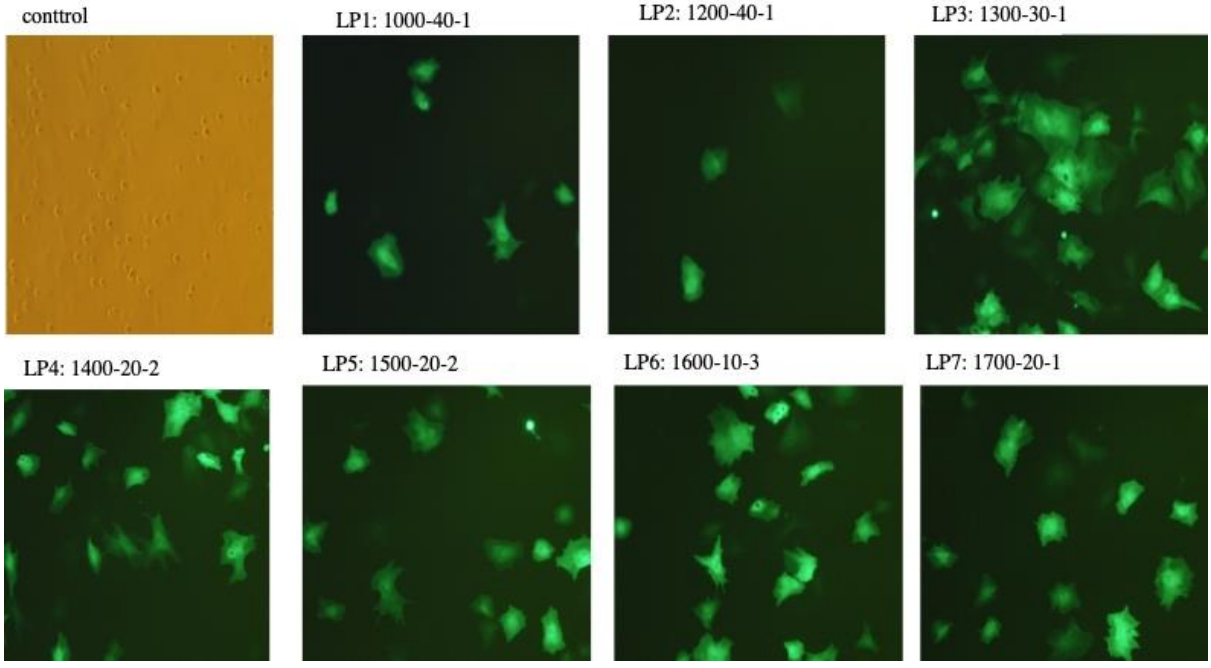

Figure 22. Flurosence microscopy images of LG-1 cells with transfected with different seven programs in Neon^{TM} transfection system. First image is of control observed with light microscope and other green flourosence images are from cells tranfeceted with programs LP1:1000-40-1, LP2:1200-40-1, LP3:1300-30-1, LP4:1400-20-2, LP5:1500-20-2, LP6:1600-10-3 and, LP7:1700-20-1.

The transfected cells were analysed using flow cytometry to find out the transfection efficiency of each program after 72 hours of transfection (Fig.24). Program LP3, LP4, and LP7 gave higher transfection efficiency (Table 16).

Table 16. Results from flow cytometry analsyis of transfected LG-1 cells after 72 hours.

Program	Transfection efficiency %
Control	0
LP1: 1000-40-1	26
LP2: 1200-40-1	17.3
LP3: 1300-30-1	58.1
LP4: 1400-20-2	55.2
LP5: 1500-20-1	41.5
LP6:1600-10-3	44.7
LP7: 1700-20-1	54.1

C. LP2= 1200-40-1

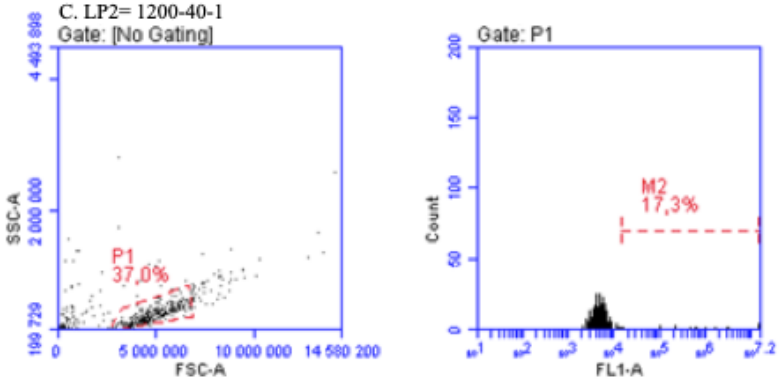

D. LP3= 1300-30-1

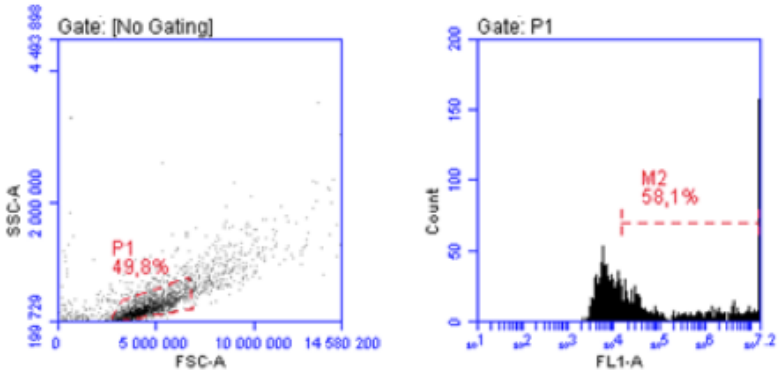

A. Control

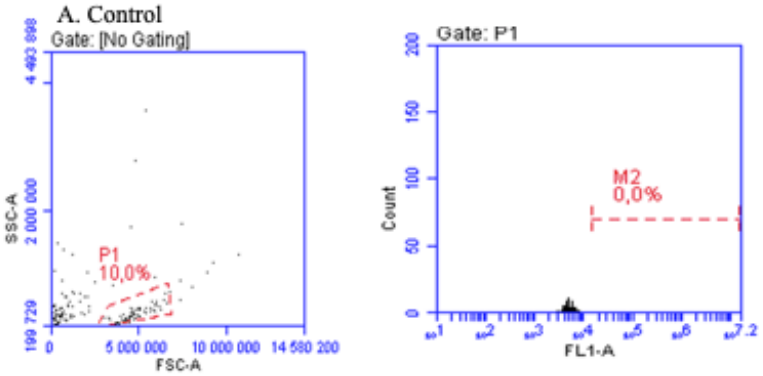

B. LP1: 1000-40-1

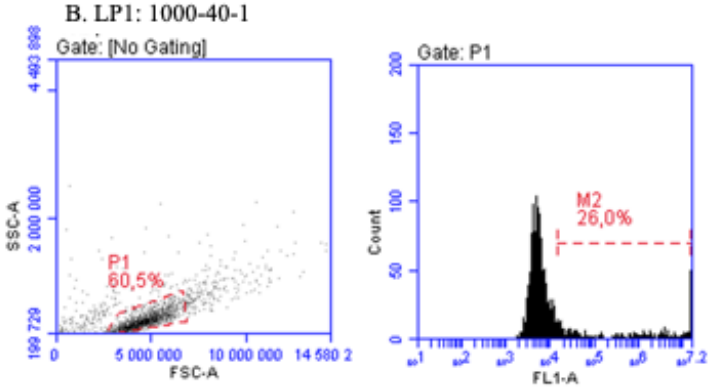

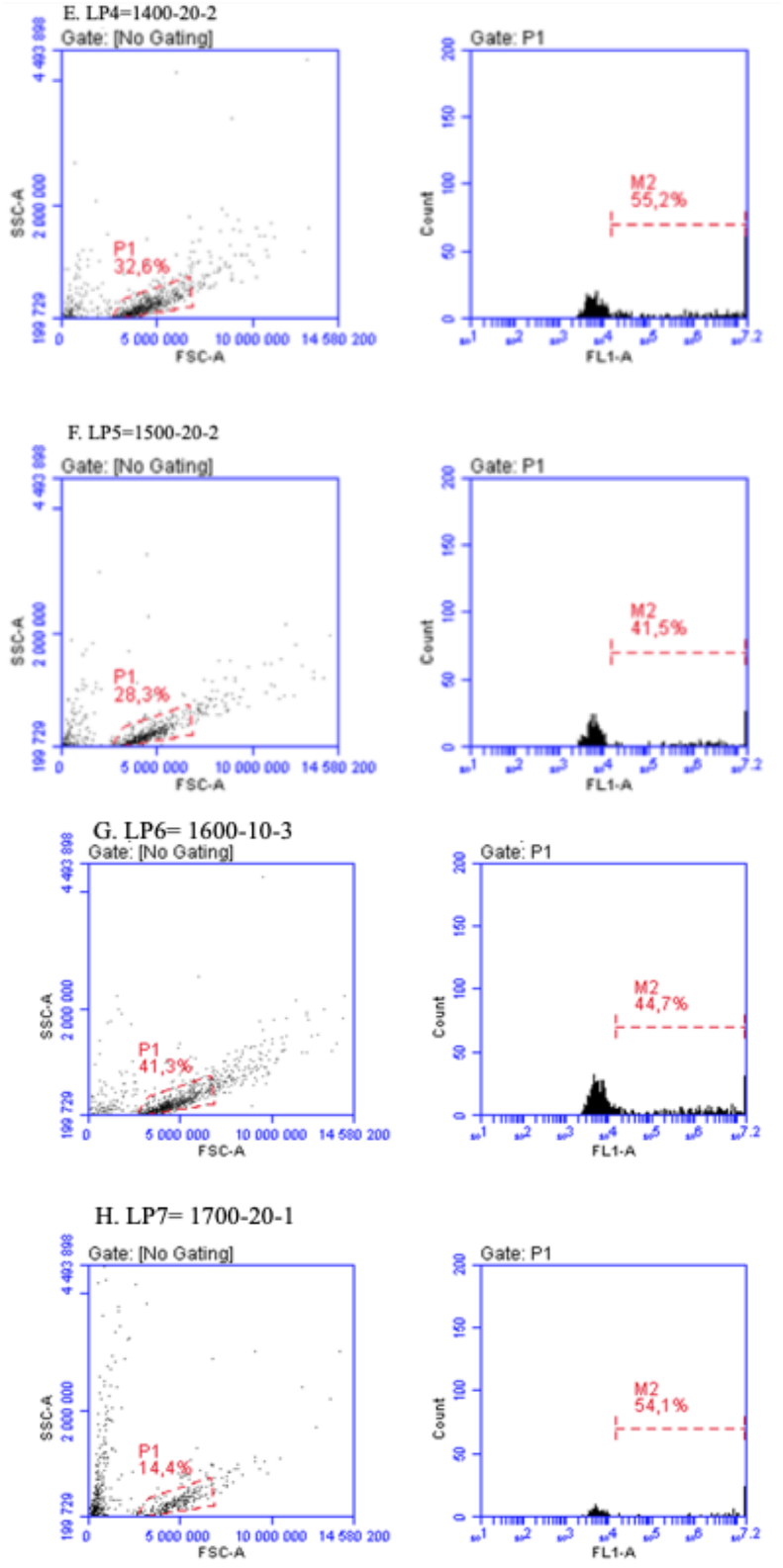

Figure 23. Images from flow cytometry analysis of transfected LG-1 cells with different seven programs in Neon device. Two images in row are for first images representing sample gating, second is image (FL1 detector) for transfection efficiency. Images A. control, B. LP1:1000-40-1, C. LP2:1200-40-1, D. LP3:1300-30-1, E. LP4:1400-20-2, F. LP5:1500-20-2, G. LP6:1600-10-3 and, H. LP7:1700-20-1.

5.4 eSpCas9-GFP protein transfection of cells by NucleofectorTM 2b Device

5.4.1 Transfection of ASG10 cells

This experiment was done to see how efficiently protein can be transfected and what kind of differences can be seen compared to plasmid transfection. One million ASG-10 cells were protein transfected with Nucleofector™ 2b Device. The programs choosen were the same programs that were used for plasmid transfection P1= U029 and P2= L029. After observing the transfected cells in flurosence microsocope, cells transfected with both programs showed green fluorescence (Fig.24).

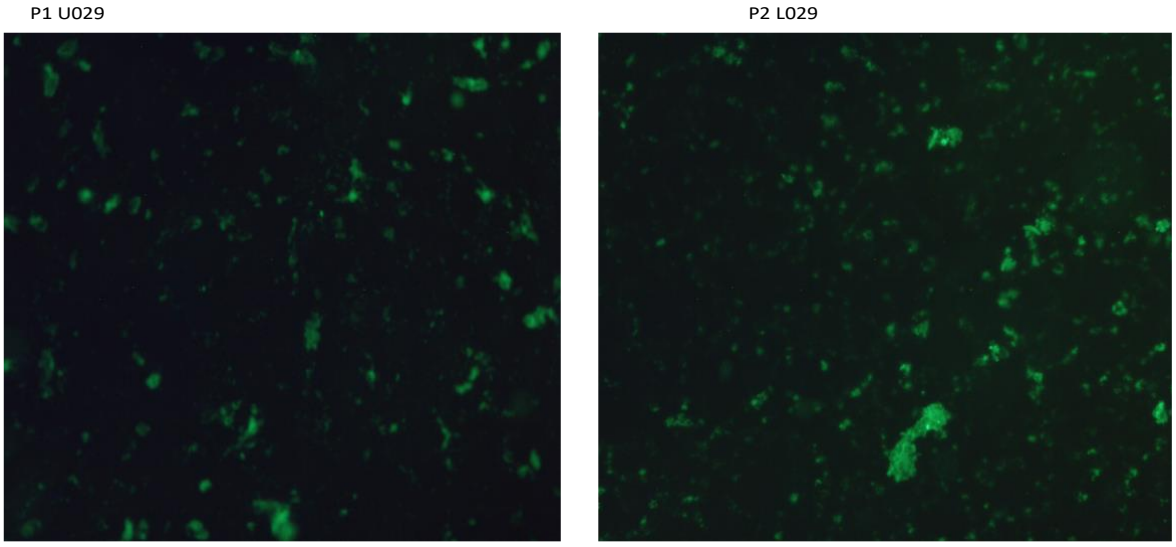

Figure 24. Fluorescence microscopy image for protein transfected ASG-10 cells with Nucleofector™ 2b Device. The first image is for P1 U029 transfected cells and second image is for L029 cells.

The images of specific program were taken from flow cytometric analysis of cells (Fig. 25). The flow cytometry analsysis of transfected cells after 72 hours showed higher transfection for program U029 compared to program L029 (Table 17).

Table 17. Results from flow cytometric analsysis of prtoein transfected cells after 72 hours.

Program	Transfection efficiency %	Viability %
Control	0	99.3
U-029	69	98.3
L-029	41.4	96.8

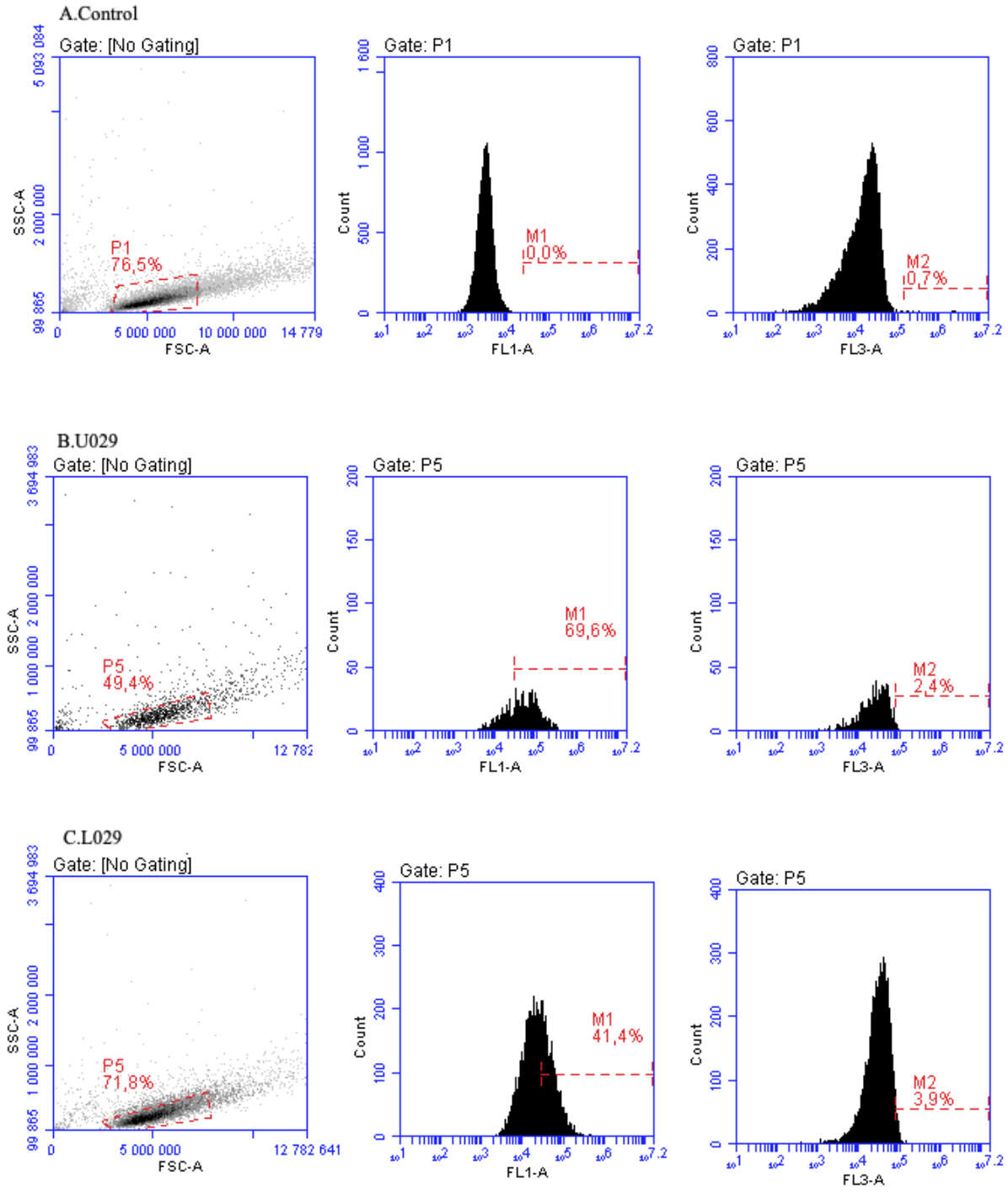

Figure 25. Image from flowcytometry analsysis of protein transfected ASG-10 cells with Nucleofector™ 2b Device. There are three images in the row for each sample first image is sample gating, second is image (FL1 detector) for transfection efficiency and third image (FL3 detector) for viability. Image A. Control B. cells transfected with program U029 and C. progam transfected with L029 cells.

5.4.2 Transfection of CHSE 214

Two million cells with 70-80% confluency was protein transfected using NucleofectorTM 2b Device. This experiment was performed to find the best program for protein transfection and to see the differences with programs that were used for plasmid transfection. The same two programs that were used for plasmid transfection were used for protein transfection Program Y-001 (CP1) and program T-20 (CP2).

After 72 hours of transfection, the cells were observed in a fluorescence microscope and images were captured (Fig. 26) Very few green fluorescences were observed in the cells transfected with Program Y-001 and a higher level of fluorescence was observed in the cells transfected with Program T-20.

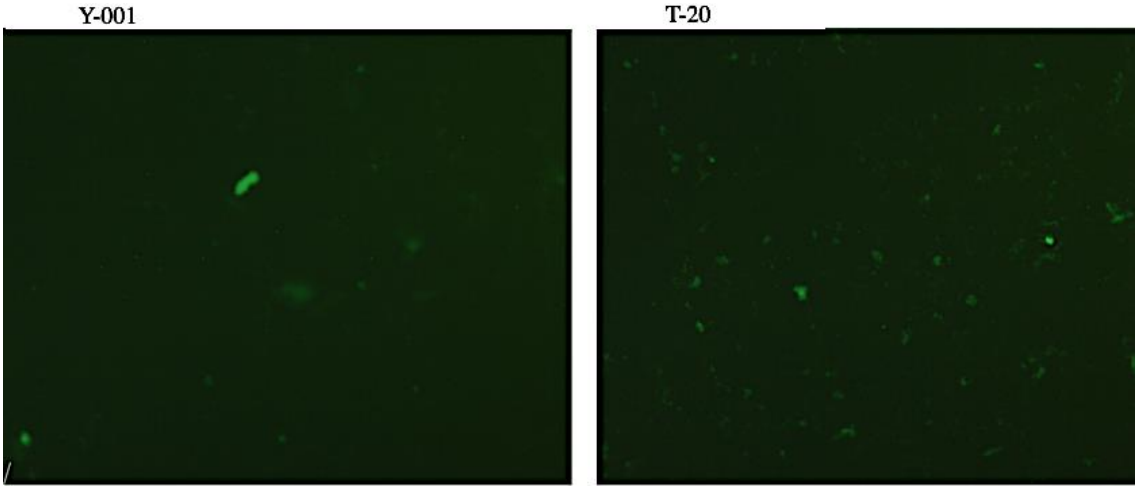

Figure 26. Fluorescence microscopy image for protein transfected CHSE 214 cells with Nucleofector™ 2b Device. The first image is for P1= Y-001 transfected cells and second image is for P2= T-20 cells.

The flowcytometeric analsysis of transfected cells were done after 72 hours. From the analysis it was observed program T-20 has higher transfection efficiency around five time more compared to program Y-001 (Table 18). Control also showed 1% transfection effeiciency due to GFP cas9 that were attached with cells and remained unwashed by PBS during preparation of cells for flow cytometry.

Table 18. Results from flow cytometric analyis of protein transfected CHSE 214 cells.

Program	Transfection efficiency %
Control	1
Y-001	9.6-1=8.6
T-20	47.9-1= 46.9

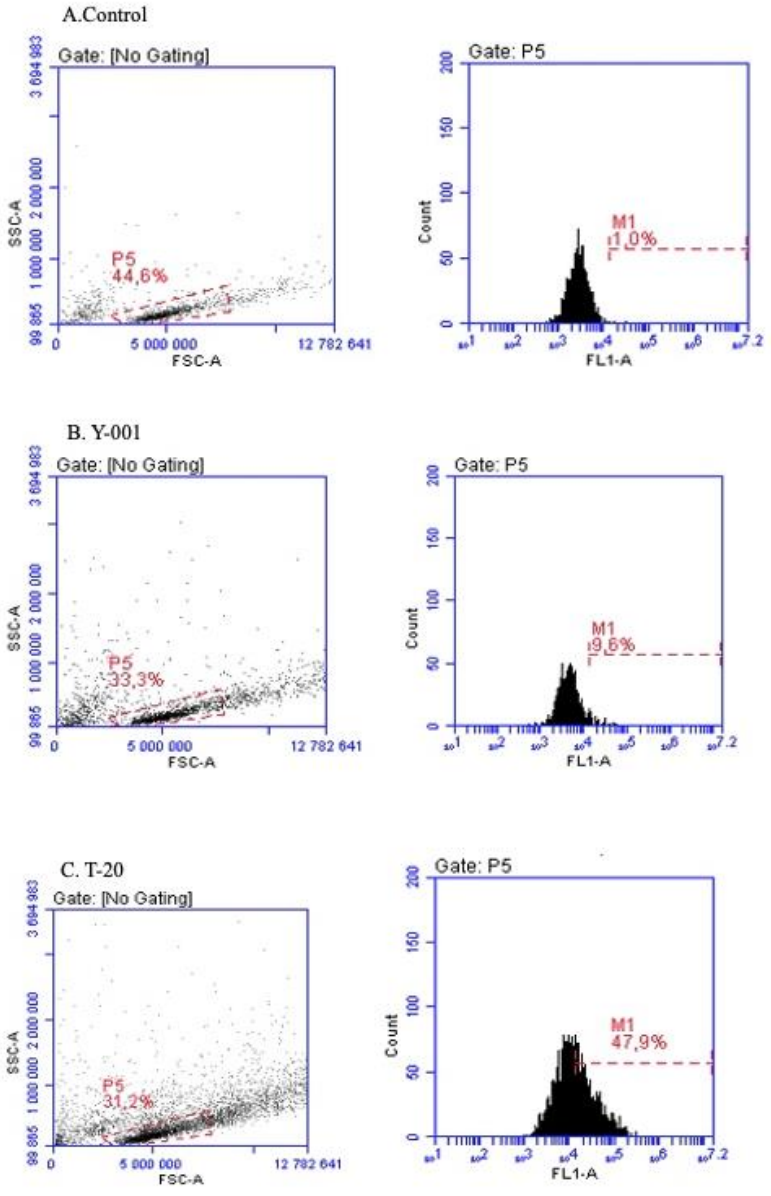

Figure 27. Image from flowcytometry analsysis of protein transfected CHSE 214 cells with Nucleofector™ 2b Device. There are two images in the row for each sample first image is sample gating, second is image (FL1 detector) for transfection efficiency and third image (FL3 detector) for viability. The images shown are A. control, B. cells transfected with program Y-001, and C. cells transfected with program T-20.

5.5 Gene editing attempt in ASG-10 cells

5.5.1 Identification of CYP1a gene in Atlantic salmon

The target gene should be analyzed before designing gRNA. The number of copies of the tareget CYP1a gene in the genome were identified by searching in a genome browser of the Ensembl and National Center for Biotechnology Information (NCBI). Chromosomes 26 and chromosome 11 with CYP1a gene were identified (Table 19). Then gene sequences were downloaded for further analysis works.

Table 19. Table showing identification of CYP1a gene in different chromosomes

Chromosome number	Information about gene
ssa11	**Gene symbol:** LOC100136926 Gene ID: 100136926 Exon count: 7
ssa26	**Gene symbol:** LOC100136916 Gene ID: 100136916 Exon count: 7

5.5.2 Identification of target sequences using ChopChop browser

The second step after identification of the gene was to identify the target region where gRNA will act on. For this purpose, the ChopChop browser (https://chopchop.cbu.uib.no/) was used. Based on efficiency score and off-target scores best three targets were choosen (Table 20). The browser shows the results with different informatuons like GC content, self complementarity, off-target score, and efficiency (Fig. 28).

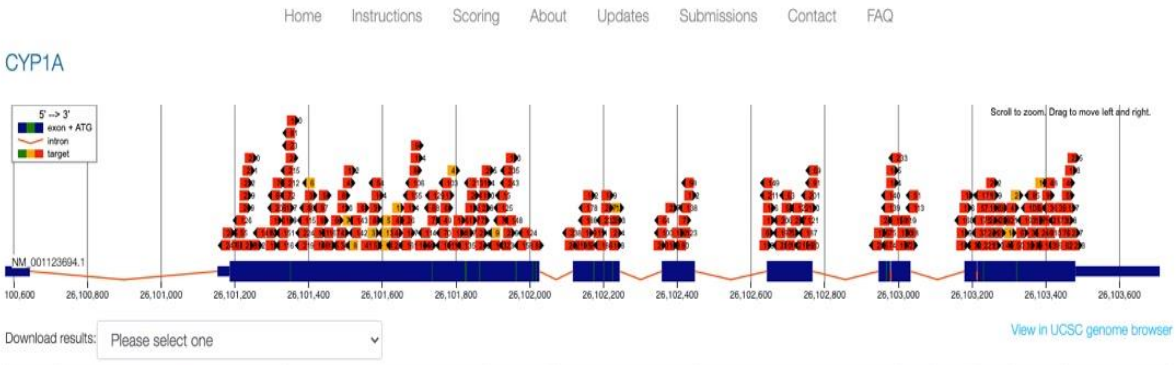

Rank	Target sequence	Genomic location	Strand	GC content (%)	Self-complementarity	MM0	MM1	MM2	MM3	Efficiency
1	CGCTCTTTCGCTACGCTGGAGGG	NC_027310.1:26101629	+	60	0	0	0	1	0	51.93
2	TGAGGCCATCGGACGCAATGAGG	NC_027310.1:26103307	+	60	2	0	1	0	0	69.35
3	CTTGGCCTTTAGCACCGACAAGG	NC_027310.1:26101562	+	55	2	0	1	0	0	60.55
4	TCGGTGGCCAACGTCATCTGTGG	NC_027310.1:26101779	+	60	0	1	0	0	0	62.60
5	GGGCGCTCATAGCTAGCTTGCGG	NC_027310.1:26101604	-	60	2	1	0	0	0	62.76
6	TGAGCCGTAGCGCTCACTCATGG	NC_027310.1:26101396	-	60	1	1	0	0	0	61.59
7	AAGCAAGGGGAAGACTTCGCCGG	NC_027310.1:26101494	+	55	2	1	0	0	0	57.23
8	GCTGTATAGATCGGGCCTCCCGG	NC_027310.1:26101513	-	60	1	1	0	0	0	55.11
9	AGGATGGGAATGAAGTCTGCAGG	NC_027310.1:26101899	-	50	1	1	0	0	0	51.25
10	CAAGCGCCGCTGCATCGGTGAGG	NC_027310.1:26103289	+	70	1	1	0	0	0	51.14
11	GGAGAAACCTGGGCACCCGCTGG	NC_027310.1:26103373	+	70	0	1	0	0	0	47.81
12	GTCAATGATCTGTTTGGGGCAGG	NC_027310.1:26102224	+	50	0	1	0	0	0	45.78
13	CGCTCATAGCTAGCTTGCGGCGG	NC_027310.1:26101601	-	60	2	1	0	0	0	44.77

Figure 28. Image showing the result after serching target for CYP1a gene from ChopChop browser for Salmo salar GCF_0002333375.1

The three target sequences (4,5, and 8) were selected from the result (Fig. 28) with the highest efficiency score and off-target scores, and the reverse complement sequence was designed for those target sequences to use further in Invitro Transcription of gRNA work.

Table 20. List of selected target sequnences from the result shown after search.

Name of target DNA	Sequence
4: TCGGTGGCCAACGTCATCTG (F)	Complement: TCGGTGGCCAACGTCATCTG Reverse Complement: CAGATGACGTTGGCCACCGA
5: CAAGCTAGCTATGAGCGCCC (R)	Reverse Complement: GGGCGCTCATAGCTAGCTTG Complement: CAAGCTAGCTATGAGCGCCC
8: GGAGGCCCGATCTATACAGC (R)	Reverse Complement: GCTGTATAGATCGGGCCTCC Complement: GGAGGCCCGATCTATACAGC

5.5.3 Design of DNA oligos for IVT synthesis of gRNA

The DNA oligos for IVT synthesis of gRNA were designed using the complement and reverse complement of the selected target DNA sequence from the Table 20. These are responsible for the synthesis of DNA oligos which in transcription gave gRNA needed for CRISPR transfection.

A. Sequence 4
   Forward: TAATACGACTCACTATAGTCGGTGGCCAACGTCATCTG (38)
   Reverse: TCTAGCTCTAAAACCAGATGACGTTGGCCACCGA (34)

B. Sequence 5
   Forward: TAATACGACTCACTATAGGGCGCTCATAGCTAGCTTG (37)
   Reverse: TCTAGCTCTAAAACCAAGCTAGCTATGAGCGCCC (34)

C. Sequence 8
   Forward: TAATACGACTCACTATAGCTGTATAGATCGGGCCTCC (37)
   Reverse: TCTAGCTCTAAAACGGAGGCCCGATCTATACAGC (34)

D. Sequence Slc45a2 (exon1)
   Forward: TAATACGACTCACTATAGGACTGTAGGGAGTCTACGA (37)
   Reverse: TCTAGCTCTAAAACTCGTAGACTCCCTACAGTCC (34)

5.5.4 PCR assembly of DNA oligos

The gel image below shows the result for PCR assembly of DNA oligos. In the *in-vitro* transcription these DNA oligos are responsible for giving gRNA after transcription. Before performing *in-vitro* transcription it is necessary to know whether PCR assembly gives the expected size DNA oligos or not.

The expected band size was around 120 bp which we see for all four samples target 4, target 5, target 8, and Slc45a2 (Fig. 29). The faint background is seen in positive control and sometimes it is seen in the samples due to the primer dimer formation. Positive control was from the kit and negative control was water control without DNA oligos template.

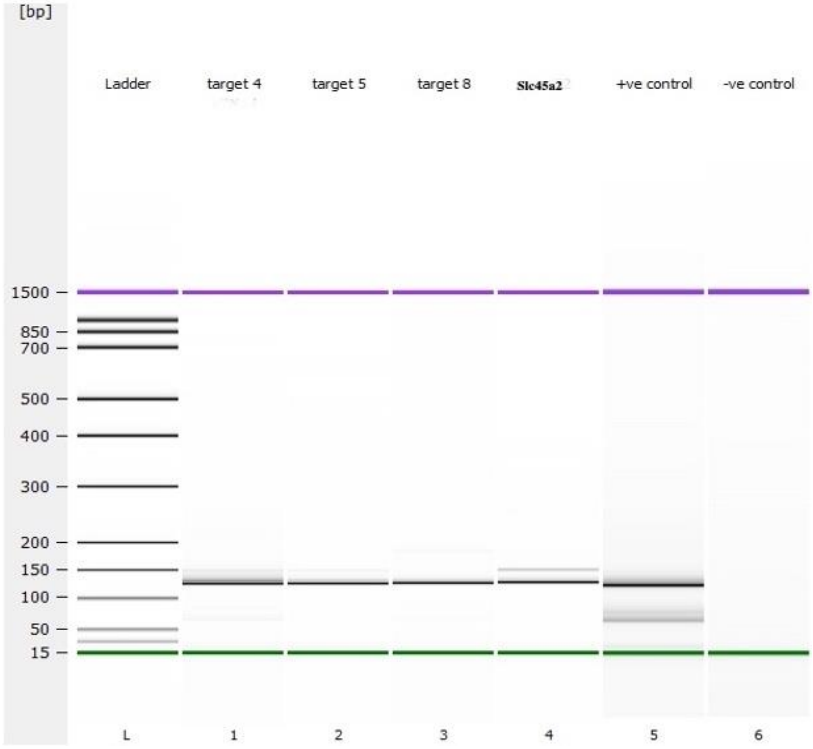

Figure 29. Gel image of PCR assembled DNA oligos analyzed using Agilent bioanalyzer 2100

The in-vitro transcription of DNA oligos resulted in the formation of gRNA. The RNA integrity was checked after purification of synthetic gRNA produced using the gel electrophoresis method (Fig. 30). The product size observed was expected to be 100 bp and the intact images with sizes nearly 100 bp indicate successful synthesis of gRNA which will be used in CRISPR-Cas9 transfection

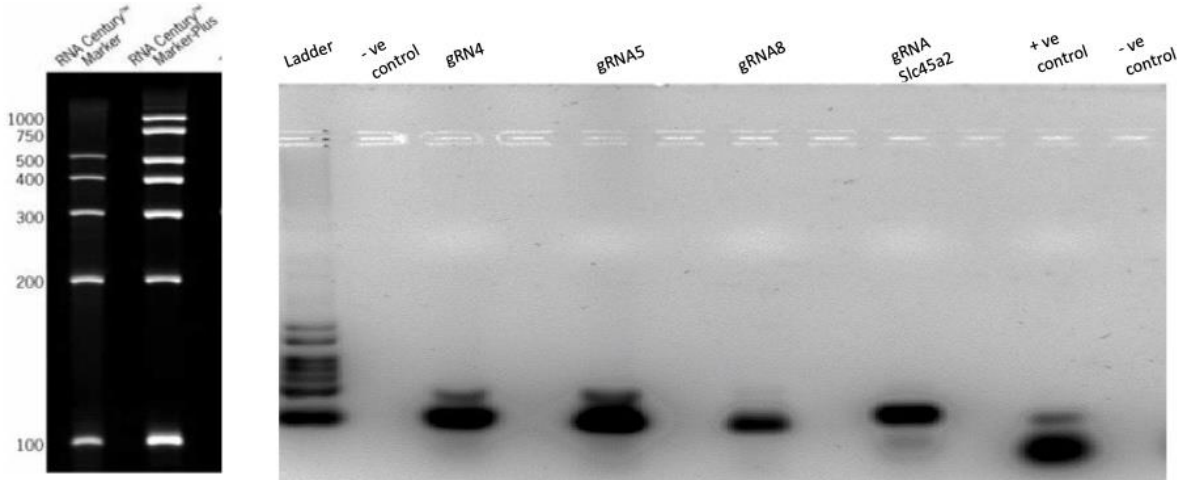

Figure 30. Gel image for checking IVT gRNA integrity.

5.5.5 Primers designed for PCR

The forward and reverse primer were designed for PCR amplification of the target region in a gene where gRNA acts and editing activity occurs. The tables show forward and reverse primer for the CYP1a gene and Slc45a2 gene.

Table 21. List of forward and reverse primer for CYP1a and Slc45a2 gene target regions.

Gene	Primer sequences	Product size	Tm
CYP1a	Forward: CTACGGCTCAGTCTTCCAGATC Reverse: TGCTCACTGACAATCTTCTGC	600 bp	56.7°C 52.4°C
Slc45a2	Forward: GCCATTGACAAGCGGGCTGA Reverse: TGCGAGGATGTAGGGCCTCC	469 bp	55.9°C 57.9°C

5.5.6 PCR of target gene CYP1a

The genomic DNA was extracted from all CRISPR transfected cells with different ribonucleoprotein complexes to analyze the result of transfection. The extracted genomic DNA was used to check whether editing has occurred or not.

The gel image in Fig. 31 shows the PCR amplification of the Slc45a2 gene from genomic DNA of different samples with naming S1, S2, S3, S4 and, S5. Slc45a2 was used as positive control for the CRISPR/Cas9 experiment. Positive control for PCR amplification was from the kit which was the HPRT1 human gene. Negative control was without any DNA template. The Table 22 shows the information about the samples. Different Cas9 enzymes were choosen based on the compatibility with electroporation systems like eSpCas9-GFP with Nucleofector™ 2b Device and TrueCut™ Cas9 with Neon™ transfection system.

From the gel electrophoresis of PCR amplified samples, we saw successful amplification of Slc45a2 genomic DNA region. Samples with higher concentration shows bigger band size and the PCR product size was expected to be 469 bp. In the image we saw bands near 500 bp band compare to ladder indicating the products were of right size.

Table 22. Sample information based on the CRISPR transfection method forASG-10 cells targeting for Slc45a2 gene.

Samples	Transfection method
S1	Nucleofector™ 2b Device + eSpCas9-GFP protein + gRNA slc45a2
S2	Nucleofector™ 2b Device + TrueCut™ Cas9 + gRNA slc45a2
S3	Nucleofector™ 2b Device + eSpCas9-GFP protein + gRNA slc45a2
S4	Neon™ transfection system + TrueCut™ Cas9 + gRNA slc45a2
S5	Non edited

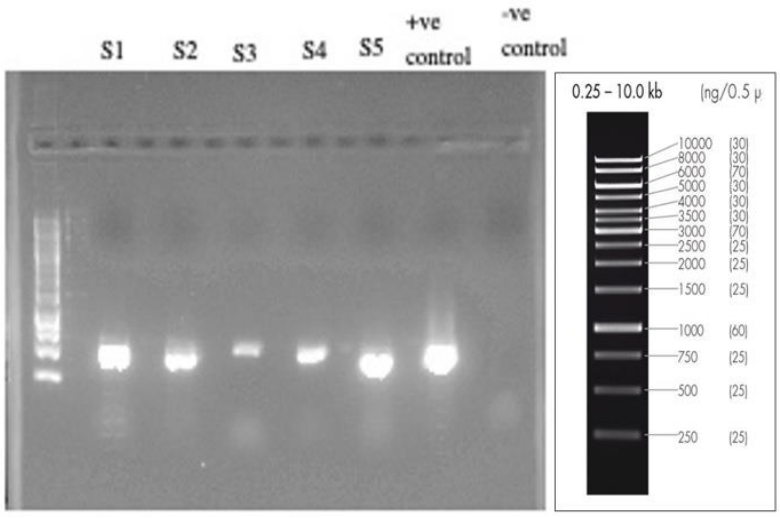

Figure 31. Gel image for PCR amplification of Slc45a2 gene for cell samples which are transfected with diffrent electropration systems and Cas9s. DNA ladder 1kb peqGold is used as marker to know size of the PCR product.

The gel electrophoresis result for the amplification of CYP1a region from genomic DNA as expected which was extracted from different CRISPR-Cas9 transfected cells (Fig. 32). In this transfection experiment TrueCut™ Cas9 was also used with Nucleofector™ 2b Device as both are compatible with each other. Table 23 gives the information about samples. Positive control for PCR amplification was from the kit which was the HPRT1 human gene. Negative control was without any DNA template

Table 23. Sample information based on the CRISPR transfection method for CYP1a cells targeting for Slc45a2 gene.

Sample	Transfection strategy
Sg1	Nucleofector™ 2b Device +eSpCas9-GFP protein+ gRNA4
Sg2	Nucleofector™ 2b Device +eSpCas9-GFP protein + gRNA5
Sg3	Nucleofector™ 2b Device +eSpCas9-GFP protein + gRNA8
Sg4	Nucleofector™ 2b Device +eSpCas9-GFP protein
St1	Nucleofector™ 2b Device + TrueCut™ Cas9 + gRNA4
St2	Nucleofector™ 2b Device + TrueCut™ Cas9 + gRNA5
St3	Nucleofector™ 2b Device + TrueCut™ Cas9 + gRNA8
St4	Nucleofector™ 2b Device + TrueCut™ Cas9

The gel image below shows the PCR amplification of genomic DNA for the CYP1a target region. The product size was expected to be 600 bp. In the gel image, we saw bands that were above 500 bp size bands compared to the band in the ladder. This showed the right size products were amplified.

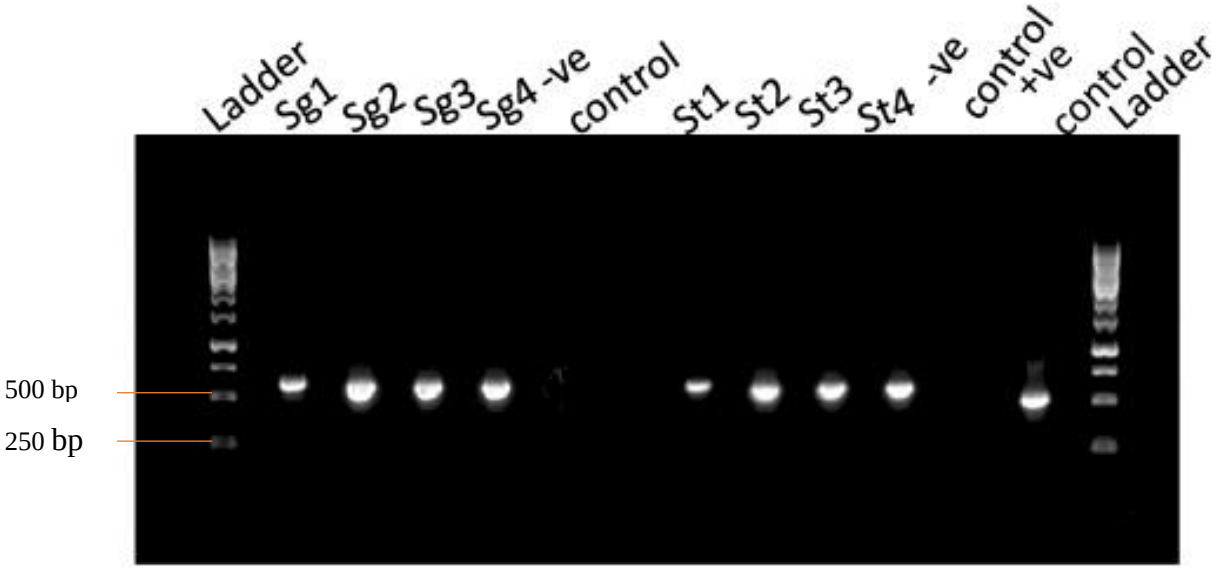

Figure 32. Gel image for PCR amplification of CYP1 gene gene for cell samples which are transfected with diffrent electropration systems and Cas9s. DNA ladder used as marker is1kb peqGold DNA ladder.

5.5.7 Genomic cleavage detectation assay

The gel images shown below are for checking whether editing was occurred or not in the Slc45a2 gene (Fig. 33). The samples were the same PCR amplified sample from table 22 (Table 22). Which was added with endonuclease enzyme from Alt-R Genome Editing Detection Kit. The first negative control was for homodimer which doesn't show cleavage bands, positive control was the heterodimers which showed cleavages due to mismatch in the nucleotide sequences during reannealing. The second negative control wass water control for the whole cleavage reaction. For Slc45a2 samples cleavage bands were not seen so clear compared to the positive control. The faint images in the background could be primer dimers from PCR.

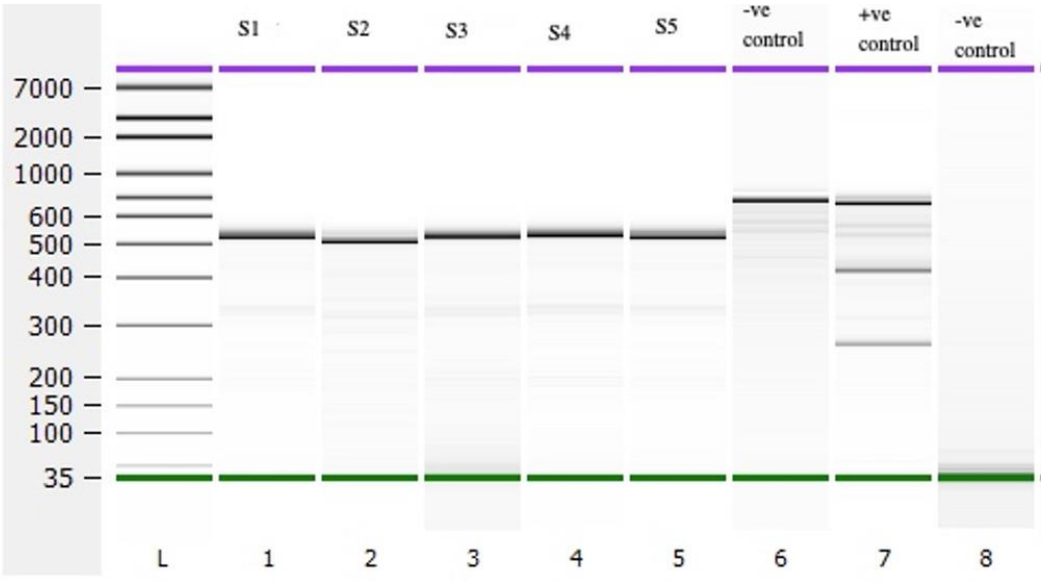

Figure 33. Gel image from Cleavage assay of Slc45a2 PCR ampliifeid samples from Agilent Bioanalyzer 2100.

The result is for the CRISPR/Cas9 transfection of the CYP1a gene using gRNA4, gRNA5, and gRNA8 with different Cas9 enzymes (eSpCas9-GFP and TrueCut Ca9) (Fig. 34). The samples are the same PCR amplified samples from table 23 (Table 23). which is added with endonuclease enzyme from GeneArt Genomic Cleavage Detection Kit. But sg4 was without an endonuclease enzyme. The positive control is from the kit and the negative is water control with template DNA.

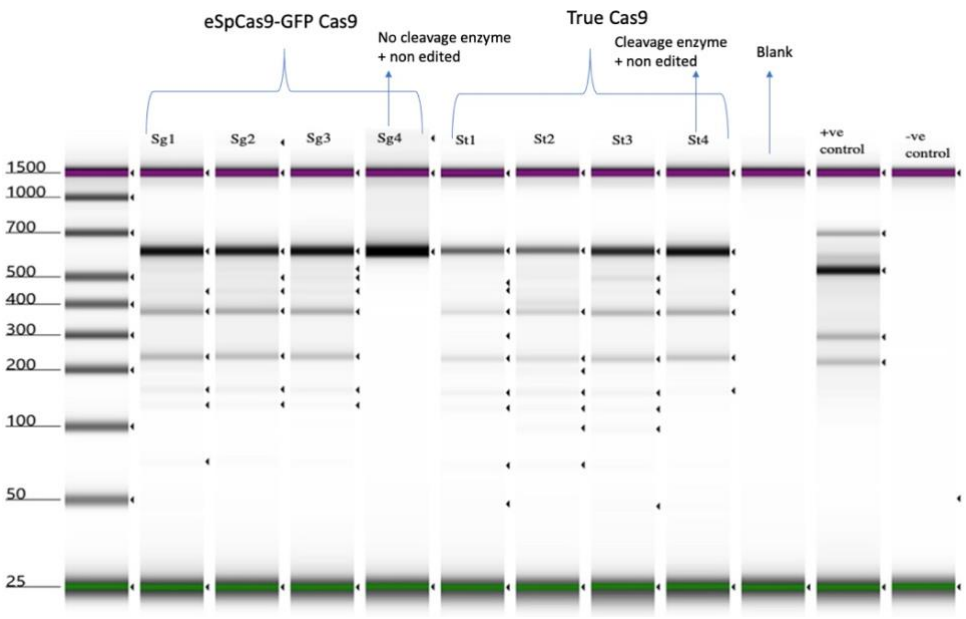

Figure 34. Gel image from Cleavage assay of CYP1a gene of PCR amplified samples from Agilent Tapestation 4200.

After analyzing the samples in Agilent tape station 4200, similar cleaved DNA bands were observed in all samples including negative control, which was not expected. The expectation was different bands sizes in different samples. For Sg1/St1 expected band size were370 bp and 230 bp, for Sg2/St2 expected band size were 404 bp and 196 bp for Sg3/St3 expectec band size were 495 bp and 105 bp. Positive control was from kit, so it had different bands compare to samples.

5.5.8 Results from PCR clonning

The restricitions sites in construct was identified using Genious 8.0 software (Fig. 35). The result from restricition digestion of extracted purified plasmid showed the ligation worked rightly as expected. It gave two bands with size of 2212 bp and 1388 bp (Fig. 36).

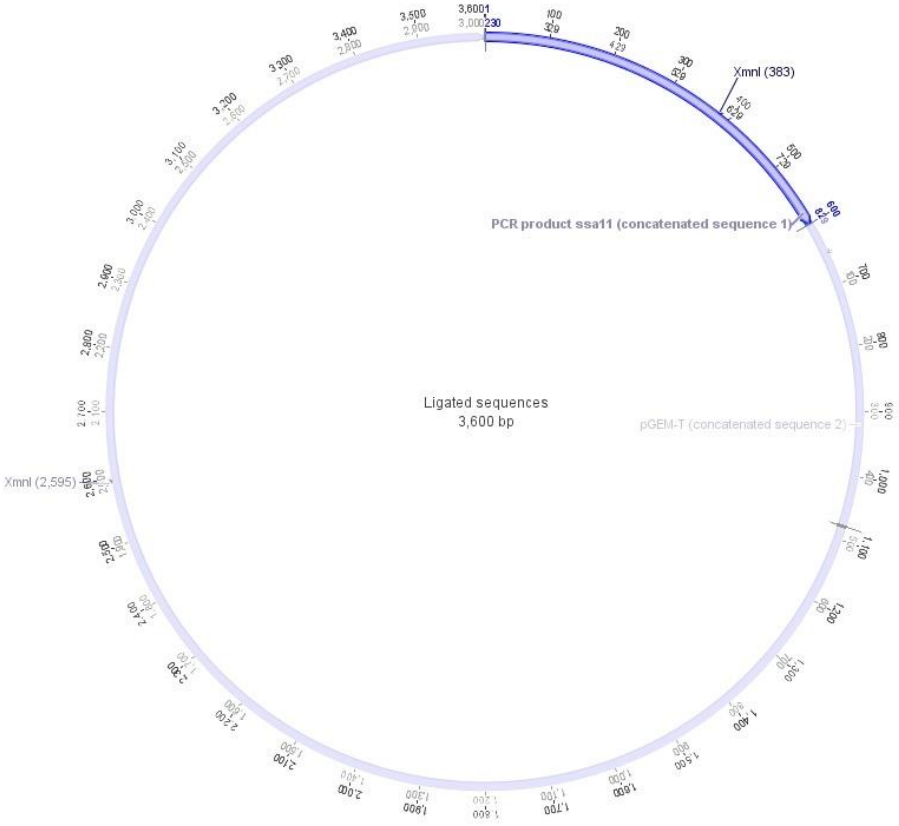

Figure 35. Diagram showing vector construct with ligation of PCR product and the restriction sites for restricition enzyme Xmnl using Geneious. 08.

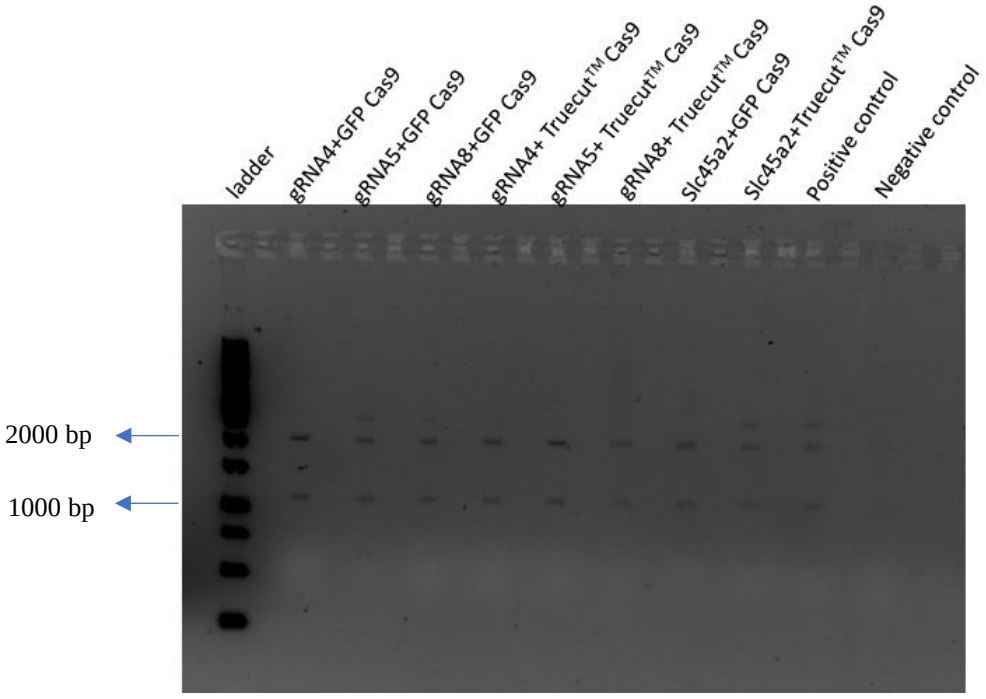

Figure 36. Gel image showing result of restriction digestion of PCR prouct ligated plasmid Vector.

5.5.9 Sanger sequencing

After direct sanger sequencing of PCR product and PCR clonned plasmid DNA, similar results were seen from the sequence analysis after Sanger sequencing for CYP1a within chromosome 11 and chromosome 26, which were subjected to gene editing with different gRNAs (gRNA4, gRNA5, and gRNA8) and Cas9s (TrueCut™ Cas9 and eSpCas9-GFP protein) to determine whether editing has occurred or not. For the analysis of sequencing results software Geneious 8.0 was used (Geneious, 2014).

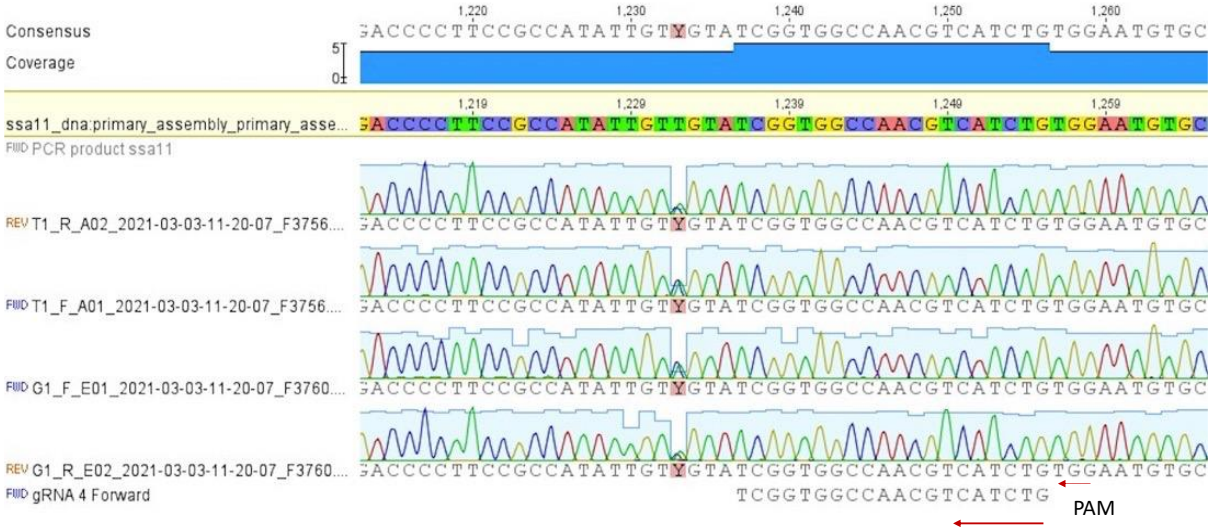

Figure 37. Diagram showing result from sanger sequencing of samples transfected with gRNA4 in chromosome 11 (ssa11). This image shows results after transfection for both eSpCas9-GFP protein and TrueCut-Cas9, complexed with gRNA4 targeting CYP1a ssa11 for gene editing.

Fig.37 shows the result of analysis of edits within the CYP1a gene sequence of chromosome 11 which was transfected with the gRNA 4 Cas9 complex. gRNA4 acted on the forward DNA sequence. After analysis, we saw no evidence of editing. The first two strands are for forward and reverse strand from samples which were transfected with enzyme TrueCut™ Cas9 and third and fourth strands are from samples with eSpCas9-GFP protein. Therse was seen mismatach in the position 1283, it is due to sanger error in sanger sequencing where it mistunderstood for C/T nucleotide.

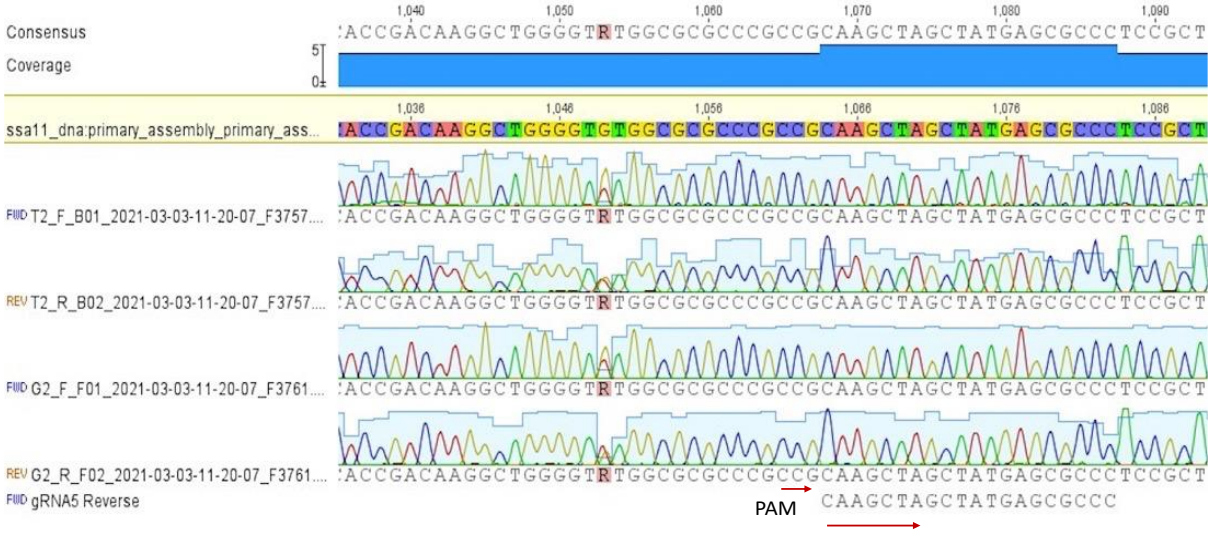

Figure 38. Diagram showing result from sanger sequencing of samples transfected with gRNA5 in ssa11. This image shows results after transfection for both eSpCas9-GFP protein and TrueCut-Cas9, complexed with gRNA5 targeting CYP1a on chromosome 11 (ssa11) for gene editing.

Fig 38. shows the result of analysis of edits within the CYP1a gene sequence of chromosome 11 which was transfected with gRNA5 Cas9 complex. gRNA5 acted on the reverse DNA sequence. After analysis, we saw no evidence of editing. The first two strands are for forward and reverse strand from samples which were transfected with enzyme TrueCut™ Cas9 and third and fourth strand are from samples with eSpCas9-GFP protein. The mismatach in position 1053 in consensus sequences and other aligned sequnences from sequencing are due to the error from sanger sequencing where it failed to identify A/G and there was overlapping peak of chromatogram for both A and G.

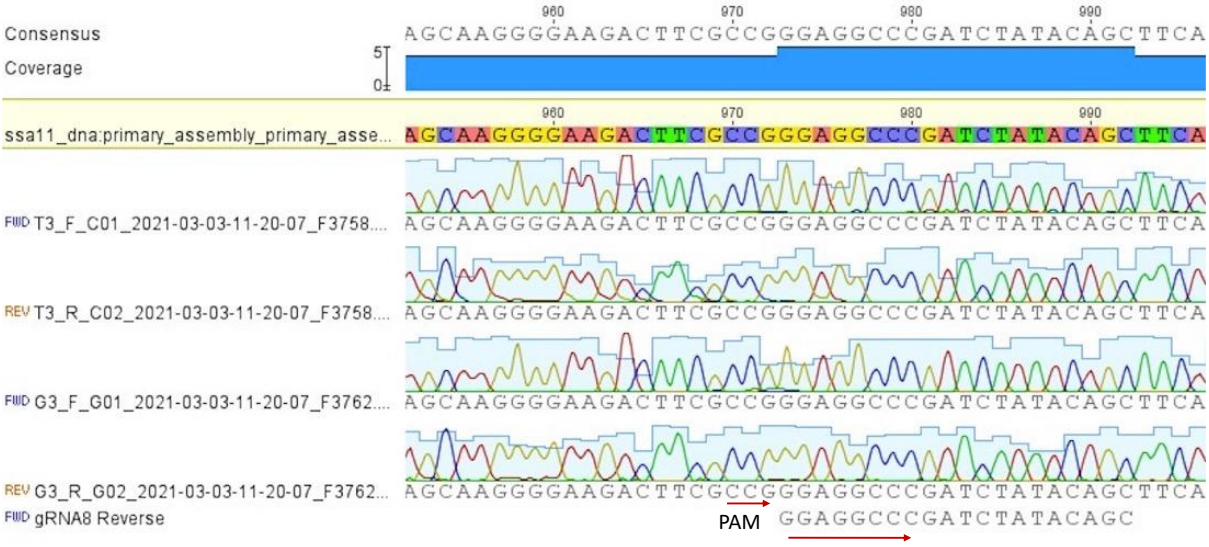

Figure 39. Diagram showing result from sanger sequencing of samples transfected with gRNA8 in chromosome 11 (ssa11). This image shows results after transfection for both eSpCas9-GFP protein and TrueCut-Cas9, complexed with gRNA8 targeting CYP1a ssa11 for gene editing

Fig 39. shows the result of analysis of edits within the CYP1a gene sequence of chromosome 11 which was transfected with gRNA8 Cas9 complex (Fig. 39). gRNA8 acted on the reverse DNA strand. After analysis, we saw no evidence of editing. The first two strands are for forward and reverse strand from samples which were transfected with enzyme TrueCut™ Cas9 and third and fourth strand are from samples with eSpCas9-GFP protein.

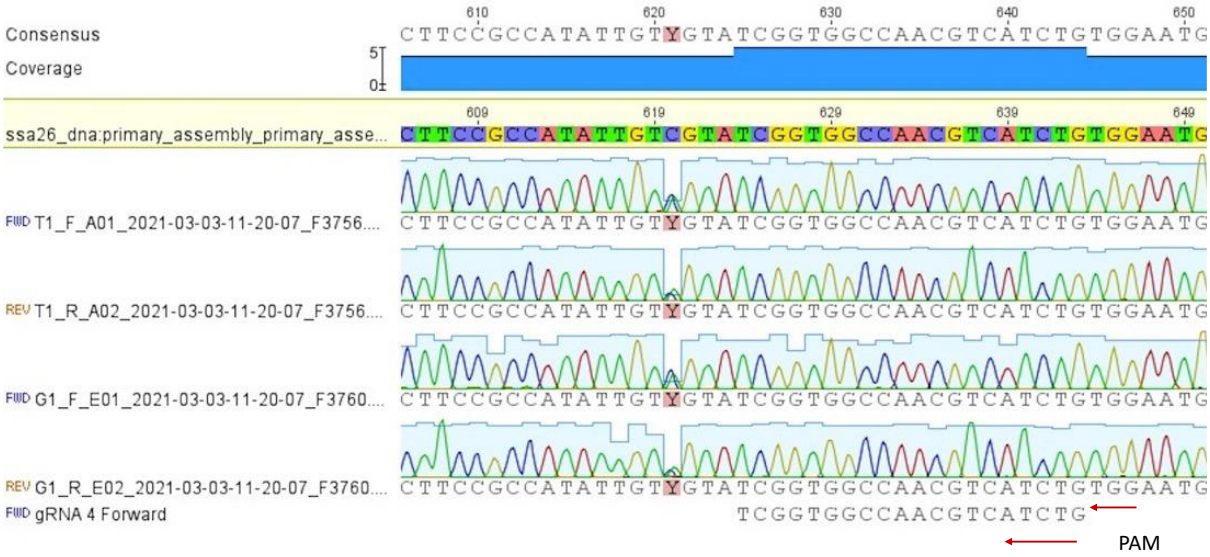

Figure 39. Diagram showing result from sanger sequencing of samples transfected with gRNA4 in chromosome 26 (ssa26). This image shows results after transfection for both eSpCas9-GFP protein and TrueCut-Cas9, complexed with gRNA4 targeting CYP1a in ssa26 for gene editing

Figure 40. shows the result of analysis of edits within the CYP1a gene sequence of chromosome 26 which was transfected with gRNA4 Cas9 complex (40). gRNA4 acted on the forward DNA sequence. After analysis, we saw no evidence of editing. The first two strands are for forward and reverse strand from samples which were transfected with enzyme TrueCut™ Cas9 and third and fourth strand are from samples with eSpCas9-GFP protein. Therse was seen mismatach in the position 621, it is due to error in sanger sequencing where it mistunderstood for C/T nucleotide and there is overlapping peak of chromatogram for both C and T.

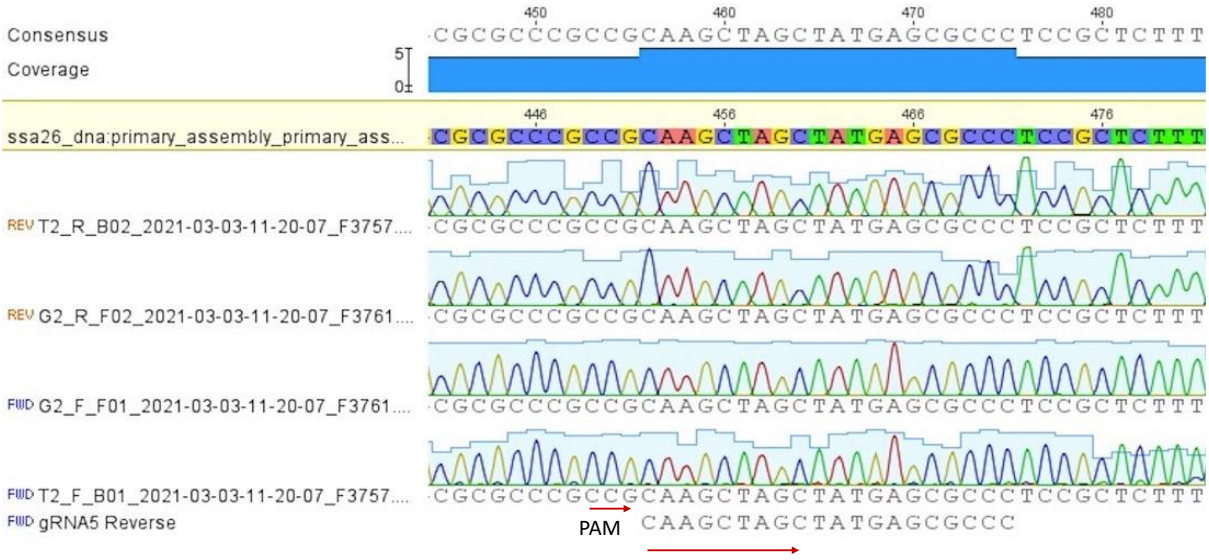

Figure 40. Diagram showing result from sanger sequencing of samples transfected with gRNA5 in chromosome 26 (ssa26). This image shows results after transfection for both eSpCas9-GFP protein and TrueCut-Cas9, complexed with gRNA5 targeting CYP1a in ssa26 for gene editing

Figure 41. shows the result of analysis of edits within the CYP1a gene sequence of chromosome 26 which was transfected with gRNA5 Cas9 complex (Fig. 41). gRNA5 acted on the reverse DNA sequence. After analysis, we saw no evidence of editing. The first two strands are for forward and reverse strand from samples which were transfected with enzyme TrueCut™ Cas9 and third and fourth strand are from samples with eSpCas9-GFP protein.

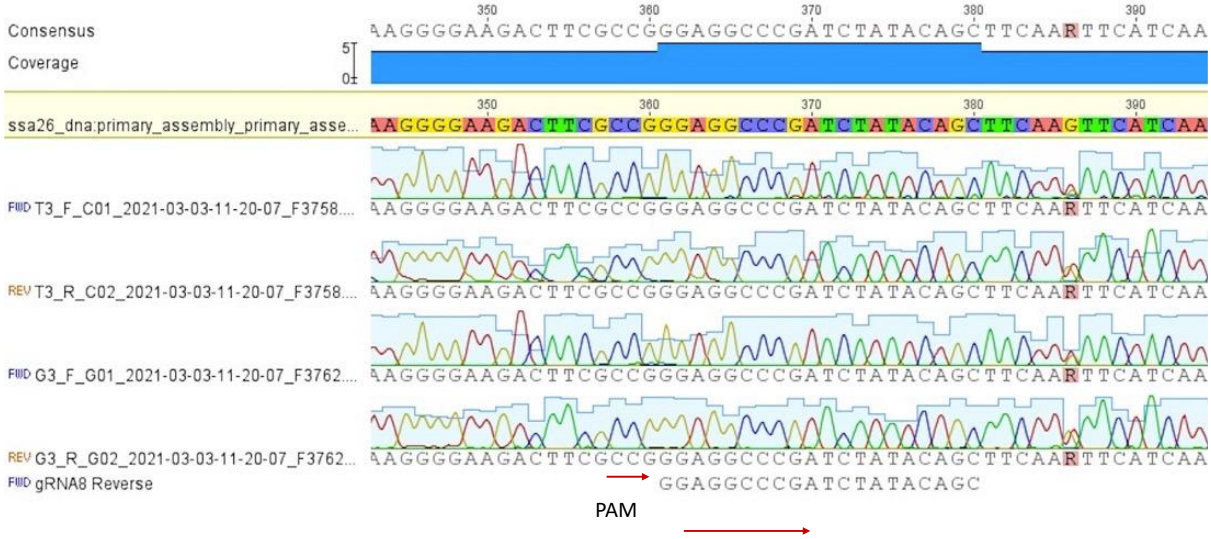

Figure 41. Diagram showing result from sanger sequencing of samples transfected with gRNA8 in chromosome 26 (ssa26). This image shows results after transfection for both eSpCas9-GFP protein and TrueCut-Cas9, complexed with gRNA8 targeting CYP1a in ssa26 for gene editing

Figure 42. shows the result of analysis of edits within the CYP1a gene sequence of chromosome 26 which was transfected with gRNA8 Cas9 complex (Fig. 42). gRNA8 acted on the reverse DNA sequence. After analysis, we saw no evidence of editing. The first two strands are for forward and reverse strand from samples which were transfected with enzyme TrueCut™ Cas9 and third and fourth strand are from samples with eSpCas9-GFP protein. The mismatach in position 386 in consensus sequences and other aligned sequnences from sequencing are due to the error from sanger sequencing where it failed to identify A/G and there is overlapping peak of chromatogram for both A and G.

6 Discussion

6.1 Identification of factors affecting transfection efficiency in GFP tagged plasmid DNA transfection

From section 5.1.1 and 5.1.2 transfection of ASG -10 cells with pmaxGFPTM plasmid using Neon™ transfection system, it is seen parameters like confluency of cells (between 70% to 80 %) (Table 11) and a higher number of cells (Table 12) showed an increase in transfection efficiency. The criteria followed in each step were to increases transfection efficiency which was based on the recommendation from published works (Promega Corporation, 2021; Zhang et al., 2018), and it is proved by the results that confluency of 70-80 % and higher number of cells increases transfection efficiency. The reason why lower cell confluency contributed to higher transfection efficiency is that less confluent cells can uptake more DNA/protein as they are in the dividing stage and fully confluent cells exhibit contact inhibitions which negatively affects the uptake of DNA/protein resulting in less transfection efficiency (Brunner et al., 2000). Different cells have different sizes and when fewer cells are used, they have less cell-to-cell contact and lower availability for uptake of DNA/protein in electroporation, so increasing the cell number shows positive effectiveness (Potter, 2003). In the section when fully confluent cells with less cell number were used the transfection efficiency was very low compared to the section with 70-80% with five times more cells.

The CHSE 214 cell line was used as a control cell line for transfection using NeonTM transfection system. Programs that were tested earlier in published works were used as references. The result from transfection using program CNP2: 1600-10-3 in Neon device gave 97.6 % with GFP plasmid in our experiment (Table. 14) comparable to previously published work which claimed 99.9 -100 % transfection with tracrRNA–ATTO550 (Gratacap et al., 2020a). The other two programs (CNP1: 1400-30-1 and CNP3: 1700-20-1) were used randomly to see how efficiently they transfect the cells when using a parameter for a lower voltage (1400) and higher voltage (1700) compared to 1600 V. It was observed the program CNP3 1700-20-1 also gave similar transfection efficiency with CNP2: 1600-10-3. Here the success in results with CNP2: 1600- 10- 3 proved the system is working as expected. In the case of, Nucleofector™ 2b device it was already optimized by previous master student Kathrine Andersen in ASG-10 (work not published yet) and the same system was continued. In the Nucleofector™ 2b Device, transfection program Y-001 showed higher transfection efficiency 51% and 47.8 % for program T-20 for GFP plasmid transfection. The reason for Nucleofector™ 2b device transfection of CHSE 214 with GFP plasmid cells was to make a foundation for protein transfection using the tested program.

The result from transfection of LG-1 cells showed success in transfection from the test of seven different programs where three programs (LP3: 1300-30-1, LP4: 1400-20-2, and LP7: 1700-20-2) worked effectively showing more than 50% transfection efficiency (Table 16). If we look at these three-best programs (LP3, LP4, and LP7) there was a different combination of voltage, width, and pulse, so sometimes increasing width like in P1 can be best, or sometimes increasing voltage like in P3 can be best. If we compare this result with ASG-10 in Table 12. higher voltage can affect lowering viability of cells which can be focused on the next experiment to study and these three programs (P3, P4, and P7) can be further used in the optimization of transfection efficiency and the program which gives both higher transfection efficiency and viability can be chosen.

6.2 Identification of Nucleofector™ 2b device programs giving higher transfection efficiency in protein transfection

There were no prior works that have information about direct protein transfection in cell lines from Atlantic salmon and Lumpsucker and the efficiency of transfection. It is important to know the success of transfection of fish cells, for example, with GFP -tagged proteins for effective CRISPR/Cas9 transfection using RNP complex. In protein transfection experiments, the eSpCas9-GFP protein was chosen to transfect cells using the Nucleofector™ 2b device, as the protein was compatible with Nucleofector™ 2b device transfection kit, and it was easier to analyze the cells after transfection by flow cytometry to know the transfection efficiency. If the cell after transfection shows green fluorescence, then they can be sorted by fluorescence-activated cell sorting (FACS) which is very useful in selecting transfected cells after CRISPR-Cas9 transfection (Jin et al., 2020).

In both ASG-10 and CHSE 214, protein transfection was successful showing good results. In the ASG-10 program, U-029 gave higher transfection efficiency 69% with viability of 98.3% and L-029 gave 41.4 % transfection efficiency and 96.8% viability for protein transfection (Table 17). In both plasmid DNA transfection and protein transfection, U-029 was effective in giving higher transfection results. Plasmid transfection result from the master thesis of Kathrine Andersen in ASG-10 (work not published yet) was compared for the programs U-029 and L-029.

In CHSE 214, program T-20 gave 46.9 % transfection efficiency and program Y-001 gave 8.6% transfection efficiency (Table 18). In CHSE 214 the program T-20 gave higher transfection efficiency for protein but less with Y-001 which was just the opposite with plasmid transfection

where program T-20 gave 47.8% transfection efficiency and Y-001 gave 51% transfection efficiency.

From the transfection of ASG-10 and CHSE 214, it is seen that the program for plasmid transfection may or may not be effective equally for protein transfection. So, different programs should be tested for different transfection components (DNA/Protein) in different cell types. So, there is no generic program that can work equally in all the environment. In Nucleofector™ 2b device there is no clear information about voltage, width, and pulse used in the specific program so it's difficult to say which factor is playing role in giving different results in plasmid transfection and protein transfection. If the GFP tagged protein that is compatible with the Neon™ transfection system will be available then we can know the effect of different factors like voltage, width, and pulse in protein transfection.

6.3 Attempt to gene edit in ASG-10 cells

6.3.1 Analysis of target gene (CYP1a) and identification of target sequences

The gRNA designing step is very crucial in CRISPR design, so proper annotation of target genes and selection of target sequences for gene editing using appropriate software is important (Mohr et al., 2016). Off-target effect and on-target efficiency are always a big problem with gRNA, so the selection of appropriate software helps to solve such problems (Xu et al., 2015; Zhang et al., 2015). Ensembl genome browser is effective in gene annotation of vertebrate species, so for Atlantic salmon (Howe et al., 2021). ChopChop is effective in target selection for gRNA designing as it can give results for target sequences at different exons with off-target scores, efficiency, and GC content. ChopChop is effective to work with whole exons rather than with a single exon with a limited number of nucleotide sequences, like in CRISPR (http://crispor.tefor.net/).

Ensembl genome browser revealed the presence of the CYP1a gene in chromosome 11 (ssa11) and chromosome 26 (ssa26). But when looking for the target region in ChopChop only ssa11 was available as the reference sequence for the CYP1a gene. Then three sequences from ChopChop were retrieved and aligned with ssa26 sequences by sequence alignment in Mega7 software. The reason for choosing three sequences was sometimes choosing a single sequence during optimization may not work so it is recommended to check with different gRNA (Synthego, 2021). From the sequence alignment it was seen CYP1a gene sequence in both chromosomes was highly similar, and the region where gRNAs act, were similar (Supplementary Fig. 1). Same gRNAs work for both chromosomes and all three target sequences act at exon two for both ssa11 and ssa26.

6.3.2 Analysis of gene editing after RNP transfection

Due to high sequence similarity, designing specific primer pair for PCR of the CYP1a gene in a single chromosome was difficult. For cleavage assay, PCR product size around 500 bp is supposed to be effective (Invitrogen, 2014). Designing a unique PCR primer pair that acts on the only chromosome was impossible due to high sequence similarity. The single pair of primer was designed that gave PCR product of 600 bp which gave a problem with similar band size in all the samples including a negative control in cleavage assay as shown Fig.34. It gave heterodimer formation problems due to nine nucleotide differences in PCR amplified CYP1a gene sequences in ssa11 and ssa26 (Supplementary fig.1). This caused an overlapping effect making it difficult to make any editing decision. Due to this difficulty, genomic detection assay may not be suitable for species that have undergone genome duplication with few differences in duplicated gene sequences.

After the genomic detection cleavage assay which didn't give a conclusive result, direct sequencing of PCR product was done. It was also not effective to give proof of evidence of gene editing. So, PCR cloning was done in the pGem-T vector to find colonies that are ligated with edited PCR amplicon. In sanger sequencing, instead of choosing the higher number of colonies (from vector ligated with PCR products), only one from each sample was chosen. This was due to the problem with plating media, the plates which were ordered from the media production department (NVI) had a lower concentration of antibiotics ampicillin around ten times less which was identified in a later stage, but the colonies were grown well in the plate. But there was the problem if the ligation had not worked well and if there was the presence of other contaminating vectors, there could be a loss of time and resources, so a single colony was chosen. Plates were preserved so that more colonies could be grown if a positive result for ligation was seen. From agarose gel electrophoresis it was seen the correct size of PCR product was ligated.

From the analysis of Sanger sequencing results, evidence of editing was not seen. The main reason was just single plasmid DNA sequencing and direct sequencing of PCR products which were not enough for analysis of the mixed pool of PCR amplified amplicons. There should be more colonies to be selected and sequenced (Edvardsen et al., 2014). As well as there may be less editing in the pool of cells resulting in very few PCR amplicons from edited cells.

To solve the problem in the analysis of gene edit, other approaches can be used like using qPCR-based methods for the analysis of gene edit before sequencing and next-generation sequencings like Illumina, and sorting of cells after CRISPR/cas9 transfection (Li et al., 2019; Morisaka et

al., 2019). There was a plan for FACS sorting after CRISPR-Cas9 transfection using GFP tagged Cas9, but there was difficult to book the instrument due to the Corona situation and the need to skip this step. As well as there was not enough time for colony selection of cells after transfection so we could have a pool of cells and analyze gene editing from them. Post transfection works (cell sorting, clone selection of cells, time for growing cells, genomic DNA extraction, sequencing) are more time-consuming, and time was the main limitation for this research project.

6.4 Future perspective

Fish cell lines are slow-growing and transfecting those cells for delivery for foreign DNA or protein complex is challenging, so there is the need for an effective delivery method. From the success of higher transfection efficiency using Neon™ transfection system, now there is an opportunity to test expression systems (plasmid, mRNA, ribonucleoprotein) and optimize them. The effectiveness of expression systems is the next important factor in transfection so the next door that has been opened is to study the effectiveness of expression systems (Hamar & Kültz, 2021).

There is a high demand for stable reporter cell lines which can be used for studying genes responding against different pathogens causing diseases (Collet et al., 2018). Gill cells are very important for studying various immune responses, and the success in developing a stable gene-edited gills cell line will be a milestone for fish health research. The best method till now to work on genome editing is CRISPR-Cas9 based method. In the future, the research can be directed to optimize and work effectively based on the methods/ workflow designed in this research for RNP transfection.

7 Conclusion

This master´s thesis research was successful in optimizing transfection protocols for plasmid transfection and protein transfection. In the experiment GFP tagged plasmid and GFP-tagged protein were used. The protocol for ASG-10 was completely optimized for the plasmid transfection with the Neon^{TM} transfection system obtaining 91.5% transfection efficiency and 89.4% viability from the program AP3: 1200-30-2 using 70-80% confluent $5*10^5$ cells. Protein transfection of ASG-10 with the Nucleofector^{TM} 2b device gave 69% transfection efficiency and 98.3% viability from the program U029 using 70-80% confluent $1*10^6$ cells. LG-1 was also successfully transfected with GFP tagged plasmid using the Neon^{TM} transfection system achieving the highest transection of 58.1 % with program LP3: 1300-30-1 using fully confluent $1*10^5$ cells. Protein transfection in CHSE 214 was also successful using the Nucleofector^{TM} 2b device obtaining 46.9% transfection efficiency from program T-20 using $2*10^6$ cells.

In the CRISPR-Cas9 transfection experiment, the work was successful to develop the workflow and method of transfection. All the methods were carried out successfully, but the problem was seen in the analysis of editing using genomic cleavage detection assay and Sanger sequencing which were not able to give evidence of gene editing. Analysis work can be further optimized, and better methods can be chosen for analysis of gene editings like qPCR-based methods and Next Generation Sequencing (NGS) like Illumina.

8 References

Adan, A., Alizada, G., Kiraz, Y., Baran, Y. & Nalbant, A. (2017). Flow cytometry: basic principles and applications. *Critical Reviews in Biotechnology*, 37 (2): 163-176. doi: 10.3109/07388551.2015.1128876.

Agilent Technologies. (2016). *Agilent DNA 1000*

Ahmed, N. & Thompson, S. (2019). The blue dimensions of aquaculture: A global synthesis. *Science of The Total Environment*, 652: 851-861. doi: https://doi.org/10.1016/j.scitotenv.2018.10.163.

Arukwe, A., Förlin, L. & Goksøyr, A. (1997). Xenobiotic and steroid biotransformation enzymes in Atlantic salmon (Salmo salar) liver treated with an estrogenic compound, 4-nonylphenol. *Environmental Toxicology and Chemistry: An International Journal*, 16 (12): 2576-2583.

Bailey, J. L. & Eggereide, S. S. (2020). Indicating sustainable salmon farming: The case of the new Norwegian aquaculture management scheme. *Marine Policy*, 117: 103925. doi: https://doi.org/10.1016/j.marpol.2020.103925.

BarentsWatch. (2020). *About the Norwegian aquaculture industry*. Available at: https://www.barentswatch.no/en/havbruk/about-norwegian-aquaculture.

BD Bioscience. (2013). *BD Accuri™ C6 Cytometer*. Available at: https://static.bdbiosciences.com/documents/BD_Accuri_C6_brochure.pdf.

Bergheim, A. (2012). Recent growth trends and challenges in the Norwegian aquaculture industry. *Latin American Journal of Aquatic Research*, 40: 800-807.

Bloodworth, J. W., Baptie, M. C., Preedy, K. F. & Best, J. (2019). Negative effects of the sea lice therapeutant emamectin benzoate at low concentrations on benthic communities around Scottish fish farms. *Science of The Total Environment*, 669: 91-102. doi: https://doi.org/10.1016/j.scitotenv.2019.02.430.

Brooker, A. J., Papadopoulou, A., Gutierrez, C., Rey, S., Davie, A. & Migaud, H. (2018). Sustainable production and use of cleaner fish for the biological control of sea lice: recent advances and current challenges. *Veterinary Record*, 183 (12): 383-383.

CAB International. (2021). *Oncorhynchus tshawytscha (chinook salmon)*. Available at: https://www.cabi.org/isc/datasheet/71815.

CABI. (2020). *Salmo salar* Available at: https://www.cabi.org/isc/datasheet/65307#5FDBD4E5-D634-437A-8D87-60C0333683C9.

Carroll, D. (2011). Genome engineering with zinc-finger nucleases. *Genetics*, 188 (4): 773-782.

Carroll, D. (2014). Genome engineering with targetable nucleases. *Annual review of biochemistry*, 83: 409-439.

Carroll, D. (2017). Genome Editing: Past, Present, and Future. *The Yale journal of biology and medicine*, 90 (4): 653-659.

Clark, D. P., Pazdernik, N. J. & McGehee, M. R. (2019). Chapter 20 - Genome Defense. In Clark, D. P., Pazdernik, N. J. & McGehee, M. R. (eds) *Molecular Biology (Third Edition)*, pp. 622-653: Academic Cell.

Collet, B., Urquhart, K., Monte, M., Collins, C., Perez, S. G., Secombes, C. J. & Hall, M. (2015). Individual monitoring of immune response in Atlantic salmon Salmo salar following experimental infection with Infectious Salmon Anaemia Virus (ISAV). *PloS one*, 10 (9): e0137767.

Colombo, S. M. & Mazal, X. (2020). Investigation of the nutritional composition of different types of salmon available to Canadian consumers. *Journal of Agriculture and Food Research*, 2: 100056. doi: https://doi.org/10.1016/j.jafr.2020.100056.

Cong, L., Ran, F. A., Cox, D., Lin, S., Barretto, R., Habib, N., Hsu, P. D., Wu, X., Jiang, W. & Marraffini, L. A. (2013). Multiplex genome engineering using CRISPR/Cas systems. *Science*, 339 (6121): 819-823.

Costa-Pierce, B. A. (2010). Sustainable ecological aquaculture systems: the need for a new social contract for aquaculture development. *Marine Technology Society Journal*, 44 (3): 88-112.
Criddle, K. & Shimizu, I. (2014). Economic importance of wild salmon. In, pp. 269-306.
Di Giulio, R. & Clark, B. (2015). The Elizabeth River Story: A Case Study in Evolutionary Toxicology. *Journal of toxicology and environmental health. Part B, Critical reviews*, 18: 1-40. doi: 10.1080/15320383.2015.1074841.
Doudna, J. A. & Charpentier, E. (2014). The new frontier of genome engineering with CRISPR-Cas9. *Science*, 346 (6213): 1258096. doi: 10.1126/science.1258096.
Drennan, J. D., Lapatra, S. E., Samson, C. A., Ireland, S., Eversman, K. F. & Cain, K. D. (2007). Evaluation of lethal and non-lethal sampling methods for the detection of white sturgeon iridovirus infection in white sturgeon, Acipenser transmontanus (Richardson). *J Fish Dis*, 30 (6): 367-79. doi: 10.1111/j.1365-2761.2007.00817.x.
Ede, D. R., Farhang, N., Stover, J. D. & Bowles, R. D. (2017). 4.32 Gene Editing Tools. In Ducheyne, P. (ed.) *Comprehensive Biomaterials II*, pp. 589-599. Oxford: Elsevier.
El Mounadi, K., Morales Floriano, M. L. & Garcia Ruiz, H. (2020). Principles, Applications, and Biosafety of Plant Genome Editing Using CRISPR-Cas9. *Frontiers in Plant Science*, 11 (56). doi: 10.3389/fpls.2020.00056.
Elisabeth Ytteborg & Lynne Falconer. (2020). *Adaptation to climate change: lessons from Norwegian salmon aquaculture*. Available at: https://thefishsite.com/articles/adaptation-to-climate-change-lessons-from-norwegian-salmon-aquaculture.
Erkinharju, T., Dalmo, R. A., Hansen, M. & Seternes, T. (2021). Cleaner fish in aquaculture: review on diseases and vaccination. *Reviews in Aquaculture*, 13 (1): 189-237. doi: https://doi.org/10.1111/raq.12470.
European Union. (2010). Directive 2010/63/EU of the European Parliament and of the Council of 22 September 2010 on the protection of animals used for scientific purposes Text with EEA relevance.
Evans, D. H., Piermarini, P. M. & Choe, K. P. (2005). The Multifunctional Fish Gill: Dominant Site of Gas Exchange, Osmoregulation, Acid-Base Regulation, and Excretion of Nitrogenous Waste. *Physiological Reviews*, 85 (1): 97-177. doi: 10.1152/physrev.00050.2003.
FAO. (2021). *Oncorhynchus tshawytscha ,*. Available at: http://www.fao.org/fishery/species/2933/en.
Food and Agriculture Organization of the United Nations. (2018). The State of World Fisheries and Aquaculture 2018–Meeting the sustainable development goals. *FAO*.
Food and Agriculture Organization of the United Nations. (2020). The State of World Fisheries and Aquaculture 2020–Sustainablity in action. *FAO*.
Foyle, K. L., Hess, S., Powell, M. D. & Herbert, N. A. (2020). What Is Gill Health and What Is Its Role in Marine Finfish Aquaculture in the Face of a Changing Climate? *Frontiers in Marine Science*, 7 (400). doi: 10.3389/fmars.2020.00400.
Froese, R. & Pauly, D. (2014). *Fishbase, a Global Information System on Fishes: http://www. fishbase. org. World Wide Web electronic publication*: Accessed.
Garneau, J. E., Dupuis, M.-È., Villion, M., Romero, D. A., Barrangou, R., Boyaval, P., Fremaux, C., Horvath, P., Magadán, A. H. & Moineau, S. (2010). The CRISPR/Cas bacterial immune system cleaves bacteriophage and plasmid DNA. *Nature*, 468 (7320): 67-71.
Gauld, N. (2016). *PhD Thesis: The behavioural ecology of migratory salmonids in the River Tweed, UK*.
Geneious. (2014). *Geneious R8*
. Available at: https://www.geneious.com/download/previous-versions/#geneious-r8.
Gezelius, S. S. (2008). The arrival of modern fisheries management in the North Atlantic: a historical overview. In *Making fisheries management work*, pp. 27-40: Springer.
Gjessing, M. C., Aamelfot, M., Batts, W. N., Benestad, S. L., Dale, O. B., Thoen, E., Weli, S. C. & Winton, J. R. (2018). Development and characterization of two cell lines from gills of Atlantic salmon. *PloS one*, 13 (2): e0191792-e0191792. doi: 10.1371/journal.pone.0191792.

Gjessing, M. C., Steinum, T., Olsen, A. B., Lie, K. I., Tavornpanich, S., Colquhoun, D. J. & Gjevre, A.-G. (2019). Histopathological investigation of complex gill disease in sea farmed Atlantic salmon. *PloS one*, 14 (10): e0222926.

Goldstone, J. V., Goldstone, H. M., Morrison, A. M., Tarrant, A., Kern, S. E., Woodin, B. R. & Stegeman, J. J. (2007). Cytochrome P450 1 genes in early deuterostomes (tunicates and sea urchins) and vertebrates (chicken and frog): origin and diversification of the CYP1 gene family. *Molecular Biology and Evolution*, 24 (12): 2619-2631.

Gratacap, R. L., Regan, T., Dehler, C. E., Martin, S. A. M., Boudinot, P., Collet, B. & Houston, R. D. (2020). Efficient CRISPR/Cas9 genome editing in a salmonid fish cell line using a lentivirus delivery system. *BMC Biotechnology*, 20 (1): 35. doi: 10.1186/s12896-020-00626-x.

Gupta, R. M. & Musunuru, K. (2014). Expanding the genetic editing tool kit: ZFNs, TALENs, and CRISPR-Cas9. *The Journal of clinical investigation*, 124 (10): 4154-4161.

Gutierrez Rabadan, C., Spreadbury, C., Consuegra, S. & Garcia de Leaniz, C. (2021). Development, validation and testing of an Operational Welfare Score Index for farmed lumpfish Cyclopterus lumpus L. *Aquaculture*, 531: 735777. doi: https://doi.org/10.1016/j.aquaculture.2020.735777.

Hahn, M. E., Woodin, B. R., Stegeman, J. J. & Tillitt, D. E. (1998). Aryl hydrocarbon receptor function in early vertebrates: inducibility of cytochrome P450 1A in agnathan and elasmobranch fish. *Comp Biochem Physiol C Pharmacol Toxicol Endocrinol*, 120 (1): 67-75. doi: 10.1016/s0742-8413(98)00007-3.

Hamilton, M. C., Hites, R. A., Schwager, S. J., Foran, J. A., Knuth, B. A. & Carpenter, D. O. (2005). Lipid composition and contaminants in farmed and wild salmon. *Environmental science & technology*, 39 (22): 8622-8629.

Hillary, V. E., Ceasar, S. A. & Ignacimuthu, S. (2020). Chapter 18 - Genome engineering in insects: focus on the CRISPR/Cas9 system. In Singh, V. & Dhar, P. K. (eds) *Genome Engineering via CRISPR-Cas9 System*, pp. 219-249: Academic Press.

Howe, K. L., Achuthan, P., Allen, J., Allen, J., Alvarez-Jarreta, J., Amode, M. R., Armean, I. M., Azov, A. G., Bennett, R., Bhai, J., et al. (2021). Ensembl 2021. *Nucleic Acids Research*, 49 (D1): D884-D891. doi: 10.1093/nar/gkaa942.

Hsu, P. D., Lander, E. S. & Zhang, F. (2014). Development and applications of CRISPR-Cas9 for genome engineering. *Cell*, 157 (6): 1262-1278.

Imsland, A. K. D., Hanssen, A., Nytrø, A. V., Reynolds, P., Jonassen, T. M., Hangstad, T. A., Elvegård, T. A., Urskog, T. C. & Mikalsen, B. (2018). It works! Lumpfish can significantly lower sea lice infestation in large-scale salmon farming. *Biology open*, 7 (9).

Institute of Marine Research. (2020). *Lumpfish*.

Integrated DNA Technologies. (2021). *Alt-R® Genome Editing Detection Kit*.

invitrogen. (2016). *GeneArt™ Precision gRNA Synthesis Kit USER GUIDE*.

Ishino, Y., Krupovic, M. & Forterre, P. (2018). History of CRISPR-Cas from Encounter with a Mysterious Repeated Sequence to Genome Editing Technology. *Journal of bacteriology*, 200 (7): e00580-17. doi: 10.1128/JB.00580-17.

ITIS. (2020). *Salmonidae* Available at: https://www.itis.gov/servlet/SingleRpt/SingleRpt?search_topic=TSN&search_value=161931#null.

Iversen, A., Asche, F., Hermansen, Ø. & Nystøyl, R. (2020). Production cost and competitiveness in major salmon farming countries 2003–2018. *Aquaculture*, 522: 735089. doi: https://doi.org/10.1016/j.aquaculture.2020.735089.

Jinek, M., Jiang, F., Taylor, D. W., Sternberg, S. H., Kaya, E., Ma, E., Anders, C., Hauer, M., Zhou, K., Lin, S., et al. (2014). Structures of Cas9 endonucleases reveal RNA-mediated conformational activation. *Science*, 343 (6176): 1247997. doi: 10.1126/science.1247997.

Joung, J. K. & Sander, J. D. (2013). TALENs: a widely applicable technology for targeted genome editing. *Nature reviews. Molecular cell biology*, 14 (1): 49-55. doi: 10.1038/nrm3486.

Kazakov, R. (1992). Distribution of Atlantic salmon, Salmo salar L., in freshwater bodies of Europe. *Aquaculture Research*, 23 (4): 461-475.
Kim, T. K. & Eberwine, J. H. (2010). Mammalian cell transfection: the present and the future. *Analytical and bioanalytical chemistry*, 397 (8): 3173-3178. doi: 10.1007/s00216-010-3821-6.
Koonin, E. V. & Makarova, K. S. (2019). Origins and evolution of CRISPR-Cas systems. *Philos Trans R Soc Lond B Biol Sci*, 374 (1772): 20180087. doi: 10.1098/rstb.2018.0087.
Koppang, E. O., Kvellestad, A. & Fischer, U. (2015). 5 - Fish mucosal immunity: gill. In Beck, B. H. & Peatman, E. (eds) *Mucosal Health in Aquaculture*, pp. 93-133. San Diego: Academic Press.
Krøvel, A. V., Søfteland, L., Torstensen, B. & Olsvik, P. A. (2008). Transcriptional effects of PFOS in isolated hepatocytes from Atlantic salmon Salmo salar L. *Comparative Biochemistry and Physiology Part C: Toxicology & Pharmacology*, 148 (1): 14-22.
Kumar, S., Stecher, G. & Tamura, K. (2016). MEGA7: molecular evolutionary genetics analysis version 7.0 for bigger datasets. *Molecular biology and evolution*, 33 (7): 1870-1874.
Labun, K., Montague, T. G., Krause, M., Torres Cleuren, Y. N., Tjeldnes, H. & Valen, E. (2019). CHOPCHOP v3: expanding the CRISPR web toolbox beyond genome editing. *Nucleic Acids Research*, 47 (W1): W171-W174. doi: 10.1093/nar/gkz365.
Lafferty, K. D., Harvell, C. D., Conrad, J. M., Friedman, C. S., Kent, M. L., Kuris, A. M., Powell, E. N., Rondeau, D. & Saksida, S. M. (2015). Infectious Diseases Affect Marine Fisheries and Aquaculture Economics. *Annual Review of Marine Science*, 7 (1): 471-496. doi: 10.1146/annurev-marine-010814-015646.
Leaver, M. J. & George, S. G. (2000). A cytochrome P4501B gene from a fish, Pleuronectes platessa. *Gene*, 256 (1): 83-91. doi: https://doi.org/10.1016/S0378-1119(00)00373-5.
Lee, L. E. J., Dayeh, V. R., Schirmer, K. & Bols, N. C. (2009). Applications and potential uses of fish gill cell lines: examples with RTgill-W1. *In Vitro Cellular & Developmental Biology - Animal*, 45 (3): 127-134. doi: 10.1007/s11626-008-9173-2.
Lewis, D., Watson, E. & Lake, B. (1998). Evolution of the cytochrome P450 superfamily: sequence alignments and pharmacogenetics. *Mutation Research/Reviews in Mutation Research*, 410 (3): 245-270.
Liang, F., Han, M., Romanienko, P. J. & Jasin, M. (1998). Homology-directed repair is a major double-strand break repair pathway in mammalian cells. *Proceedings of the National Academy of Sciences*, 95 (9): 5172. doi: 10.1073/pnas.95.9.5172.
Life Technologies Corporation. (2014). *GeneArt® Genomic Cleavage Detection Kit*. A.0 ed.
Little, D., Newton, R. & Beveridge, M. (2016). Aquaculture: a rapidly growing and significant source of sustainable food? Status, transitions and potential. *Proceedings of the Nutrition Society*, 75: 274-286. doi: 10.1017/S0029665116000665.
MacCrimmon, H. R. & Gots, B. L. (1979). World distribution of Atlantic salmon, salmo solar. *Journal of the Fisheries Board of Canada*, 36 (4): 422-457.
Makarova, K. S., Haft, D. H., Barrangou, R., Brouns, S. J., Charpentier, E., Horvath, P., Moineau, S., Mojica, F. J., Wolf, Y. I., Yakunin, A. F., et al. (2011). Evolution and classification of the CRISPR-Cas systems. *Nat Rev Microbiol*, 9 (6): 467-77. doi: 10.1038/nrmicro2577.
Makarova, K. S., Wolf, Y. I., Alkhnbashi, O. S., Costa, F., Shah, S. A., Saunders, S. J., Barrangou, R., Brouns, S. J., Charpentier, E. & Haft, D. H. (2015). An updated evolutionary classification of CRISPR–Cas systems. *Nature Reviews Microbiology*, 13 (11): 722-736.
Manghwar, H., Lindsey, K., Zhang, X. & Jin, S. (2019). CRISPR/Cas System: Recent Advances and Future Prospects for Genome Editing. *Trends in Plant Science*, 24 (12): 1102-1125. doi: https://doi.org/10.1016/j.tplants.2019.09.006.
Markussen, T., Dahle, M. K., Tengs, T., Løvoll, M., Finstad, Ø. W., Wiik-Nielsen, C. R., Grove, S., Lauksund, S., Robertsen, B. & Rimstad, E. (2013). Sequence analysis of the genome of piscine orthoreovirus (PRV) associated with heart and skeletal muscle inflammation (HSMI) in Atlantic salmon (Salmo salar). *PloS one*, 8 (7): e70075-e70075. doi: 10.1371/journal.pone.0070075.

Marraffini, L. A. & Sontheimer, E. J. (2010). Self versus non-self discrimination during CRISPR RNA-directed immunity. *Nature*, 463 (7280): 568-571. doi: 10.1038/nature08703.
Martos-Sitcha, J. A., Mancera, J. M., Prunet, P. & Magnoni, L. J. (2020). Editorial: Welfare and Stressors in Fish: Challenges Facing Aquaculture. *Frontiers in Physiology*, 11 (162). doi: 10.3389/fphys.2020.00162.
McMillan, D. B. & Harris, R. J. (2018). Chapter L - Respiratory Systems. In McMillan, D. B. & Harris, R. J. (eds) *An Atlas of Comparative Vertebrate Histology*, pp. 389-425. San Diego: Academic Press.
Mikalsen, K. H. & Jentoft, S. (2003). Limits to participation? On the history, structure and reform of Norwegian fisheries management. *Marine Policy*, 27 (5): 397-407. doi: https://doi.org/10.1016/S0308-597X(03)00025-3.
Miller, J. C., Holmes, M. C., Wang, J., Guschin, D. Y., Lee, Y.-L., Rupniewski, I., Beausejour, C. M., Waite, A. J., Wang, N. S. & Kim, K. A. (2007). An improved zinc-finger nuclease architecture for highly specific genome editing. *Nature biotechnology*, 25 (7): 778-785.
Moon, S. B., Kim, D. Y., Ko, J.-H., Kim, J.-S. & Kim, Y.-S. (2019). Improving CRISPR Genome Editing by Engineering Guide RNAs. *Trends in Biotechnology*, 37 (8): 870-881. doi: https://doi.org/10.1016/j.tibtech.2019.01.009.
MOWI. (2019). *Salmon Farming Industry Handbook 2019*.
National Institute of Water and Atmospheric Research. (2016). Chinook salmon.
National Wildlife Federation. (2020). *Chinook salmon*. Available at: https://www.nwf.org/Educational-Resources/Wildlife-Guide/Fish/Chinook-Salmon.
Nelson, D. R., Kamataki, T., Waxman, D. J., Guengerich, F. P., Estabrook, R. W., Feyereisen, R., Gonzalez, F. J., Coon, M. J., Gunsalus, I. C. & Gotoh, O. (1993). The P450 superfamily: update on new sequences, gene mapping, accession numbers, early trivial names of enzymes, and nomenclature. *DNA and cell biology*, 12 (1): 1-51.
Nelson, J. S., Grande, T. C. & Wilson, M. V. (2016). *Fishes of the World*: John Wiley & Sons.
NOAA Fisheries. (2021). *Chinook Salmon*. Available at: https://www.fisheries.noaa.gov/species/chinook-salmon.
Noguera, P. A., Grunow, B., Klinger, M., Lester, K., Collet, B. & Del-Pozo, J. (2017). Atlantic salmon cardiac primary cultures: An in vitro model to study viral host pathogen interactions and pathogenesis. *PloS one*, 12 (7): e0181058-e0181058. doi: 10.1371/journal.pone.0181058.
Olsvik, P. A., Vikeså, V., Lie, K. K. & Hevrøy, E. M. (2013). Transcriptional responses to temperature and low oxygen stress in Atlantic salmon studied with next-generation sequencing technology. *BMC Genomics*, 14 (1): 817. doi: 10.1186/1471-2164-14-817.
Paisley, L. G., Ariel, E., Lyngstad, T., Jónsson, G., Vennerström, P., Hellström, A. & Østergaard, P. (2010). An overview of aquaculture in the Nordic countries. *Journal of the World Aquaculture Society*, 41 (1): 1-17.
Pastwa, E. & Błasiak, J. (2003). Non-homologous DNA end joining. *Acta Biochim Pol*, 50 (4): 891-908.
Pattanayak, V., Guilinger, J. P. & Liu, D. R. (2014). Determining the specificities of TALENs, Cas9, and other genome-editing enzymes. *Methods in enzymology*, 546: 47-78.
Pennell, W. & Prouzet, K. (2009). Salmonid fish: bology, conservation status, and economic importance of wild and cultured stocks. *Fisheries and aquaculture. P. Safran, Enciclopedia of life suport system*: 42-65.
Powell, A., Treasurer, J. W., Pooley, C. L., Keay, A. J., Lloyd, R., Imsland, A. K. & Garcia de Leaniz, C. (2018). Use of lumpfish for sea-lice control in salmon farming: Challenges and opportunities. *Reviews in aquaculture*, 10 (3): 683-702.
Promega corporation. (2018). *pGEM®-T and pGEM®-TEasy Vector Systems*.
Public Health England. (2021). *ECACC General Cell Collection: CHSE-214*. Available at: https://www.phe-culturecollections.org.uk/products/celllines/generalcell/detail.jsp?refId=91041114&collection=ecacc_gc#:~:text=ECACC%20General%20Cell%20Collection%3A%20CHSE%2D214&text=Ce

ll%20Line%20Description%3A,many%20instances%20replicate%20high%20titres.&text=Freeze%20cells%20in%205%25%20DMSO,foetal%20bovine%20serum%20(FBS).
Rabanal, H. R. (1988). History of aquaculture.
Rahman, M. S. & Thomas, P. (2012). Effects of hypoxia exposure on hepatic cytochrome P450 1A (CYP1A) expression in Atlantic croaker: molecular mechanisms of CYP1A down-regulation. *PloS one*, 7 (7): e40825.
Ran, F. A., Hsu, P. D., Lin, C.-Y., Gootenberg, J. S., Konermann, S., Trevino, A. E., Scott, D. A., Inoue, A., Matoba, S. & Zhang, Y. (2013). Double nicking by RNA-guided CRISPR Cas9 for enhanced genome editing specificity. *Cell*, 154 (6): 1380-1389.
Rath, D., Amlinger, L., Rath, A. & Lundgren, M. (2015). The CRISPR-Cas immune system: Biology, mechanisms and applications. *Biochimie*, 117: 119-128. doi: https://doi.org/10.1016/j.biochi.2015.03.025.
Rees, C. B., McCormick, S. D., Heuvel, J. P. V. & Li, W. (2003). Quantitative PCR analysis of CYP1A induction in Atlantic salmon (Salmo salar). *Aquatic Toxicology*, 62 (1): 67-78.
Rees, C. B., McCormick, S. D. & Li, W. (2005). A non-lethal method to estimate CYP1A expression in laboratory and wild Atlantic salmon (Salmo salar). *Comparative Biochemistry and Physiology Part C: Toxicology & Pharmacology*, 141 (3): 217-224.
Rees, C. B., Wu, H. & Li, W. (2005). Cloning of CYP1A in Atlantic salmon (Salmo salar). *Aquaculture*, 246 (1): 11-23. doi: https://doi.org/10.1016/j.aquaculture.2004.12.025.
Rice, J. (2013). *NOAA report establishes Chinook monitoring framework*. Available at: https://www.eopugetsound.org/articles/noaa-report-establishes-chinook-monitoring-framework.
Rodger, H. D. (2016). Fish Disease Causing Economic Impact in Global Aquaculture. In Adams, A. (ed.) *Fish Vaccines*, pp. 1-34. Basel: Springer Basel.
Rombough, P. (2007). The functional ontogeny of the teleost gill: Which comes first, gas or ion exchange? *Comparative Biochemistry and Physiology Part A: Molecular & Integrative Physiology*, 148 (4): 732-742. doi: https://doi.org/10.1016/j.cbpa.2007.03.007.
Sanden, M. & Olsvik, P. A. (2009). Intestinal cellular localization of PCNA protein and CYP1A mRNA in Atlantic salmon Salmo salar L. exposed to a model toxicant. *BMC Physiology*, 9 (1): 3. doi: 10.1186/1472-6793-9-3.
Sandersen, H. T., Olsen, J., Hovelsrud, G. K. & Gjertsen, A. (2020). Climate Change and Norwegian Arctic Aquaculture: Perception, Relevance and Adaptation.
Scientific, T. (2021). *Neon Transfection System Cell Line Data and Transfection Parameters*. Available at: https://www.thermofisher.com/no/en/home/life-science/cell-culture/transfection/neon-transfection-system/neon-transfection-system-cell-line-data.html.
Sekine, M. (2018). Recent Development of Chemical Synthesis of RNA. In *Synthesis of Therapeutic Oligonucleotides*, pp. 41-65: Springer.
Sekkingstad AS. (2021). *Norwegian salmon (salmo salar)*.
Sentmanat, M. F., Peters, S. T., Florian, C. P., Connelly, J. P. & Pruett-Miller, S. M. (2018). A Survey of Validation Strategies for CRISPR-Cas9 Editing. *Scientific Reports*, 8 (1): 888. doi: 10.1038/s41598-018-19441-8.
Smith, T. (2014). Greening the Blue Revolution: How History Can Inform a Sustainable Aquaculture Movement.
SSB Norway. (2020). *Aquaculture*.
Sternberg, S. H., Redding, S., Jinek, M., Greene, E. C. & Doudna, J. A. (2014). DNA interrogation by the CRISPR RNA-guided endonuclease Cas9. *Nature*, 507 (7490): 62-7. doi: 10.1038/nature13011.
Stickney, R. R. & Treece, G. D. (2000). History of aquaculture. *Enclyclopedia of Aquaculture, John Wiley & Sons Inc., New York, 1063p*.

Sun, N. & Zhao, H. (2013). Transcription activator-like effector nucleases (TALENs): a highly efficient and versatile tool for genome editing. *Biotechnology and bioengineering*, 110 (7): 1811-1821.

Terns, M. P. & Terns, R. M. (2011). CRISPR-based adaptive immune systems. *Current Opinion in Microbiology*, 14 (3): 321-327. doi: https://doi.org/10.1016/j.mib.2011.03.005.

The Norwegian National Research Ethics Committees. (2015). *Animals in research*. Available at: https://www.forskningsetikk.no/en/resources/the-research-ethics-library/research-and-environment/animals-in-research/.

Torrissen, O., Jones, S., Asche, F., Guttormsen, A., Skilbrei, O. T., Nilsen, F., Horsberg, T. E. & Jackson, D. (2013). Salmon lice–impact on wild salmonids and salmon aquaculture. *Journal of fish diseases*, 36 (3): 171-194.

Trump, B. F., Kane, A. S. & Jones, R. T. (2000). Development of an in vitro model of fish skin and gill. *Marine Environmental Research*, 50 (1): 546-547. doi: https://doi.org/10.1016/S0141-1136(00)00234-8.

Uno, T., Ishizuka, M. & Itakura, T. (2012). Cytochrome P450 (CYP) in fish. *Environmental Toxicology and Pharmacology*, 34 (1): 1-13. doi: https://doi.org/10.1016/j.etap.2012.02.004.

Urnov, F. D., Rebar, E. J., Holmes, M. C., Zhang, H. S. & Gregory, P. D. (2010). Genome editing with engineered zinc finger nucleases. *Nature Reviews Genetics*, 11 (9): 636-646.

Waples, R. S., Teel, D. J., Myers, J. M. & Marshall, A. R. (2004). Life-History Divergence in Chinook Salmon: Historic Contingency and Parallel Evolution. *Evolution*, 58 (2): 386-403.

Wegner, N. (2011). Gill Respiratory Morphometrics. In vol. 2, pp. 803-811.

Wood, C. M., Kelly, S. P., Zhou, B., Fletcher, M., O'Donnell, M., Eletti, B. & Pärt, P. (2002). Cultured gill epithelia as models for the freshwater fish gill. *Biochimica et Biophysica Acta (BBA) - Biomembranes*, 1566 (1): 72-83. doi: https://doi.org/10.1016/S0005-2736(02)00595-3.

9 Appendix

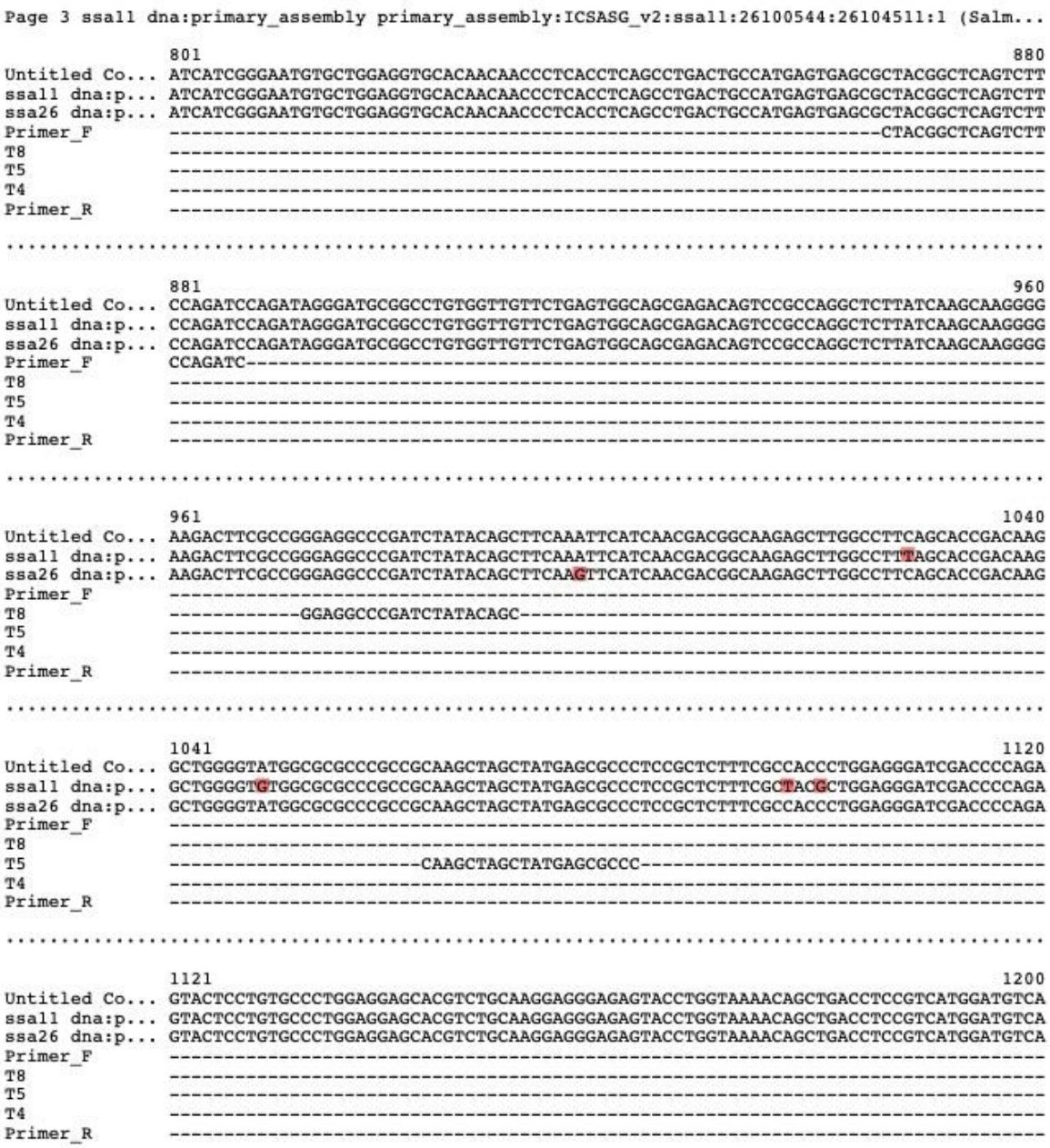
Page 3 ssa11 dna:primary_assembly primary_assembly:ICSASG_v2:ssa11:26100544:26104511:1 (Salm...
801 880
Untitled Co... ATCATCGGGAATGTGCTGGAGGTGCACAACAACCCTCACCTCAGCCTGACTGCCATGAGTGAGCGCTACGGCTCAGTCTT
ssa11 dna:p... ATCATCGGGAATGTGCTGGAGGTGCACAACAACCCTCACCTCAGCCTGACTGCCATGAGTGAGCGCTACGGCTCAGTCTT
ssa26 dna:p... ATCATCGGGAATGTGCTGGAGGTGCACAACAACCCTCACCTCAGCCTGACTGCCATGAGTGAGCGCTACGGCTCAGTCTT
Primer_F ----------CTACGGCTCAGTCTT
T8 ----------
T5 ----------
T4 ----------
Primer_R ----------
881 960
Untitled Co... CCAGATCCAGATAGGGATGCGGCCTGTGGTTGTTCTGAGTGGCAGCGAGACAGTCCGCCAGGCTCTTATCAAGCAAGGGG
ssa11 dna:p... CCAGATCCAGATAGGGATGCGGCCTGTGGTTGTTCTGAGTGGCAGCGAGACAGTCCGCCAGGCTCTTATCAAGCAAGGGG
ssa26 dna:p... CCAGATCCAGATAGGGATGCGGCCTGTGGTTGTTCTGAGTGGCAGCGAGACAGTCCGCCAGGCTCTTATCAAGCAAGGGG
Primer_F CCAGATC----------
T8 ----------
T5 ----------
T4 ----------
Primer_R ----------
961 1040
Untitled Co... AAGACTTCGCCGGGAGGCCCGATCTATACAGCTTCAAATTCATCAACGACGGCAAGAGCTTGGCCTTCAGCACCGACAAG
ssa11 dna:p... AAGACTTCGCCGGGAGGCCCGATCTATACAGCTTCAAATTCATCAACGACGGCAAGAGCTTGGCCTTTAGCACCGACAAG
ssa26 dna:p... AAGACTTCGCCGGGAGGCCCGATCTATACAGCTTCAAGTTCATCAACGACGGCAAGAGCTTGGCCTTCAGCACCGACAAG
Primer_F ----------
T8 ----------GGAGGCCCGATCTATACAGC----------
T5 ----------
T4 ----------
Primer_R ----------
1041 1120
Untitled Co... GCTGGGGTATGGCGCGCCCGCCGCAAGCTAGCTATGAGCGCCCTCCGCTCTTTCGCCACCCTGGAGGGATCGACCCCAGA
ssa11 dna:p... GCTGGGGTGTGGCGCGCCCGCCGCAAGCTAGCTATGAGCGCCCTCCGCTCTTTCGCTACGCTGGAGGGATCGACCCCAGA
ssa26 dna:p... GCTGGGGTATGGCGCGCCCGCCGCAAGCTAGCTATGAGCGCCCTCCGCTCTTTCGCCACCCTGGAGGGATCGACCCCAGA
Primer_F ----------
T8 ----------
T5 ----------CAAGCTAGCTATGAGCGCCC----------
T4 ----------
Primer_R ----------
1121 1200
Untitled Co... GTACTCCTGTGCCCTGGAGGAGCACGTCTGCAAGGAGGGAGAGTACCTGGTAAAACAGCTGACCTCCGTCATGGATGTCA
ssa11 dna:p... GTACTCCTGTGCCCTGGAGGAGCACGTCTGCAAGGAGGGAGAGTACCTGGTAAAACAGCTGACCTCCGTCATGGATGTCA
ssa26 dna:p... GTACTCCTGTGCCCTGGAGGAGCACGTCTGCAAGGAGGGAGAGTACCTGGTAAAACAGCTGACCTCCGTCATGGATGTCA
Primer_F ----------
T8 ----------
T5 ----------
T4 ----------
Primer_R ----------

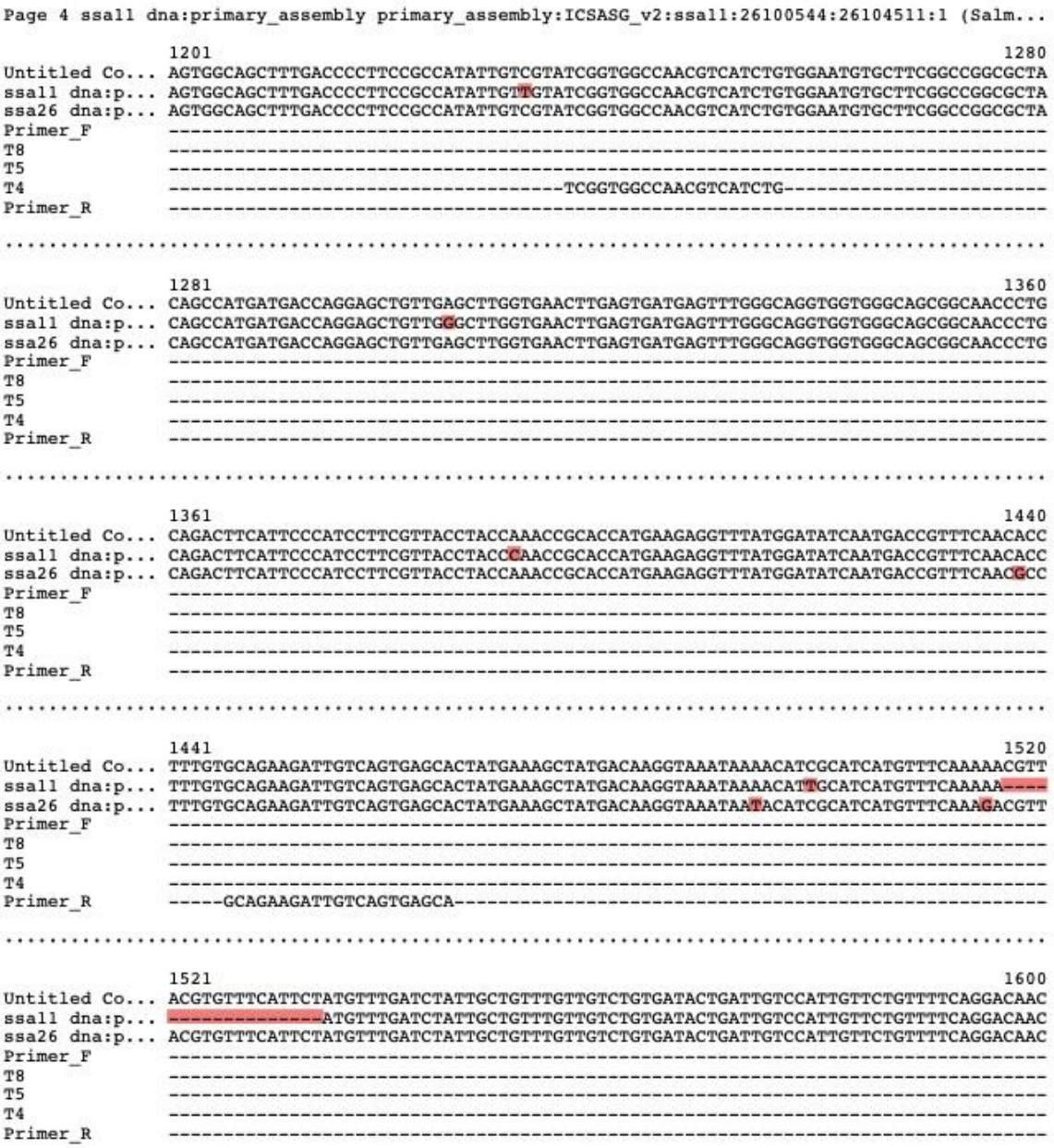

Supplementary Figure 1: Diagram showing sequence alignment of ssa11 and ssa26 along with target sequences and PCR primers for CYP1a. This alignment shows where the target sequence acts on CYP1a gene in chromosome 11 and 26, as well as the location where PCR primers acts.

Supplementary Figure 1: TC20™ automated cell counter

Supplementary Figure 2: Pico™ 17 Microcentrifuge

Supplementary Figure 3: Neon™ Transfection System

Supplementary Figure 4: Nucleofector™ 2b Device

Supplementary Figure 5: BD Accuri™ C6 flow cytometer

Supplementary Figur 6: T100™ thermal cycler

Norges miljø- og biovitenskapelige universitet
Noregs miljø- og biovitskapelege universitet
Norwegian University of Life Sciences

Postboks 5003
NO-1432 Ås
Norway